



venterra

Helping wind power grow

Kriegers Flak II South – Integrated 3D GeoModel



ENERGINET

Client	Energinet
Document Ref.	24004-REP-003-03
Project Title	Kriegers Flak II South
Date	04/09/2024

Project Title:	Kriegers Flak II South
Project Reference	24004-REP-003-03
Report Title:	Kriegers Flak II South – Integrated 3D GeoModel
Document Reference	24004-REP-003-03
Client Report Reference	24004-REP-003-03

Client:	Energinet
Ultimate Client:	Energinet
Confidentiality	Non Confidential

REVISION HISTORY

Rev	Date	Reason for Issue	Originator	Checker	Reviewer	Approver
00	02/08/2024	Draft for Comment	EM, TB, MG	GMcA	LT/TJ	LT
01	07/08/2024	Draft, Geotechnical Parameters included	JM, EM, GM, MG	AL	TJ	LT
02	26/08/2024	Updated to address client comments	JM, EM, GM, MG, TB	TB	GMcA/TJ	GMcA, TJ
03	04/09/2024	Updated to address client comments	JM, EM, GM, MG	TB	JQ	TJ

DISCLAIMER

Gavin & Doherty Geosolutions Ltd (GDG), part of the Venterra Group, has prepared this report for the sole use of Energinet (hereafter the “Client”) in accordance with the terms of a contract between the Client and GDG. No other warranty, expressed or implied, is made as to the professional advice contained in the report or any other services provided by GDG. Any party other than our Client that relies upon this report in whole or in part does so at their own risk. GDG assumes no liability or duty of care to any third party in respect of or arising out of or in connection with this report and/or the professional advice contained within.

This report is the copyright of GDG. All rights reserved.

TABLE OF CONTENTS

Chapter	Page
Table of Contents	3
Executive Summary	12
1 Introduction	14
1.1 Purpose and Scope of Work	14
1.2 Limitations and Exclusions	14
1.3 Geodetic Information	15
1.4 Vertical Datum	15
1.5 Summary of Previous Studies and Site-Specific Reports	15
2 The site	17
3 Method description and deliverables	18
4 Geological Background and Previous Studies	20
4.1 Preliminary Ground Model (GeoXYZ, 2024)	20
4.2 Geotechnical Site Investigation (Gardline, 2024)	21
4.3 Regional Geological Background	21
4.3.1 Regional Geological History	21
4.3.1.1 Pre-Quaternary	21
4.3.1.2 Quaternary	25
4.3.2 Expected Seabed Sediments	33
4.4 Conceptual Geological Model	33
5 Integrated 3D GeoModel Development	37
5.1 Geophysical Survey - Interpretation Refinement	39
5.1.1 UHRS Data Quality Grading	39
5.2 Geotechnical Data Summary	41
5.3 Geotechnical Data Integration	42
5.4 Velocity Model Revision	46
5.5 Gridding and Depth Conversion	48
5.5.1 Gridding	48
5.5.2 SEGY Depth Conversion	49
6 Discussion of Spatial Integrated 3D GeoModel	51
6.1 Seafloor Interpretation	51
6.1.1 Multibeam Echosounder Bathymetry and Slope	51
6.1.2 Side Scan Sonar	54
6.1.3 Seafloor Lithology	55
6.1.4 Seafloor Morphology	57
6.1.5 Seafloor Objects	59
6.1.6 Magnetic Anomalies	60
6.2 Sub-seafloor Interpretation	61
6.2.1 Seismic Unit I (SU I) - Marine Sediments	66
6.2.1.1 Geophysical Description	66
6.2.1.2 Spatial Distribution	66
6.2.1.3 Geotechnical Description	68
6.2.1.4 Interpretation	68

6.2.2	Seismic Unit IIIa (SU IIIA) - Upper Glaciolacustrine	71
6.2.2.1	Geophysical Description	71
6.2.2.2	Spatial Distribution	71
6.2.2.3	Geotechnical Description	72
6.2.2.4	Interpretation	72
6.2.3	Seismic Unit IIIb (SU IIIb) - Lower Glaciolacustrine	75
6.2.3.1	Geophysical Description	75
6.2.3.2	Spatial Distribution	75
6.2.3.3	Geotechnical Description	77
6.2.3.4	Interpretation	77
6.2.4	Seismic Unit Va (SU Va) - Unlithified CHalk	82
6.2.4.1	Geophysical Description	82
6.2.4.2	Spatial Distribution	82
6.2.4.3	Geotechnical Description	83
6.2.4.4	Interpretation	83
6.2.5	Seismic Unit Vb (SU Vb) - Lithified CHalk	86
6.2.5.1	Geophysical Description	86
6.2.5.2	Spatial Distribution	86
6.2.5.3	Geotechnical Description	86
6.2.5.4	Interpretation	86
6.2.6	Geological Units Summary	89
6.3	Soil Zonation	91
6.4	Geotechnical Unitisation	93
6.5	Integrated 3D GeoModel Uncertainty	93
6.6	Statistical Correlation of GI with Geophysical Data	97
7	Geotechnical Parameters	98
7.1	General	98
7.2	Geotechnical Soil Parameters	98
7.3	Recommended Parameter Bounding Framework	99
7.4	Interpretation Strategy	100
7.5	Selection of CPT Classification Method	100
7.5.1	General	100
7.5.2	Soil Classification Based on CPT Data	101
7.6	Summary of Laboratory Tests	102
7.7	Classification Properties and Unit Weight	103
7.8	Engineering Properties	105
7.9	Cone Penetration Test Parameters	105
7.9.1	General	105
7.9.1.1	Relative Density	107
7.9.2	Static Undrained Shear Strength	107
7.9.3	Remoulded Undrained Shear Strength	108
7.9.4	Sensitivity	108
7.9.6	Coefficient of Lateral Earth Pressure at Rest	109
7.9.7.1	General	110
7.9.8.4	Small Strain Shear Modulus	111

7.9.8.5	Strain at 50% Peak Deviator Stress	112
7.10	Rock Parameters	112
7.10.2	RQD	112
7.10.5	Intact Youngs Modulus	113
8	Hazards and Geohazards	114
8.1	Seafloor hazards	114
8.1.1	Boulders and Debris	114
8.1.2	Depressions	114
8.1.3	Seafloor Scarring	115
8.1.4	Slope	115
8.1.5	Wrecks	115
8.1.6	Other	115
8.2	Sub-Seafloor Hazards	115
8.2.1	Boulders and Coarse Sediments	115
8.2.2	Shallow Gas	116
8.2.3	Channels and Channel Infill	117
8.2.4	Faults and Faulting	119
8.2.5	Glacial Features	120
8.2.6	Low Strength Sediment	120
8.2.7	Shallow Bedrock	120
9	Risk Register	121
10	Recommendations	123
10.1.1	Desk Studies	123
10.1.2	Data Re-Processing	123
10.1.3	Further Surveys and Investigations	123
11	Conclusion	125
12	References	129
13	Appendices	132
	Appendix A – Charts and digital deliverables	132
	Appendix B - Seismic Cross Sections	133
	Appendix C - Unitised Geotechnical Parameters	133
	Appendix D - Risk Register	133
	Appendix E - Geotechnical Cross-sections	133

LIST OF TABLES

Table 1-1 - Geodetic parameters	15
Table 4-1 - Shallow geological units (GEOxyz, 2024)	20
Table 4-2 - Regional Quaternary stratigraphy and seismic facies	30
Table 4-3 - Conceptual Geological Model Summary	34
Table 5-1 - Revised seismic interpretation of the geophysical data	39
Table 5-2 - Correlation between seismic and geotechnical tops	45
Table 5-3 - UHRS line offsets from geotechnical locations	45
Table 5-4 - Velocity model parameters	46
Table 5-5 - Final velocity model	48
Table 6-1 - Sediment classification based on MBES backscatter analysis	57
Table 6-2 - Overview of the interpreted units	63
Table 6-3 - Geological units summary	90
Table 6-4 - Defined provinces	91
Table 6-5 Ground conditions and design challenges at each Province	94
Table 6-6 - IGM uncertainty	95
Table 6-7 - Statistical correlation between GI and geophysical data	97
Table 7-1 - Geotechnical soil and rock parameters determined	98
Table 7-2 CPT classification	102
Table 7-3 - Types and number of tests available at time of reporting (Gardline, 2024)	103
Table 7-4 - Measured and derived CPT parameters	106
Table 7-5 - Nkt empirical factors	107

LIST OF FIGURES

Figure 1-1 - Danish Offshore Wind Farms (www.ens.dk)	14
Figure 2-1 – The proposed Kriegers Flak II Southern site overview (Flanders Marine Institute, 2023)	17
Figure 4-1 - Geological, schematic, general arrangement of the units (GEOxyz, 2024)	20
Figure 4-2 - Regional setting, modified from Graversen (2009). AOI – Area of Interest	22
Figure 4-3 - Pre-Quaternary deposits (lithology) and faults (EMODnet, 2024)	23
Figure 4-4 - Pre-Quaternary deposits (age) and faults (EMODnet, 2024)	23
Figure 4-5 - Pre-Quaternary deposits (age) and faults (DGU, 1992; GEUS, 2024)	24
Figure 4-6 - Top pre-Quaternary surface elevation (Binzer, et al., 1994; GEUS, 2024)	25
Figure 4-7 - Ice margin evolution (Pedersen, 1998; GEUS, 2024)	26
Figure 4-8 - Danish region palaeogeography from 18 to 12 ka BP; modified from GEUS (2022; 2023)	27
Figure 4-9 - Danish region palaeogeography from 11.5 to 7 ka BP; modified from GEUS (2022; 2023)	28
Figure 4-10 - Quaternary deposits age (EMODnet, 2024)	32
Figure 4-11 - Quaternary deposits lithology (EMODnet, 2024)	32
Figure 4-12 - Seabed sediments – Folk 7 (EMODnet, 2024)	33
Figure 4-13 - Conceptual Geological Model	36
Figure 5-1 - IGM development workflow	38
Figure 5-2 - UHRS line paths and data quality grades	41
Figure 5-3 - Geotechnical site investigation locations overview (Gardline, 2024)	42
Figure 5-4 - Comparison of pre (a) and post (b) geotechnical interpretation integration UHRS line L020	44

Figure 5-5 Comparison of pre (a) and post (b) geotechnical interpretation integration UHRS line L02	44
Figure 5-6 - Seismic unit velocity model	47
Figure 5-7 - Example of the transition between well constrained velocity model (right) and interpolated model with limited vertical offset (left)	50
Figure 6-1 – Hillshaded MBES bathymetry	51
Figure 6-2 - MBES derived slope	52
Figure 6-3 - Areas of increased slope angle	53
Figure 6-4 - Bathymetry with hillshade	53
Figure 6-5 – Side scan sonar (GeoXYZ, 2023)	54
Figure 6-6 - Seafloor features identified on the SSS data (GeoXYZ, 2023)	55
Figure 6-7 - Seabed lithology classification and extents (GeoXYZ, 2023; GDG, 2024)	56
Figure 6-8 - MBES backscatter (GeoXYZ, 2023)	56
Figure 6-9 - Extensive scarring shown on the MBES slope	58
Figure 6-10 - Isolated depressions on MBES slope	59
Figure 6-11 - Example of seafloor contacts picked on SSS and MBES bathymetry	60
Figure 6-12 - Magnetic contacts and offshore infrastructure (Helcom, 2018)	61
Figure 6-13 - Schematic diagram of unit distribution in the survey area	65
Figure 6-14 - Top of Unit I elevation (mMSL)	67
Figure 6-15 - Unit I vertical thickness isochore	67
Figure 6-16 - Interpretation of SBP line 1755	69
Figure 6-17 - SBP line X011 integration	70
Figure 6-18 - Top of Unit IIIa elevation (mMSL)	71
Figure 6-19 - Unit IIIa vertical thickness isochore	72
Figure 6-20 - UHRS line L025 integration	74
Figure 6-21 - Top of Unit IIIb elevation (mMSL)	76
Figure 6-22 - Unit IIIb vertical thickness isochore	76
Figure 6-23 - Interpretation of UHRS line L021	79
Figure 6-24 - UHRS line L20 integration	80
Figure 6-25 - KFII_S_10_BH example of till to chalk interface	81
Figure 6-26 - Top of Unit Va elevation (mMSL)	82
Figure 6-27 - Interpretation of UHRS line L023	84
Figure 6-28 - UHRS line L020 integration	85
Figure 6-29 - H35 lithified chalk pick overview	87
Figure 6-30 - UHRS line L022 integration	88
Figure 6-31 Geotechnical zonation provinces	92
Figure 7-1 - Roberston (2016) classification	101
Figure 7-2 - Schneider et al (2018) classification	101
Figure 8-1 - Apparent acoustic blanking on seismic line KS_L024_UHR_T_MIG_STK	116
Figure 8-2 - Example of small incisions on seismic line KS_L018_UHR_T_MIG_STK	118
Figure 8-3 - Small subglacial channels at the southern fringe of the Scandinavian Ice Sheet (Kehew, et al., 2012).	119
Figure 9-1 - Risk Matrix	122

List of Abbreviations

Abbreviations	
Abbreviation	Description
ALARP	As Low as Reasonably Practicable
BE	Best Estimate
BH	Borehole
BP	Before Present
CIUc, CIDc, CAUc	Consolidated Triaxial Testing
CPT	Cone Penetrometer Testing
CPTU	Cone Penetrometer Testing with Pore Water
DSS	Direct Simple Shear
EEZ	Exclusive Economic Zone
EMODnet	European Marine Observation and Data Network
EPSG	European Petroleum Survey Group
GDG	Gavin and Doherty Geosolutions
GEUS	Geological Survey of Denmark and Greenland
GI	Geotechnical Investigation
GM	Ground Model
GRS	Grid Reference System
HE	High Estimate
HF, LF SSS	High, Low Frequency Side Scan Sonar
IGM	Integrated 3D GeoModel
LE	Lower Estimate
LL	Liquid Limit
MAG	Magnetometer
MBES	Multibeam Echosounder
mBSF	Metres Below seafloor
MCS	Multi-Channel Seismic
MD	Measured Depth
MLV	Miniature Lab Vanes
MSL	Mean Sea Level
OCR	Overconsolidation Ratio
OWF	Offshore Wind Farm
PGM	Preliminary Ground Model
PL	Plastic Limit
PLT	Point Load Test (Point Load Index)
PP	Pocket Penetrometers
PSD	Particle Size Distribution
pUXO	Potential UXO
SBP	Sub Bottom Profiler
SCPT	Seismic Cone Penetration Test
SCS	Single-Channel Seismic

Abbreviations	
Abbreviation	Description
SQL	Structured Query Language
SSS	Side Scan Sonar
TC	Thermal Conductivity
TV	Torvane
TWTT	Two-way Travel Time
UCS	Unconfined Compressive Strength
UHRS	Ultra-High Resolution Seismic
UTM	Universal Transverse Mercator
UU	Unconsolidated Undrained Triaxial
UXO	Unexploded Ordnance

Glossary of Terms

Glossary of Terms	
Item	Description
Artefact	A non-geological feature present in hydrographic or geophysical data because of data acquisition and/or processing. E.g. busts – where adjacent survey data are not vertically aligned giving the false impression of a step in the surface being represented
Cone Penetrometer Testing	This testing measures Tip Resistance, Sleeve Friction, Pore Pressure of a sensor lowered into the ground. Calculations with these values can give indications of sediment classification.
Diamict/Diamicton	A sediment that is unsorted to poorly sorted and contains particles ranging in size from clay to boulders, suspended in an unconsolidated matrix of mud or sand.
Folk Substrate Classification	A scheme for classifying seafloor sediment types
Geological Unit	A volume of sediments/rock with similar petrographic and lithological characteristics.
Isochore	Isochore are grids that represent the vertical thickness of a layer or unit in metres; not to be confused with the depth of a unit interface that is presented as metres below seafloor.
Isochron	Isochrons are grids that represent the vertical thickness of a layer or unit in Two-way travel time.
Kingdom	Seismic data interpretation software
Multi-Channel Seismic	A seismic survey system that typically uses one or many towed high-power sources to transmit low frequency acoustic signals into the sub-seafloor where its reflections are detected by receivers along a towed streamer. These systems can provide good penetration below seabed at high resolution.
Multibeam Echosounder	This sensor transmits an acoustic signal to the seafloor, time taken allows for Bathymetry (depth) to be calculated. The Backscatter (signal strength) measures reflectance and can give indications of seafloor texture and sediment grain size. Seafloor Slope can also be derived from the Bathymetry data.
Seismic Facies	Seismic facies can be defined as a group of seismic amplitude variations with characteristics that differ distinctly from those from other facies. Seismic facies is the manifestation of the underlying geologic facies or structural feature in the seismic-amplitude data.
Seismic/Seismostratigraphic Unit	A volume of sediments/rock with similar seismic facies.
Side scan Sonar	This is a towed sonar system that transmits an acoustic signal at an angle to the seafloor, perpendicular to the path of the sensor through the water. The reflected signal received by the system allows seafloor features and targets to be detected through variations in reflectance and acoustic shadows. Each section of data is layered and combined to form a side scan mosaic.
Single-Channel Seismic	A shallow seismic survey system that uses one towed high-power source to transmit relatively low frequency acoustic signals into the sub-seafloor where its reflections are detected by a single receiver.

Glossary of Terms	
Item	Description
	These systems can provide relatively good penetration below seafloor at relatively lower resolution.
Sub-Bottom Profiler	A shallow seismic survey system that typically uses a hull-mounted low-power source to transmit very high frequency acoustic signals into the sub-seafloor where its reflections are detected by a single receiver. Parametric systems, such as Innomar, are often employed to provide improved sub-seafloor resolution, footprint and penetration below seafloor.
Till	A sediment that is characteristically unsorted and unstratified and is not usually consolidated. Most Till consists predominantly of clay, silt, and sand, but with pebbles, cobbles, and boulders scattered through the Till.

EXECUTIVE SUMMARY

Gavin & Doherty Geosolutions Ltd (GDG) as part of the Venterra Group, was commissioned by Energinet to produce an Integrated 3D GeoModel (IGM) for the proposed Krieger's Flak II Southern Offshore Wind Farm (OWF) site as part of the Danish Offshore Wind 2030 project for the Danish government. This comprised the preparation of a Conceptual Geological Model, that formed the basis of the Integrated Geomodel (IGM) through the refinement and integration of newly acquired geophysical (GEOxyz, 2024), and geotechnical (Gardline, 2024) data. An independent interpretation of the geotechnical data was performed and then integrated with the refined seismic interpretation to constrain the model and tie-in interpreted seismic units with geotechnical unit top markers.

The recent geophysical and geotechnical surveys provide a variable coverage of the site per sensor type. Bathymetry, magnetometer, and side scan sonar datasets have full coverage (acquired at 62.5 m line spacing). The Sub-bottom profiler data have a high density across the site, spaced at approximately 60 m, whilst the ultra-high resolution seismic data were acquired at approximately 250 line spacing. Multiple geotechnical investigation methods were used across 18 locations, though only five locations had borehole samples recovered. These methods included composite boreholes, sampling boreholes, borehole CPTU's, seabed CPTU's, and seabed SCPT's. The varying line spacing and spread of investigation locations present limitations expected with this phase of investigation.

The bathymetry data shows that the site has a gentle seabed slope as the seabed elevation ranges from -18.5 m in the southwest to -41.9 m relative to mean sea level (MSL), at the eastern extents. Bedforms were not prominent at the site, though the seabed is heavily scarred from anthropogenic activity. Various seabed hazards were identified. These include but are not limited to boulders and debris, depressions (possible pock marks) and a potential wreck. Subsurface hazards include an unidentified cable crossing, magnetometer targets and glacial features such as deposits of till and evidence of potential subglacial channels within the late glacial/glaciolacustrine unit.

The IGM comprised four seismic units that consists of Holocene and Pleistocene deposits overlying Upper Cretaceous Chalk bedrock that are correlated with 12 geotechnical units. Seismic unit I consists of up to 2.8 m of surficial, marine sediments (seismic Unit I) overlying late glacial to glaciolacustrine sediments (seismic Unit III). Seismic unit II represents the post-glacial transition sediments and shares similar geotechnical properties with both geotechnical Unit Ib and IIIa1. A usable interpretation could not be made from its limited visibility within the seismic data and it was considered to have limited impact on design because the geotechnical properties are captured by the overlying and underlying geotechnical units.

Seismic Unit III was split into two sub-units based on the variable internal seismic facies. Seismic Unit IIIa (up to 8.4 m in thickness) overlies the lower glaciolacustrine seismic Unit IIIb, which reaches up to 51 m in thickness. This lower subunit is dominated by a variable lithology from a prograding sand wedge (of delta system origin during late-glacial ice lake periods) in the west of the site, to comprise clays and silts in the east with a more defined and layered facies. This variable lithology coupled with limited borehole locations presents a limitation in the velocity model and resultant depth conversion of the seismic data in the southwest of the

site. This seismic unit overlies the Upper Cretaceous chalk bedrock, which is split into seismic Units Va (unlithified) and Vb (lithified). The thickness of Unit Va cannot be constrained due to the unreliability of the Unit Vb top pick across the site because of poor visibility within the seismic data and a lack of supporting geotechnical marks to tie it in. For this iteration of IGM, only a top of Unit Va is provided, with the Unit Vb pick provided only to inform on its possible elevation. This horizon should not be used as a reliable source for the top of lithified chalk and should be constrained by future site investigations. Additionally, there is an associated uncertainty with the Unit IIIb and Unit Va interface in that till has been identified in the geotechnical data, though this could not be distinguished within the seismic facies. Recovered boreholes show gradual transitions between the interpreted till and unlithified chalk. This along with the seismic resolution may mean that an insignificant acoustic impedance difference and resolution limit the ability to clearly define a separate unit.

The acquisition, interpretation, and integration of the geophysical and geotechnical datasets has provided improved reliability of this second stage of the IGM though uncertainties remain, which without further investigation will present risks to future developments on the site. Repeated geophysical surveys are recommended to rule out temporal seabed changes, whilst optimised, site-specific seismic surveys with reduced line spacing will provide more certainty in the interpretation of the seismic units and reduce the need for large inline gridding extrapolation.

Geotechnical zonation was performed to represent broadly similar ground conditions laterally and vertical across the site. Soil provinces were defined following the sub-seafloor interpretation, seismic unitisation, geotechnical unitisation, integration of the available geophysical and geotechnical data.

Geotechnical units represent similar geotechnical properties e.g. clay or sand. Geotechnical unitisation was performed considering the seismo-stratigraphic unitisation, IGM and factual data. Unitised geotechnical parameter profiles were determined for the geotechnical units identified at the site. Geotechnical parameter bounding was performed using either statistical and/or engineering judgement.

1 INTRODUCTION

1.1 PURPOSE AND SCOPE OF WORK

Denmark intends to further expand its offshore wind energy along with associated infrastructure. The Danish government (Danish Energy Agency) has allocated new offshore wind farm sites, as shown in Figure 1-1. The government has directed Energinet (Client) to commence site characterisation activities in the form of geophysical and geotechnical site investigation campaigns, and subsequent data interpretation, integration and visualisation. This is done under the project name “Danish Offshore Wind 2030”.



Figure 1-1 - Danish Offshore Wind Farms (www.ens.dk)

Venterra were commissioned by Energinet (the Client) to undertake geophysical and geotechnical consultancy services with respect to site characterisation, and Integrated 3D GeoModel (IGM) development for the proposed Kriegers Flak II Northern and Southern OWF sites. This report details the IGM and the integration of geophysical and geotechnical datasets to refine the existing Preliminary Ground Model (PGM) (GEOxyz, 2024) developed by GEOxyz based on the most recent geophysical survey and geotechnical site investigation performed by GEOxyz (GEOxyz, 2024) and Gardline (2024).

1.2 LIMITATIONS AND EXCLUSIONS

This section will outline the limitations and exclusions associated with the IGM:

- A decision was made by the client to not proceed with interpreting some newly identified horizons. This is discussed in section 6.2 . If there is a future change to the known ground conditions and geological model, this is not the liability of Venterra.

- The supplied data (geophysical) was provided with several processing artefacts (for example, tide reduction, signal processing, depth conversion) that each impacted the work performed as part of this IGM. Every effort has been made to produce this IGM to the highest standard, though some of these artefacts create remaining uncertainties within the model. Venterra are not liable for the resultant model uncertainties based on the input data. Where processes were impacted, these have been discussed in their relevant report section.
- The associated uncertainties in the model are presented in greater detail in section 6.5.
- Unexploded Ordnance (UXO) is not included within the scope of work for this IGM and UXO related risks or recommendations have not been provided.

1.3 GEODETIC INFORMATION

The project geodetic and projection parameters are summarised in Table 1-1 below:

Table 1-1 - Geodetic parameters

Geodetic parameters	
Parameter	Value
Projection:	ETRS89 / UTM zone 33N
Projection Type:	European Terrestrial Reference System 1989 ensemble
Central Meridian:	15
Latitude of Origin:	0
False Easting:	500,000
False Northing:	0
Scale Factor:	0.9996
Unit:	m
EPSG:	25833

1.4 VERTICAL DATUM

The vertical datum is Mean Sea Level (MSL). All elevations referenced in the text relate to MSL if not otherwise specified.

1.5 SUMMARY OF PREVIOUS STUDIES AND SITE-SPECIFIC REPORTS

In 2022, the Geological Survey of Denmark and Greenland (GEUS) was commissioned by the Danish Energy Agency to undertake a geological screening study for both the proposed Kriegers Flak II Northern and Southern OWF sites (GEUS, 2022). The study aimed to inform on site conditions for future investigations via the production of a conceptual geological model for the respective sites, based on available data at the time.

In 2023, GEUS produced an additional desk study report for the seabed geological conditions for the proposed Kriegers Flak II Northern and Southern OWF sites as well the proposed cable routes, at the request of Energinet (GEUS, 2023). This study built upon the work of the existing report (GEUS, 2022) by integrating geological conditions for the proposed cable route.

In 2023, Energinet commissioned GeoXYZ to perform a hydrographic and geophysical site investigation (GEOxyz, 2024), the findings of which are outlined in section 4.1. The resulting

PGM outlined an early-stage geological model for the site and was unconstrained by geotechnical data inputs.

In 2023, Gardline performed a geotechnical data acquisition survey that included laboratory testing (Gardline, 2024), the results of which are outlined in section 4.2 and 5.2. The aim of this investigation was to understand the site ground conditions and to be integrated with the available geophysical datasets for the IGM.

2 THE SITE

The proposed Krieger's Flak II Southern OWF site is in the Danish sector of the southwest Baltic Sea, east of the Fakse Bay and Møn Island (Figure 2-1), in water depths ranging between 15 and 45 m MSL. The areal extent of the site is 76 km². The site is approximately 23.3 km at its maximum length, from the southwest corner to the eastern corner, and approximately 6.5 km at its maximum width, from the northern most point to the southern boundary.

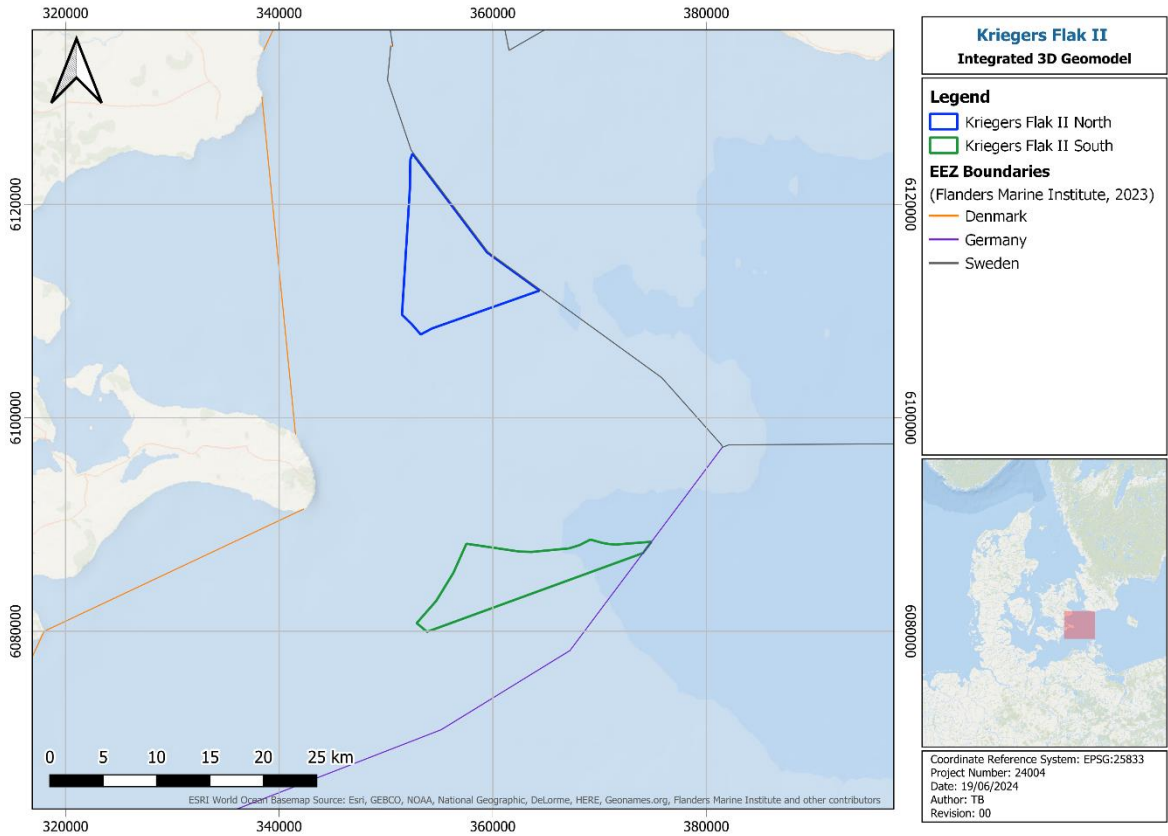


Figure 2-1 – The proposed Kriegers Flak II Southern site overview (Flanders Marine Institute, 2023)

3 METHOD DESCRIPTION AND DELIVERABLES

This IGM consists of an update of the existing PGM carried out by GEOxyz in 2023 (GEOxyz, 2024), and relies on the recently acquired project-specific hydrographic and geophysical data from their Site Investigation and its interpretation, and also inclusion of the results from the geotechnical campaign performed by Gardline (Gardline, 2024). The IGM aims to inform the understanding of the geology, geotechnical properties, and potential geohazards found/expected in the proposed Kriegers Flak II Southern OWF site.

An interpretation of the seafloor lithology, seafloor features, seafloor targets, seismic units and targets were provided by the contractor (GEOxyz, 2024). As part of the IGM development, Venterra focused on the following:

- Revising and updating the seafloor assessment. This Included a review of Multi Beam Echo Sounder (MBES) bathymetry and Side Scan Sonar (SSS) data for seafloor morphology, seafloor hazards and obstructions. Additional information on how seafloor features were identified and classified can be found in sections 6.1.1 to 6.1.6
- Updating the seafloor sediment classification to standard typology using MBES, SSS, and backscatter datasets, and available seafloor sampling data from Van Veen and Hamon grab samples (including new geotechnical data). Section 6.1.3 provides more detail into how different datasets were used to reassess the seafloor lithology distribution.
- Reviewing seismic units, attributed to geological units, through revision and reinterpretation of seismic data and building on the work of the PGM. The revision of the seismic interpretation followed the principles highlighted in section 5.1, item 2. Details on how individual units and additional sub-seafloor features were characterized and separated are found in section 0. A full description of the methodology employed to generate depth converted grids from the interpreted horizons is presented in section 5.5.
- Reviewing geotechnical units interpreted from the geotechnical data, and correlating them with geological units interpreted from geophysical data. An overview of how the geotechnical data were integrated with the IGM can be found in section 5.3.
- Investigating and applying potential improvements to the velocity model and depth conversion of seismic data, including utilisation of geotechnical velocity data where possible. An overview of the methodology employed for the velocity modelling is found in section 5.4.
- Delineating and discussing areas of uncertainty.
- Identifying any observed and potential hazards and geohazards that may present risk to the development and longevity of the OWF and need to be taken into consideration during the design, construction, operational and decommissioning stages.

A risk register for the site was generated and is provided in Appendix D. The identified risks are discussed and graded by likelihood of occurrence and severity (pre-mitigation) based on

the criteria defined in section 9 and an overall risk level has been determined from the risk matrix presented in the same section.

The seismic interpretation and geotechnical integration were carried out in Kingdom suite (SQL version 2019, Kingdom version 2022) and are provided in a master copy of the software (TKS format).

In addition to the above, the IGM digital data were collated in a GIS package with associated metadata and as a 3D GIS model (HTML format) to allow ease of distribution and visualisation of results.

4 GEOLOGICAL BACKGROUND AND PREVIOUS STUDIES

4.1 PRELIMINARY GROUND MODEL (GEOXYZ, 2024)

A PGM was produced by GeoXYZ following their geophysical campaign for both the proposed Kriegers Flak II Northern and Southern OWF sites. A Schematic diagram and summary of their preliminary geological units is presented below. For further details, please refer to the full report (GEOxyz, 2024).

GEOxyz’s geological schematic (Figure 4-1) illustrates their interpretation of the arrangement of units within the southern site. A detailed summary is provided in Table 4-1. The key surfaces identified are: the top of Unit III (H20/H05/seabed) which GEOxyz describe as being the top of potentially over consolidated deposits, and H20/H30, the top of the bedrock.

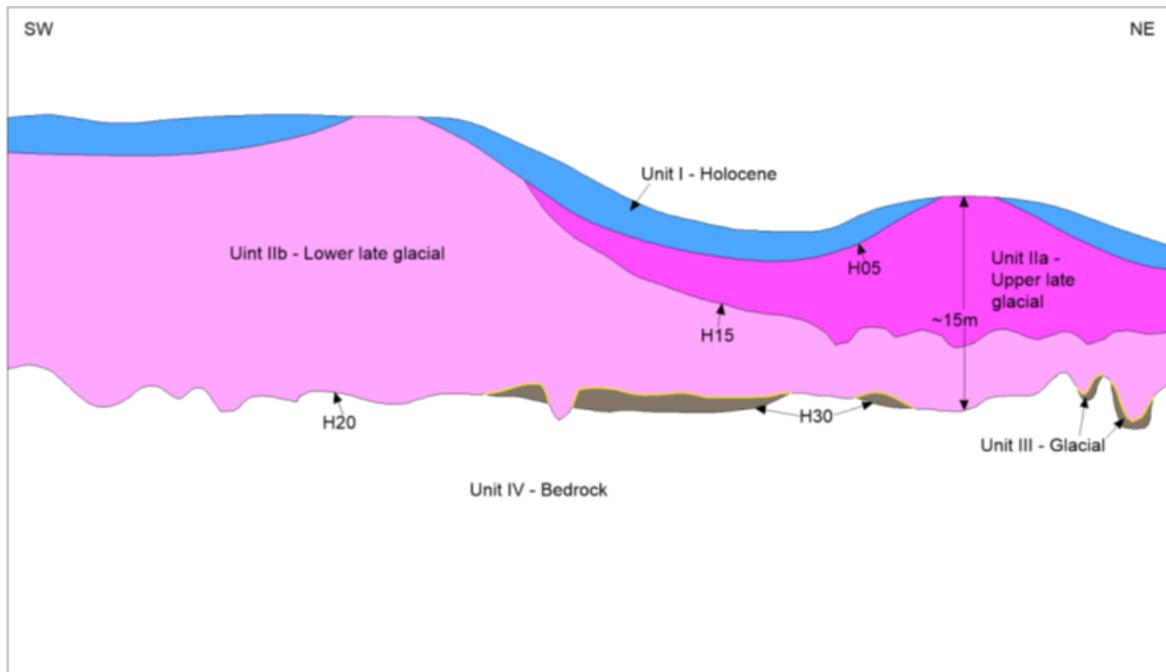


Figure 4-1 - Geological, schematic, general arrangement of the units (GEOxyz, 2024)

Table 4-1 - Shallow geological units (GEOxyz, 2024)

Shallow geological units				
Unit	Upper Surface	Lower Surface	Main Soil Description	Depositional Environment
I, H, Holocene	Seabed	H05	Silty, sandy CLAY with thin veneer of SAND at seabed	Post-glacial marine
II, LG, Late Glacial	Seabed/H05	H20	Variable, includes intervals of laminated CLAY, SAND-prone packages	Glaciolacustrine
III, GL, Glacial	H05/H15	H30	Variable, CLAY-prone, locally over consolidated	Glacial with localised direct ice contact, sandier outwash intervals
IV, BR, Bedrock	H20/H30	-	Chalk	Ancient shallow marine

4.2 GEOTECHNICAL SITE INVESTIGATION (GARDLINE, 2024)

An offshore Geotechnical Investigation (GI) campaign was performed by Gardline using the MV Kommandor Susan between 7 April and 27 August 2023, comprising:

Kriegers Flak II North

- 28 seabed Cone Penetration Tests with pore pressure measurements (CPTU), including bump-over locations;
- 12 CPTU boreholes;
- 6 Combined CPTU/sample boreholes;
- 2 P-S logging boreholes;
- Offshore geotechnical laboratory classification and strength testing.

Kriegers Flak II South

- 19 seabed CPTU's including bump-over locations;
- 2 seabed Seismic Cone Penetration Tests (SCPT);
- 18 CPTU boreholes;
- 5 Combined CPTU/sample boreholes;
- 2 P-S logging boreholes;
- Offshore geotechnical laboratory classification and strength testing.

Retrieved samples were preserved and transported to an onshore geotechnical laboratory for classification, strength and stiffness testing. The onshore laboratory test results were not available at the time of report submission. Please refer to the final factual results report for further details (Gardline, 2024).

4.3 REGIONAL GEOLOGICAL BACKGROUND

4.3.1 REGIONAL GEOLOGICAL HISTORY

4.3.1.1 PRE-QUATERNARY

The sites are located on the western margin of the Arkona Basin in the SW Baltic Sea, on the West European Platform. The latter is separated from the Fennoscandian/Baltic Shield and the East European Platform by the WNW-ESE Sorgenfrei-Tornquist Zone (part of the larger Tornquist Zone), a Palaeozoic lineament. Besides this regional structure to the north of the Arkona Basin, the sites lie east of the Norwegian-Danish Basin and the Ringkøbing-Fyn High, and west of the Bornholm Basin (Figure 4-2).

The movement along Sorgenfrei-Tornquist Zone evolved from dextral strike-slip to extension throughout its stages of reactivation during the Triassic, Jurassic, and Early Cretaceous, culminating with Late Cretaceous to Early Paleogene inversion related to the Alpine compression (Erlström & Sivhed, 2001; Mogensen & Korstgård, 2003; Graversen, 2004; 2009). Graversen (2004) also mentions an earlier episode of inversion affecting the region during the Jurassic – Early Cretaceous. The whole region is affected by faults either following

the WNW-ESE trend of this lineament, or in NW-SE and NE-SW directions (Figure 4-2). The local area, within and in the vicinity of the sites, is predominantly affected by NW-SE and NE-SW faults, as shown in Figure 4-3, Figure 4-4, and Figure 4-5 (EMODnet, 2024; GEUS, 2024).

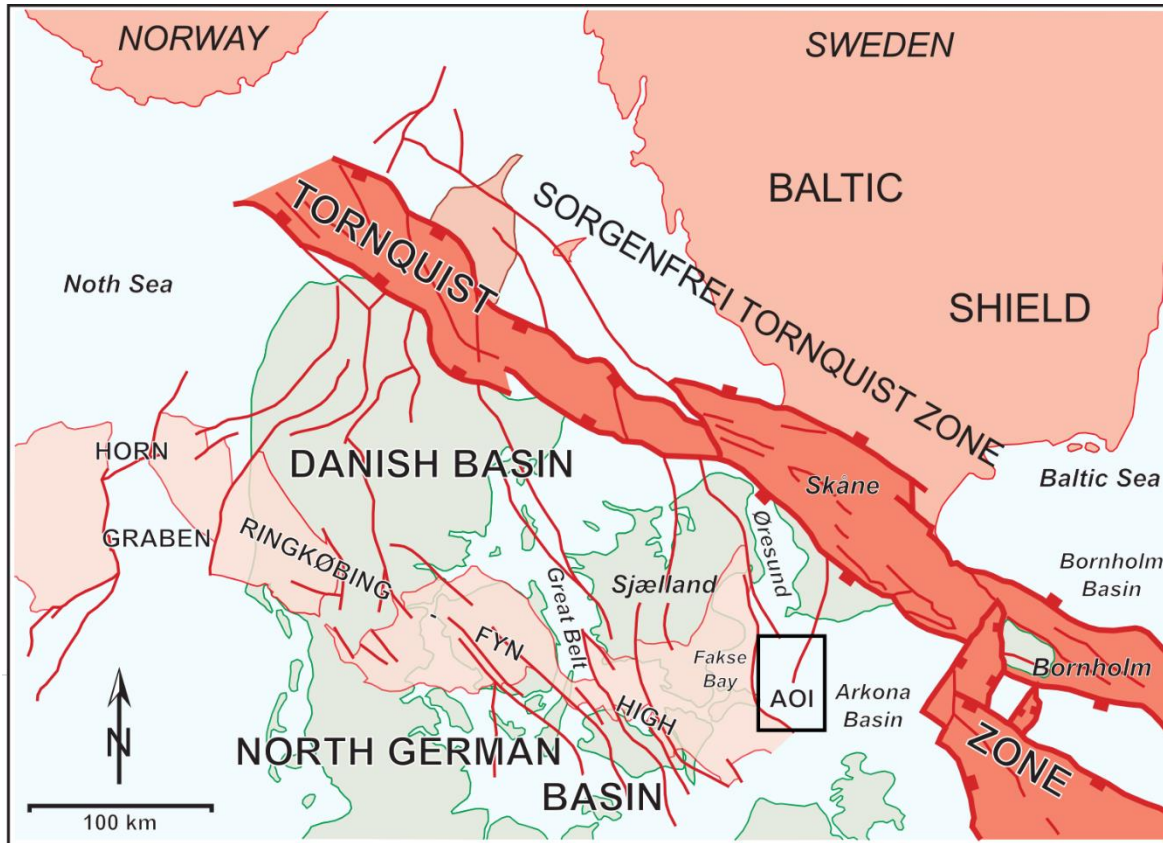


Figure 4-2 - Regional setting, modified from Graversen (2009). AOI – Area of Interest

In terms of stratigraphy, the basin area consists of Palaeozoic to Cenozoic rocks overlying Precambrian basement (Rosentau, et al., 2017). The Mesozoic to Cenozoic sedimentary infill is varied across the region, thinning from up to 10.0 km in the Norwegian-Danish Basin depocenter to less than 3.0 km along the Ringkøbing-Fyn High and within the Arkona Basin (Vejbæk & Britze, 1984; GEUS, 2024).

The lithologies expected to subcrop in the area of interest are Upper Cretaceous carbonates from the Chalk Group and Paleogene (Danian) limestone (Rosentau, et al., 2017; GEUS, 2022; 2023; 2024). The Upper Cretaceous subcrops in the entirety of the southern site. The extent of the Upper Cretaceous and Paleocene in the northern site differs between the map sources. According to the EMODnet (2024) map, the Chalk Group covers more than half of the northern site (Figure 4-4). However, from the GEUS (2024) map, the Upper Cretaceous deposits are confined to the very south-western corner of the northern site (Figure 4-5).

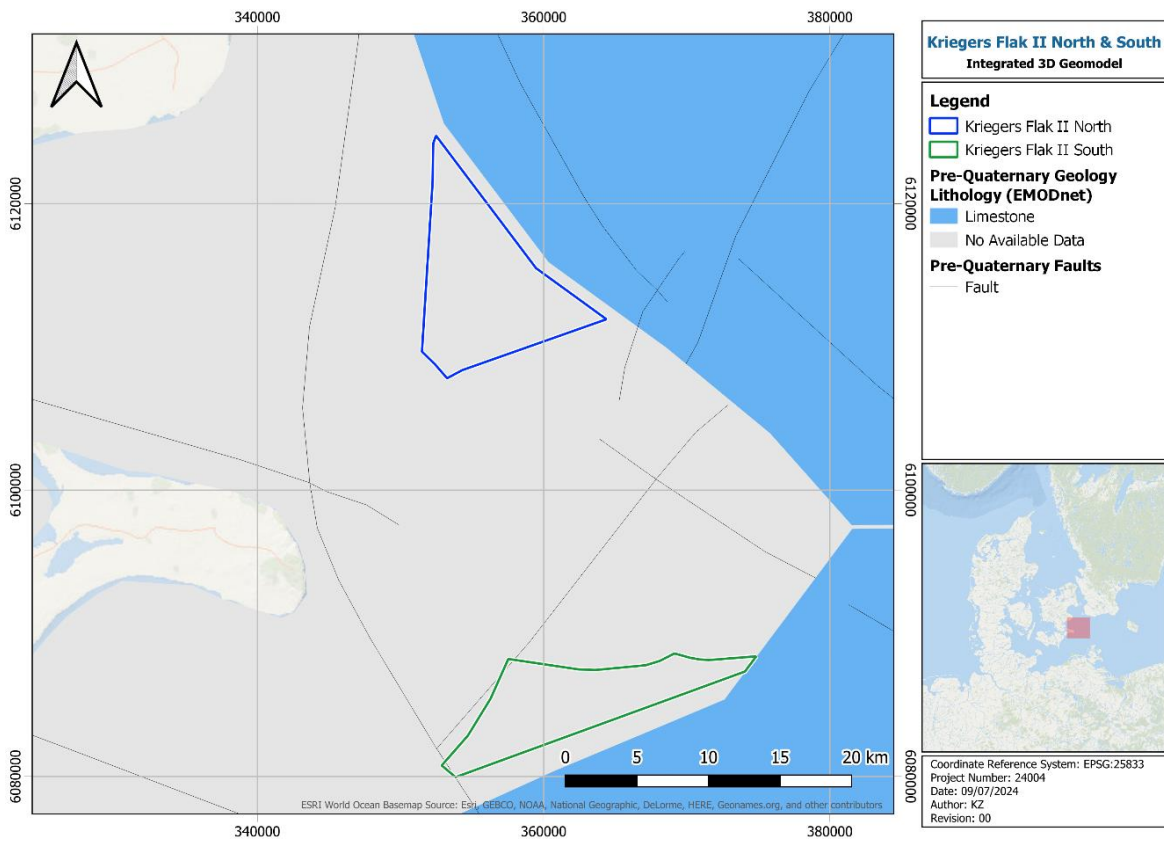


Figure 4-3 - Pre-Quaternary deposits (lithology) and faults (EMODnet, 2024)

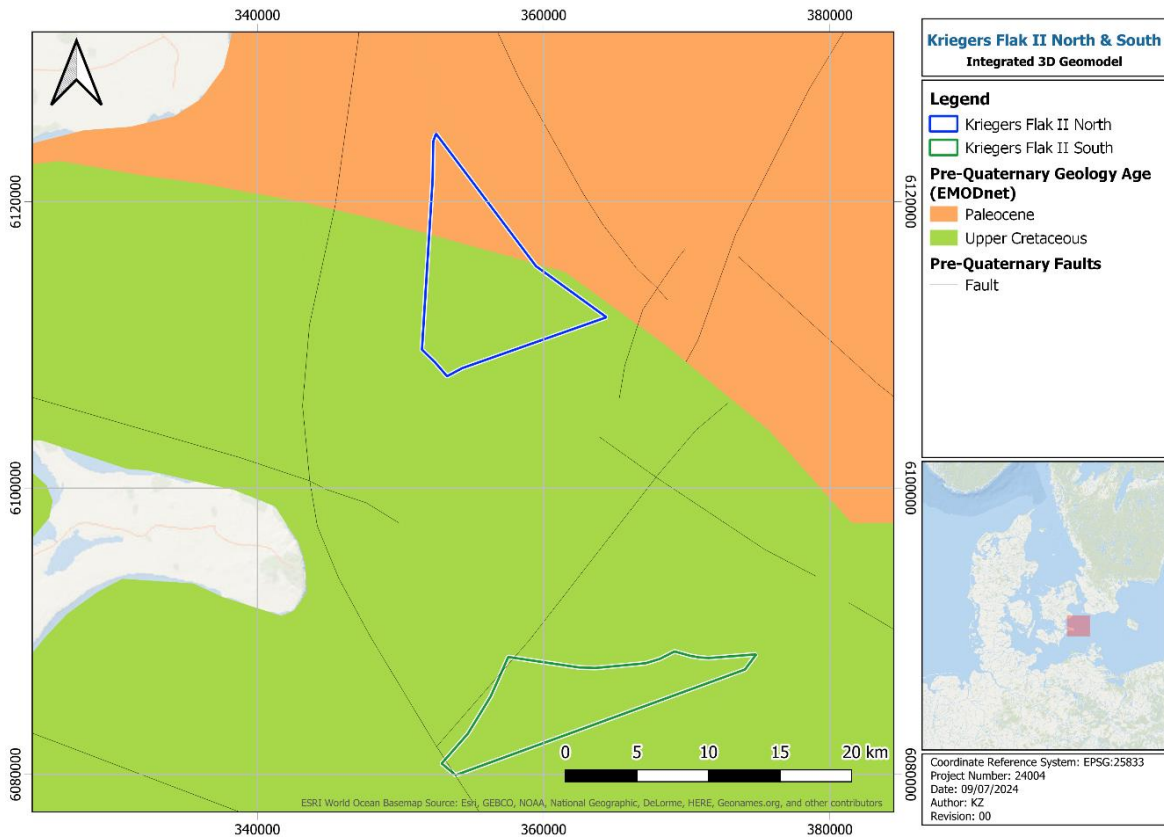


Figure 4-4 - Pre-Quaternary deposits (age) and faults (EMODnet, 2024)

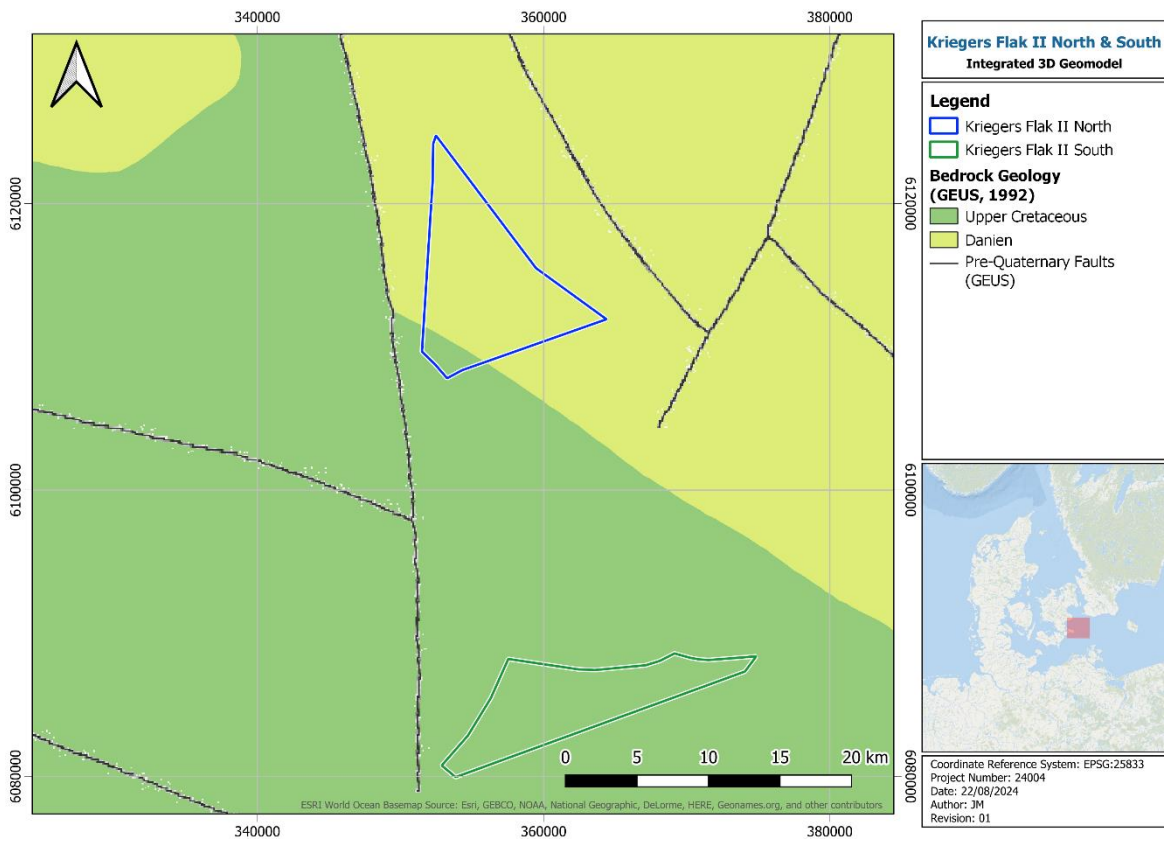


Figure 4-5 - Pre-Quaternary deposits (age) and faults (DGU, 1992; GEUS, 2024)

A map with the elevation of the top of the pre-Quaternary deposits has been generated by Binzer et al. (1994) and made available by GEUS (2024). Although this does not cover the full extent of the Arkona Basin, it can still be used to infer expected elevations. In the eastern part of the Arkona Basin the top of the pre-Quaternary was documented between -25.0 and -75.0 m relative to sea level), whereas in the west it is expected to shallow to between 0.0 and -50.0 m (Figure 4-6).

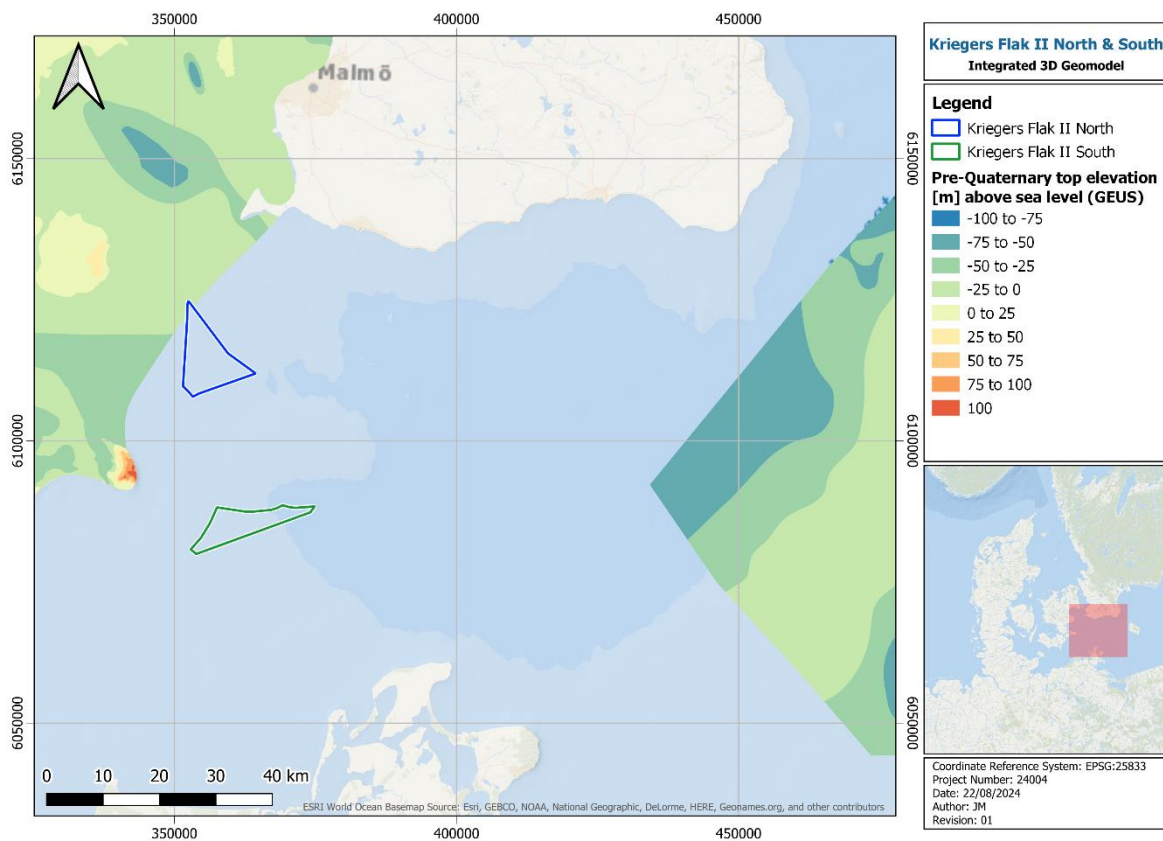


Figure 4-6 - Top pre-Quaternary surface elevation (Binzer, et al., 1994; GEUS, 2024)

4.3.1.2 QUATERNARY

The Cretaceous and Paleogene strata at each site are overlain by Quaternary deposits. These deposits show marked variability related to the palaeogeographic evolution registered by the Baltic Basin throughout this period. During the Saalian and Weichselian, the Baltic Sea region was affected by four glaciation events with the latest seeing the maximum extent of the Scandinavian Ice Sheet occurring at 22 ka before present (BP); (Figure 4-7). As the ice retreated, the Baltic Basin underwent a series of paleogeographic changes, documented in literature as the Baltic Ice Lake, Yoldia, Ancylus, and Littorina stages, during which the region alternated between the deposition of (glacio)lacustrine and transitional to marine sediments.

As the ice margin retreated from Zealand (Sjælland) through the Øresund and to the central part of Skåne and west of Bornholm at around 15 ka BP, the Baltic Ice Lake developed in front of the ice sheet, communicating with the Kattegat region through the Great Belt (Figure 4-8). The lake had several stages of damming documented, separated by regression events (Jensen, et al., 2002). The last stage of the Baltic Ice Lake occurred at around 12 k BP, had several minor channels draining it through the Great Belt and the Øresund (Figure 4-8), and was separated from the sea in central Sweden by a land bridge (Jensen, et al., 2002; Expedition 347 Scientists, 2014). Shortly after this, a connection was established between the lake and the ocean at 11.5 – 11.7 ka BP, through central Sweden, resulting in the formation of the Yoldia Sea (Figure 4-9). This stage of the Baltic Basin was short-lived as continued uplift of south-central Sweden due to ice unloading interrupted the ocean connection and led to the formation of the Ancylus Lake at around 10.2 ka BP (Figure 4-9). Continued sea level rise led

to the Littorina transgression and the formation of the Littorina Sea (Figure 4-9) at 8-7 ka BP (Emeis, et al., 2002; Jensen, et al., 2002; Expedition 347 Scientists, 2014).

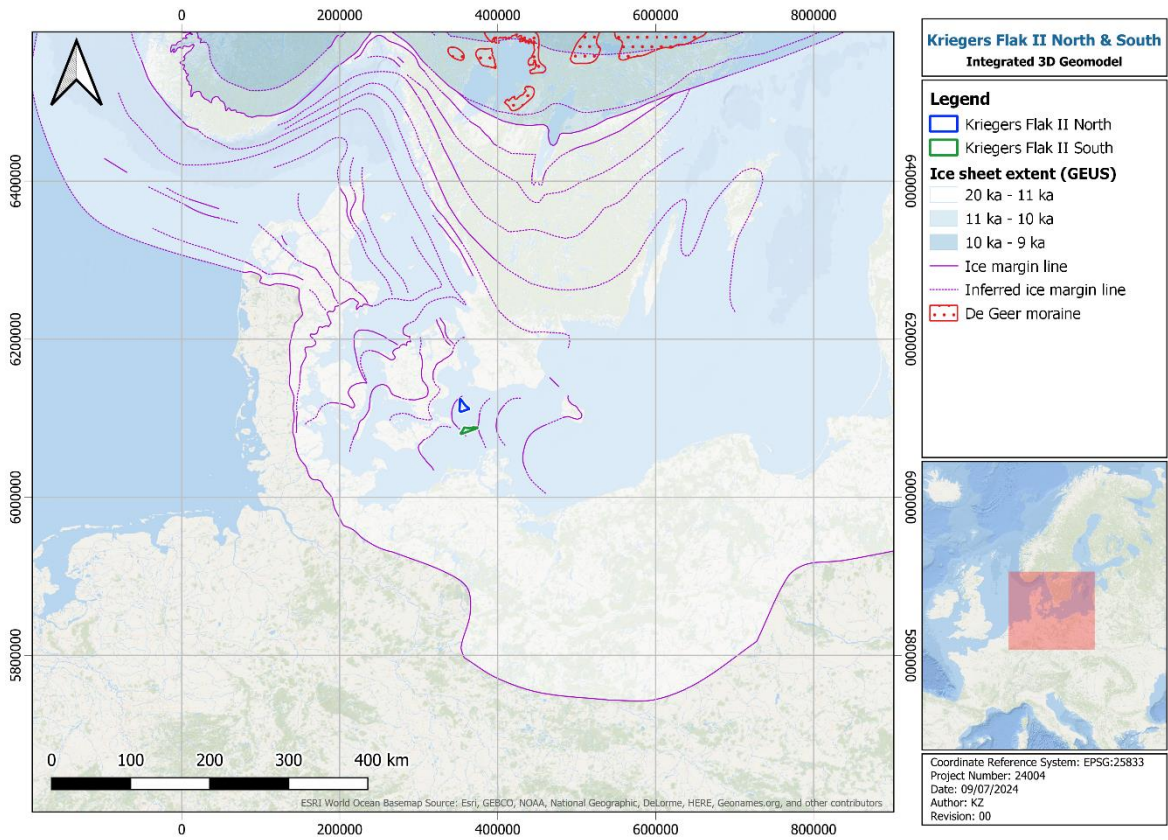


Figure 4-7 - Ice margin evolution (Pedersen, 1998; GEUS, 2024)

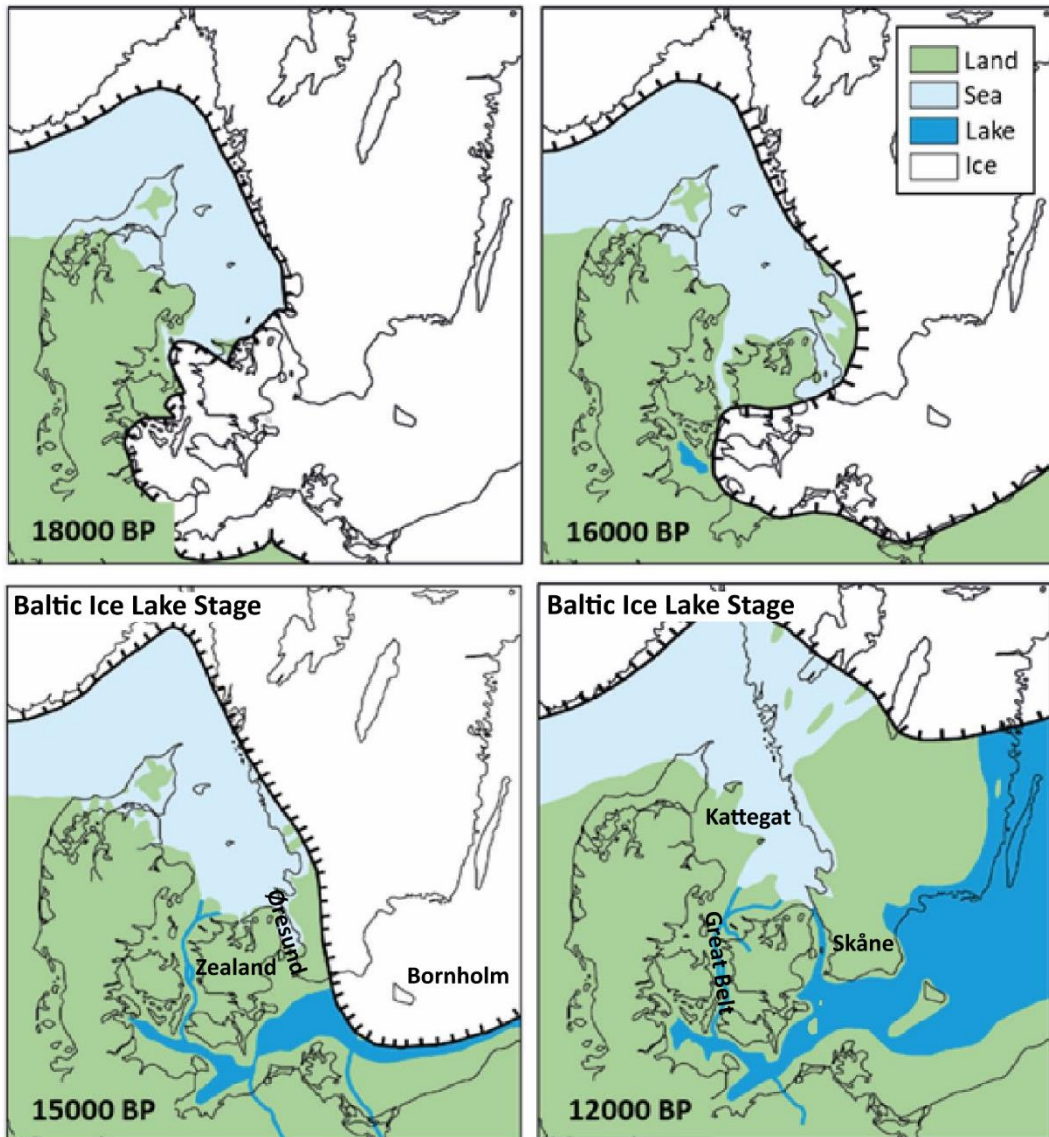


Figure 4-8 - Danish region palaeogeography from 18 to 12 ka BP; modified from GEUS (2022; 2023)

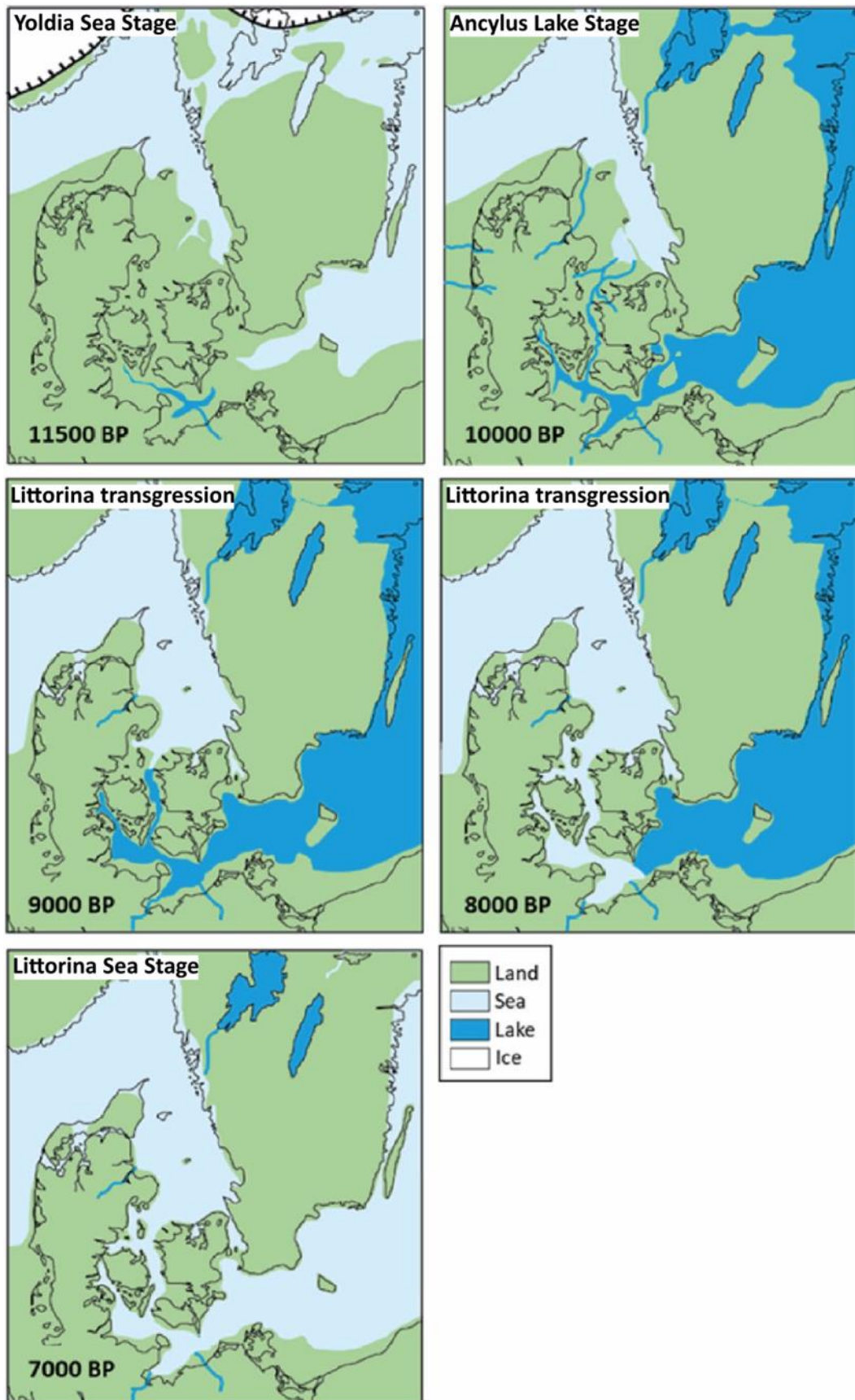


Figure 4-9 - Danish region palaeogeography from 11.5 to 7 ka BP; modified from GEUS (2022; 2023)

The nature and distribution of the Quaternary sediments deposited throughout these stages across the SW Baltic Sea have been documented by several studies. The Arkona and the Bornholm basins have a similar reported stratigraphy (Table 4-2) consisting of tills overlain by varved and/or homogeneous clays and silty clays (Jensen, et al., 2017; GEUS, 2022). Local variations are observed in the Fakse Bay (Table 4-2) where the deglaciation was accompanied by the deposition of lagoon and coastal/barrier clay, silt, sand, gravel, and peat, and south of Møn, where late glacial coastal beach barrier sandy deposits that display progradational geometries from west to east, were documented (Jensen & Nielsen, 1998; GEUS, 2022; 2023). Within the northern site, documented Quaternary shallow sediments include Holocene sand and mud across most of the site and Weichselian sand in the west (EMODnet, 2024), as shown in Figure 4-10 and Figure 4-11. Within the southern site, Holocene sand is reported across most of the site, with sand and mud present in the east (EMODnet, 2024).

Based on the top pre-Quaternary map (Binzer, et al., 1994) and current bathymetry of the area, the thickness of the Quaternary deposits are expected to vary between a few metres to 40.0 m in the Fakse Bay, up to 30.0 m in the eastern part of the Arkona Basin, and between a few metres and 60.0 m in the Bornholm Basin. In addition to this, the maps of Lemke (1998) presented in the reports of GEUS (2022; 2023) provide additional information on the thickness of Quaternary deposits and/or depths to intra-Quaternary interfaces within the Arkona Basin. Based on their analysis, the top of the till reaches 65.0 m below sea level in the central part of the basin, shallowing to 45.0 m in the southern site and to 25.0 m further north (their maps do not cover the northern site). Late glacial clays have documented thicknesses of up to 12.0 m in the central part of the basin, shallowing to 4.0 m or less towards the two sites, while proximal sandy coastal deposits are interpreted on the western margin of the basin with an estimated thickness of 30.0 m, as reported by GEUS (2022; 2023). Holocene muds have interpreted thicknesses of up to 12.0 m in the central part of the basin, shallowing to less than 3.0 m in the vicinity of the two sites.

Table 4-2 - Regional Quaternary stratigraphy and seismic facies

Regional Quaternary stratigraphy and seismic facies											
Baltic Basin Stage	Environment	Bornholm Basin (Jensen, et al., 2017; GEUS, 2022)				Arkona Basin (Moros, et al., 2002; Mathys, et al., 2005)				Fakse Bay (Jensen & Nielsen, 1998; GEUS, 2022)	
		Unit	Member	Lithology	Seismic Facies	Unit	Unit	Lithology	Seismic Facies	Local Environment	Lithology
Littorina Sea	Post-glacial marine	I	a	organic rich CLAY	low amplitude, concave and onlapping parallel reflections	F	VI	greenish silty MUD	high amplitude reflection with onlapping geometries	coastal	SAND and GRAVEL
			b								
			c								
Ancylus Lake	Post-glacial transition	II	a	laminated CLAY	close spaced parallel reflection with decreasing amplitude upwards, strong upper reflection	E	V	silty grey CLAY	high amplitude reflection with onlapping geometries	lagoon and coastal /barrier	PEAT +/- SILT and CLAY; SAND and GRAVEL
D											
Yoldia Stage			b			homogenous CLAY					
B											
Baltic Ice Lake II	Glacio-lacustrine	III	a	rhythmic CLAY	parallel internals	All	III	red-brownish varved CLAY with dropstones	sub-parallel reflection with high amplitudes; transparent to chaotic	lagoon and coastal /barrier	SILT and CLAY; SAND and GRAVEL
Baltic Ice Lake I			b	homogenous CLAY	homogenous						
			c	rhythmic CLAY	parallel internals	AI					

Regional Quaternary stratigraphy and seismic facies											
Baltic Basin Stage	Environment	Bornholm Basin (Jensen, et al., 2017; GEUS, 2022)				Arkona Basin (Moros, et al., 2002; Mathys, et al., 2005)				Fakse Bay (Jensen & Nielsen, 1998; GEUS, 2022)	
		Unit	Member	Lithology	Seismic Facies	Unit	Unit	Lithology	Seismic Facies	Local Environment	Lithology
									in the north and east		
-	Glacial	IV	a	SAND (outwash deposits)	high amplitude upper reflection (unconformity), internally chaotic	-	II	DIAMICTON	sub-parallel low amplitude reflections	-	-
			b	DIAMICTON (till)							
-	<i>Sedimentary bedrock</i>	V		LIMESTONE and calcareous SHALE	-	-	I	-	-	-	-

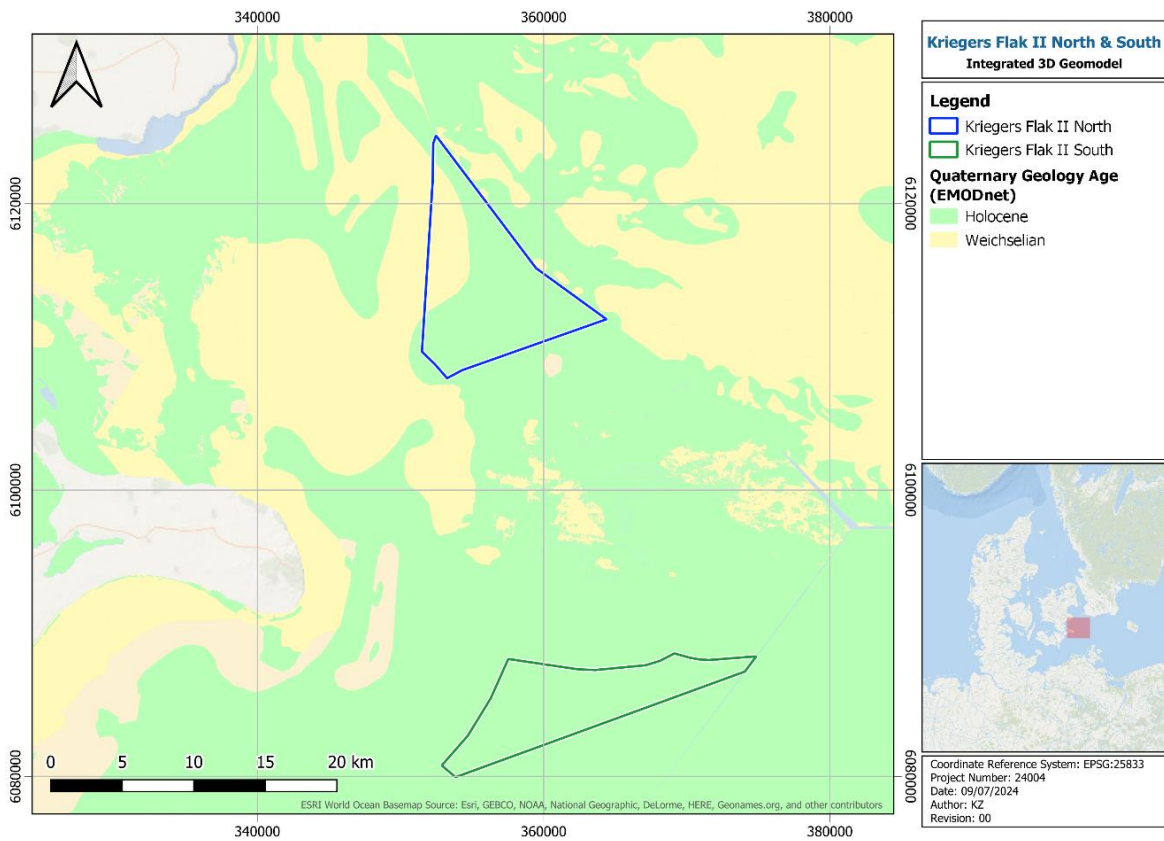


Figure 4-10 - Quaternary deposits age (EMODnet, 2024)

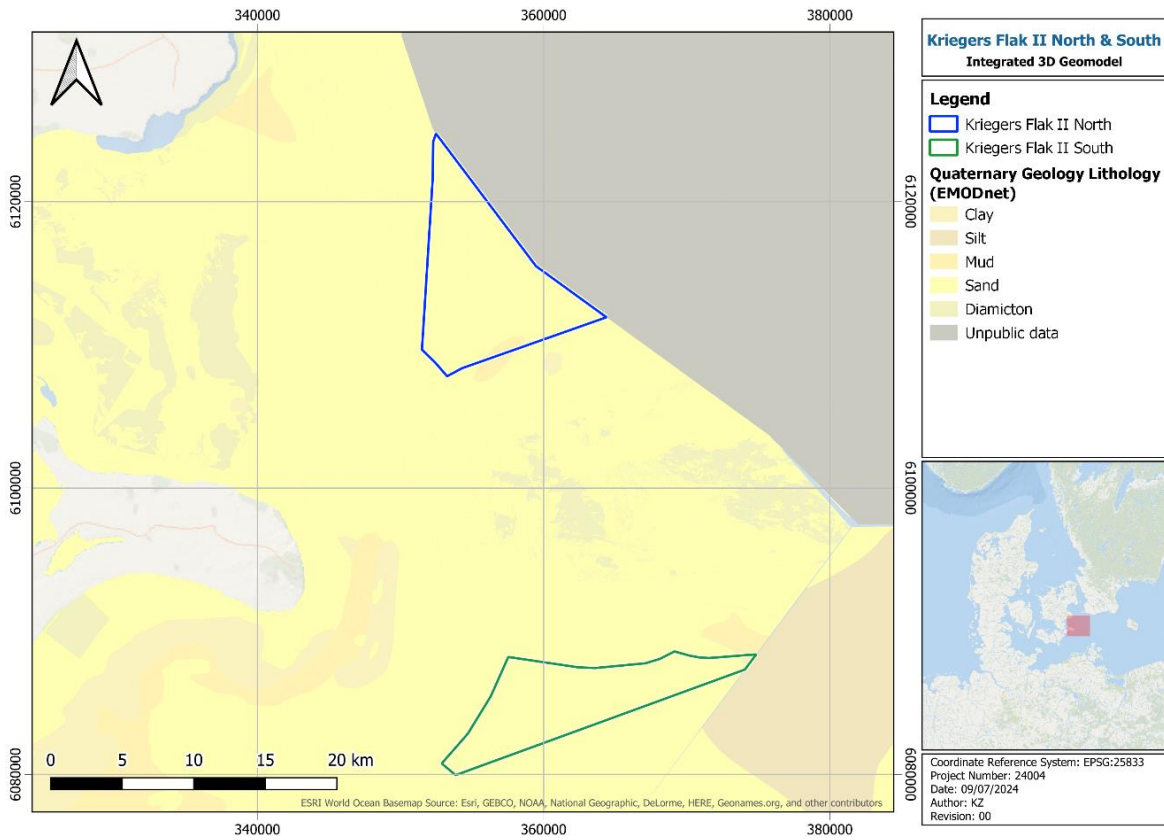


Figure 4-11 - Quaternary deposits lithology (EMODnet, 2024)

4.3.2 EXPECTED SEABED SEDIMENTS

The seabed sediments expected within the southern site have been extracted from EMODnet (2024) Folk 7 classification data (Figure 4-12). These show predominantly sand, with muddy sand in the eastern part of the site and mud documented only in the eastern corner (Figure 4-12). A similar seabed sediment distribution is reported by GEUS (2024). However, the area classified as mixed sediment by EMODnet is documented as diamicton (till) by GEUS.

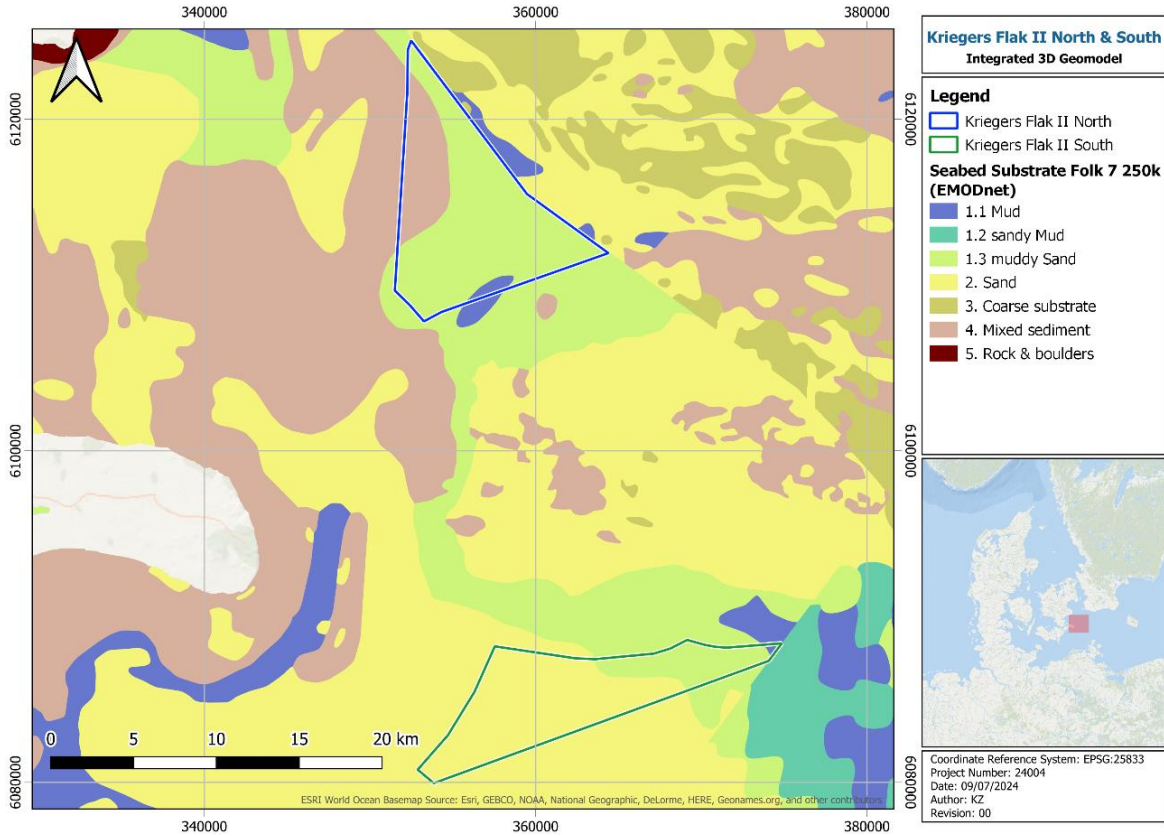


Figure 4-12 - Seabed sediments – Folk 7 (EMODnet, 2024)

4.4 CONCEPTUAL GEOLOGICAL MODEL

A conceptual geological model is presented for the site in Table 4-3 and Figure 4-13. The model consists of three seismic units (I, III, and V), with units III and V sub-divided into IIIa, IIIB, and Va and V5, respectively. Unit I consists of Holocene marine sands and clays, overlying a more variable Unit III. Unit III is of late glacial/glaciolacustrine origin, composed of low strength clays and silty sands and has been subdivided based on the variable seismic facies observed (discussed in more detail in sections 6.2.2 and 6.2.3). Underlying unit III is Unit V, consisting of unlithified chalk (Dm/Dc, Unit Va) and lithified chalk (A1-B4, Unit Vb), of Upper Cretaceous origin.

Figure 4-13 illustrates the typical vertical stratigraphy of the units identified and their associated internal seismic facies. Section 6.2 and section 7 provide further detail on the seismic unitisation, geotechnical data integration and the variability of these units across the site as well as the associated geotechnical parameters.

Table 4-3 - Conceptual Geological Model Summary

Conceptual Geological Model				
Seismic Unit	Geotechnical Unit	Age	Geotechnical Description	Depositional Environment
Unit I (SU I)	Ia	Holocene	loose to medium dense SAND	Marine
	Ib		Very low to low strength CLAY	
Unit IIIa (SU IIIa)	IIIa1	Pleistocene (Weichselian)	Medium to high plasticity, very low to low strength CLAY	Late glacial/ glaciolacustrine
	IIIa2		Dense to very dense silty SAND	
Unit IIIb (SU IIIb)	IIIb1	Pleistocene (Weichselian)	Silty to very silty, slightly sandy, medium to high plasticity, very low to low strength, CLAY	Late glacial/ glaciolacustrine
	IIIb2		Very dense, sorted to well sorted, micaceous, slightly calcareous fine to medium, SAND with trace to rare organic matter	
	IIIb3		Medium dense to dense silty SAND with closely to widely spaced thin beds of clay	

Conceptual Geological Model				
Seismic Unit	Geotechnical Unit	Age	Geotechnical Description	Depositional Environment
	IIIb4		Slightly to very sandy, medium to high slightly clayey to clayey SILT/ Interbedded sandy CLAY	
	IIIb5		sandy, slightly gravelly, medium to extremely high strength CLAY	
	IIIb6		CLAY TILL, very silty, very sandy, slightly gravelly, low plasticity, micaceous, highly calcareous (Very high to extremely high strength), sand is fine to medium, gravel is fine, of mixed lithology	
Subunit Va (SU Va)	Va	Upper Cretaceous	CHALK (Dm/Dc), unlithified (H1), very light grey to white (N8-N9), highly calcareous, with fine to medium gravel sized fragments of chalk (A1), slightly indurated (H2), white (N9), highly calcareous	Marine (sedimentary bedrock)
Subunit Vb (SU Vb)	Vb	Upper Cretaceous	CHALK (A1-B4), slightly indurated (H2), slightly fractured (S2), white (N9), highly calcareous (Very weak), interbedded with thin laminations to very thin beds of marl, medium grey (N5), highly calcareous and with rare medium gravel to stone sized fragments of chert, very strongly indurated (H5), dark grey to black (N3-N1), non-calcareous (Very strong to extremely strong)	Marine (sedimentary bedrock)

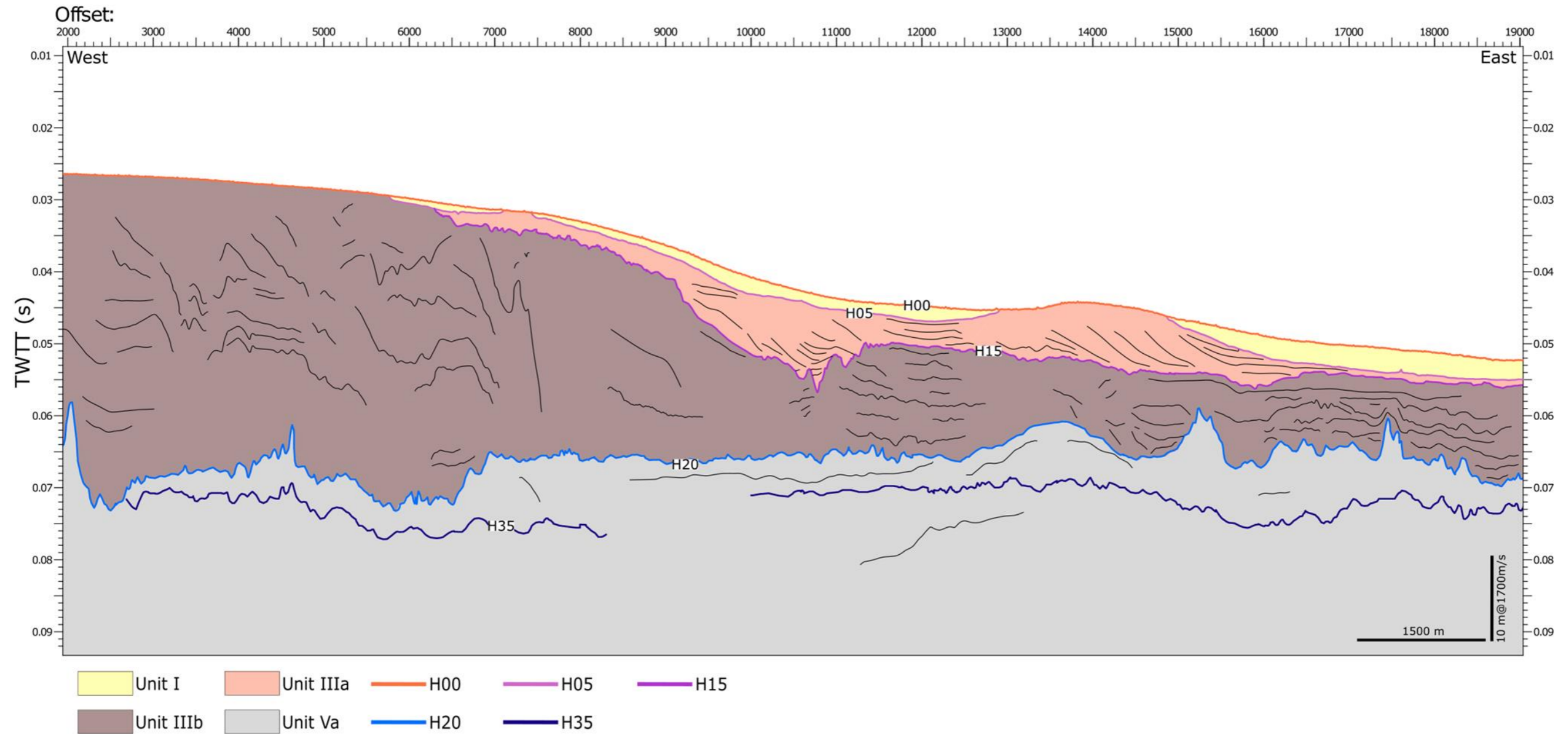


Figure 4-13 - Conceptual Geological Model

5 INTEGRATED 3D GEOMODEL DEVELOPMENT

This section comprises a summary of the main steps undertaken to develop the IGM. These included a revision of the provided geophysical survey interpretation, a review of the acquired geotechnical data and their integration in the IGM, a review of the velocity model, and an overview of how the final grids were generated and depth converted.

Seafloor lithology, seafloor contacts, and seismic unit grids have been revised from the interpretation originally provided by the contractor (GEOxyz, 2024). The revision of the seismic interpretation, presented as elevation and thickness grids in sections 6.2.1 to 6.2.5, included changes in the extent of individual seismic units, picked TWTT of the base or top horizon, and/or changes in the depth distribution following depth conversion. Magnetic targets and buried contacts have remained as per the original contractor delivery (GEOxyz, 2024).

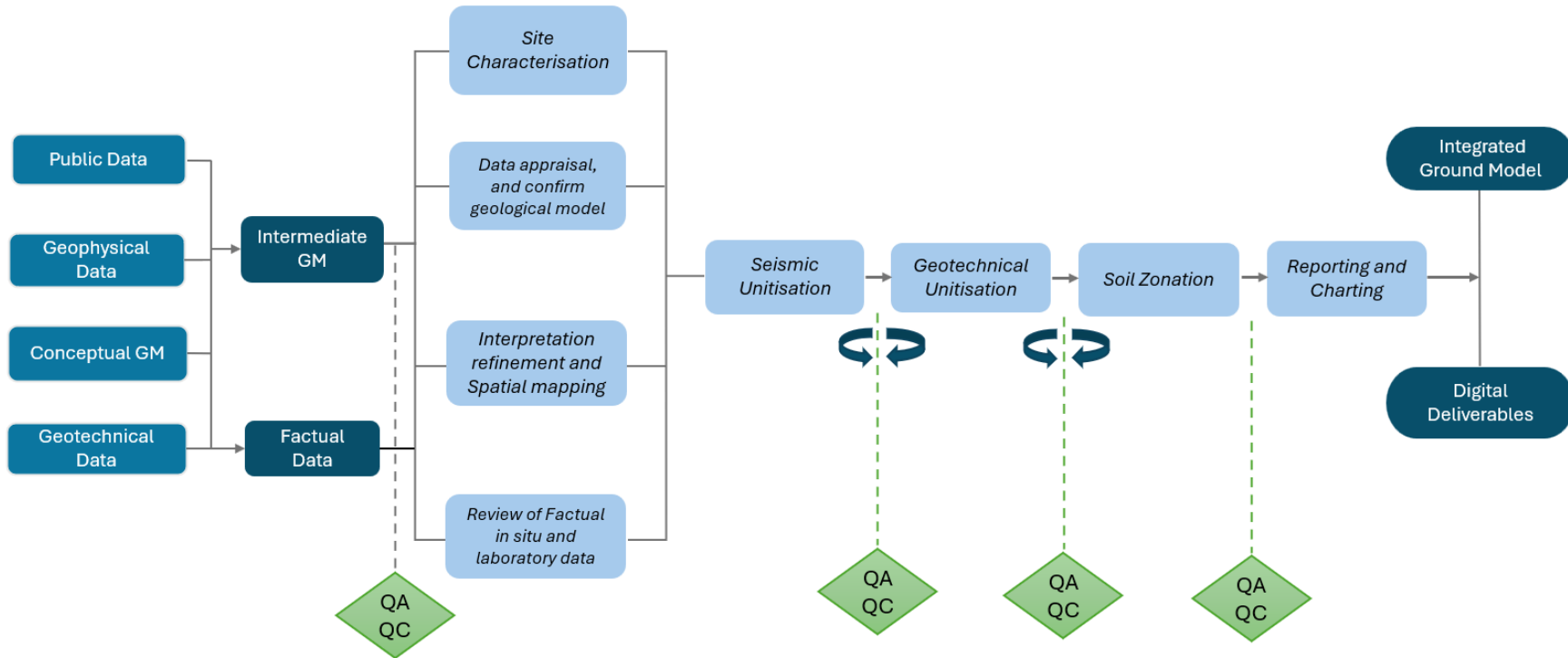


Figure 5-1 - IGM development workflow

5.1 GEOPHYSICAL SURVEY - INTERPRETATION REFINEMENT

- 1) Review seafloor data to identify any areas that will need refined interpretation.
- 2) Review seismic interpretation to identify any areas that will need refinement. This includes ensuring that the interpretation:
 - a) represents an update to the archived PGM (GEOxyz, 2024) based on Venterra's interpretation of the data in conjunction with the available geotechnical data.
 - b) is reliable between SBP and 2D-ultra-high resolution seismic (SCS and MCS) datasets.
 - c) shows minimal mis-ties (vertical differences in interpretation where seismic lines intersect).
 - d) makes geological sense given the information available.
- 3) Identify additional horizons for interpretation. A summary of the revised seismic interpretation is provided in Table 5-1.
- 4) Review geotechnical data to highlight if there are any concerns with the reliability of in-situ or lab tests which may affect the IGM.
- 5) Review the velocity model and time-to-depth conversion of the seismic data interpretation, which was derived from the 2D multichannel ultra-high resolution seismic processing carried out by the contractor, and ensure that the model accounts for real variations in the seismic velocities, as far as the data supports, in particular by reviewing any possible integration of geotechnical data into the velocity model. This is discussed in Section 5.4.

Table 5-1 - Revised seismic interpretation of the geophysical data

Revised Seismic interpretation of the geophysical data		
Seismic Reflector	Corresponding Seismic Unit	Comments (following client approval)
H00	Top of Unit I - Marine	Horizon refined
H05	Base of Unit I - Marine	Horizon refined and extent updated
H15	Base of Unit IIIa - Upper Glaciolacustrine	Horizon refined using UHRS dataset
H20	Base of Unit IIIb - Lower Glaciolacustrine / Top of Unlithified Chalk (Unit Va)	Horizon refined
H35	Top of Unit Vb - Lithified Chalk	Horizon refined based on limited available geotechnical data, though it has low confidence and has not been gridded. This horizon serves to inform on the lithified surface only.

5.1.1 UHRS DATA QUALITY GRADING

The UHRS data were graded for their data quality, the results of which are presented in Figure 5-2 and chart 24004-OVR-001-02-01, in Appendix A.

The following data quality grades were utilised:

Good (G):

- Seabed is clear and continuous
- The depth of penetration, data resolution, and effective attenuation of the ghost and multiple signals is sufficient to allow interpretation of the data, with minimal artefacts.
- The data have been correctly tidally reduced with no significant offsets between lines.
- The signal has been effectively filtered and gains are well balanced across the record with a lack of remnant ambient and mechanical noise.

Fair (F):

- Seabed is clear and continuous
- The depth of penetration, data resolution, and attenuation of the ghost and multiple signals limits the interpretability of the data locally, though it is generally good.
- The applied tidal reduction is suitable with local variations.
- The signal filtering and gain balancing is generally good, with minimal noise present.

Poor (P):

- Seabed is unclear and/or discontinuous.
- The depth of penetration, data resolution, and attenuation of the ghost and multiple signals is poor, affecting the continuity of reflectors and the interpretability of the data.
- Tidal reduction and static corrections are variable and affect the continuity of the data.
- The data require further filtering and balancing of gains to improve the record and remove the remnant noise that impacts interpretability.

Though all data have either been categorised as good, or good to fair, it is possible that the data may benefit from reprocessing to remove the de-multiple artefact that is present within the data. This is discussed in detail in section 6.2 regarding its variable affect across the site and dataset. Reprocessing may provide improved results and help to further constrain affected horizons and interpreted units affected by the artefacts.

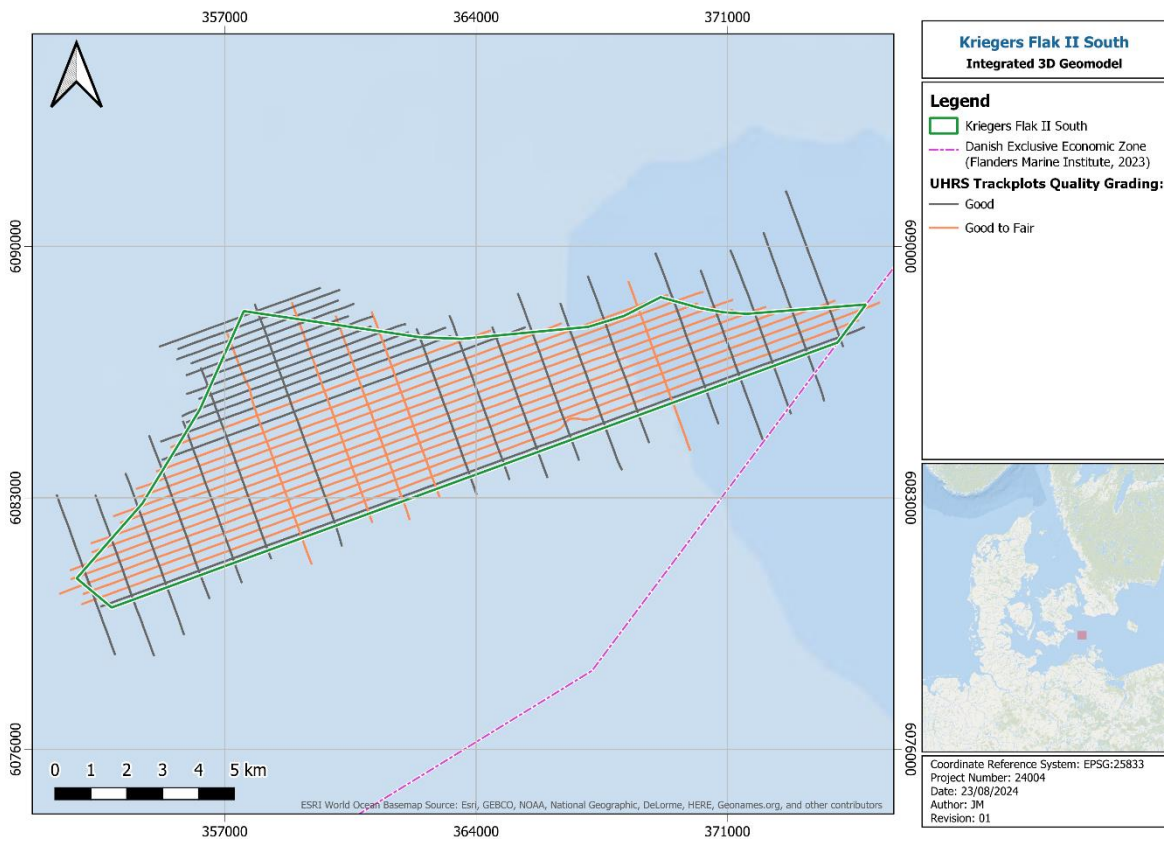


Figure 5-2 - UHRS line paths and data quality grades

5.2 GEOTECHNICAL DATA SUMMARY

Figure 5-3 shows the geotechnical testing and/or sampling locations. Section 4.2 summarises the number and geotechnical site investigations performed at the site.

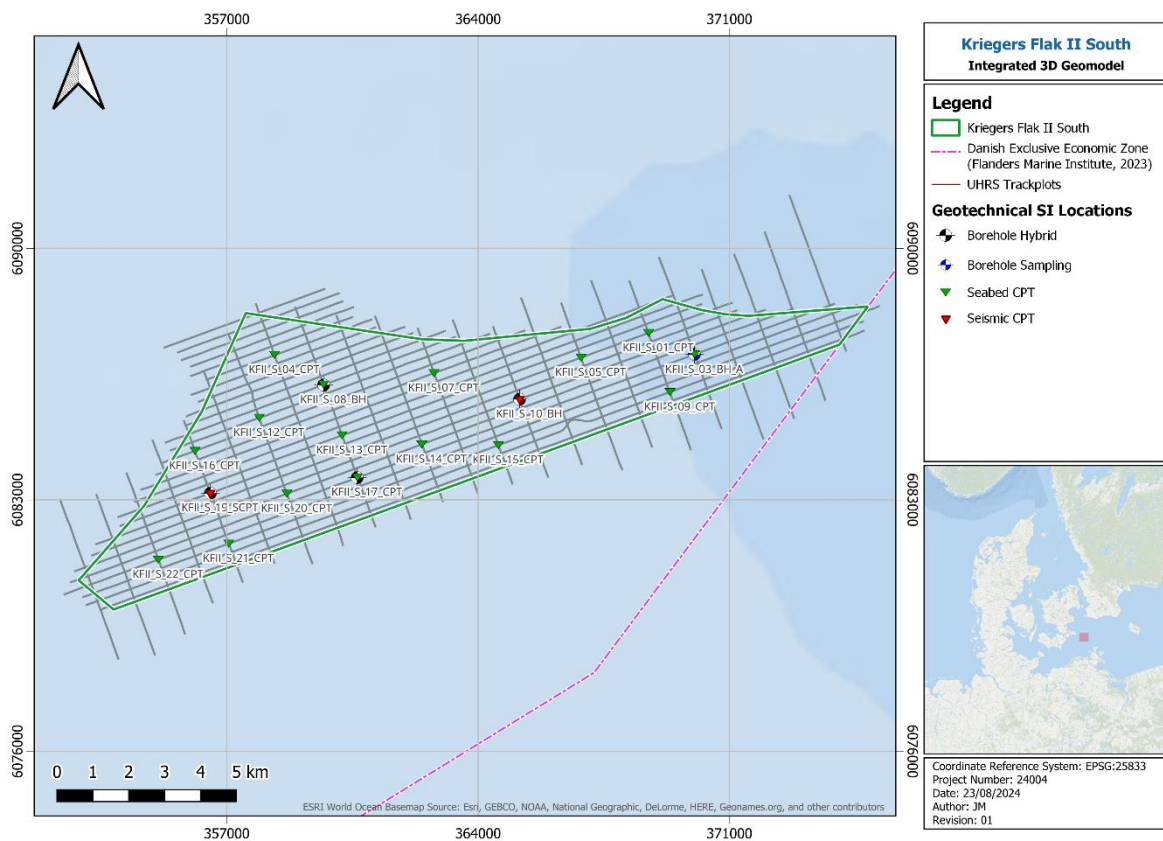


Figure 5-3 - Geotechnical site investigation locations overview (Gardline, 2024)

5.3 GEOTECHNICAL DATA INTEGRATION

At this stage, the model is primarily led by the interpretation of geophysical data. To verify it, the seismic interpretation and gridded seismic horizons are compared against the preliminary geotechnical tops that are interpreted from notable and spatially consistent variations in the available ground-truthed geotechnical data – from CPT and BH log and sample testing measurements.

The integration of geotechnical data proceeded as follows:

- To avoid bias, geotechnical data was interpreted in isolation with no consideration for existing interpreted seismic units. For this,
 - CPT and BH data were projected along depth-corrected pseudo-sections.
 - Significant changes in measurement properties were identified in each GI location, generally representing a change in sediment type.
 - Corresponding sediment type boundaries were matched between GI locations and denoted geotechnical tops.
- Geotechnical tops were then compared against seismic data and interpreted seismostratigraphic horizons in Kingdom. Initially, this was done using the GEOxyz provided velocity model to convert the tops to TWTT to overlay on seismic data (GEOxyz, 2024). Subsequently, when available, the improved velocity model was used.
- Where correlations did not immediately provide confirmation of reliable interpretation, the horizons were reinterpreted, and reliability of interpretation improved. On occasion, the

seismic horizon was clear but associated geotechnical top was not sharply defined, possibly presenting a more gradual change of geotechnical parameters. In this case, the geotechnical top was reassessed and ultimately revised to align with the seismic interpretation more closely.

- In order to ensure the most consistent interpretation of both contributing datasets, multiple workshops between the geotechnical and geophysical interpreters were undertaken, resulting in multiple iterations of the interpretation
- Based on the analysis of the geotechnical data, a total of 12 geotechnical units were identified. The geotechnical unitisation was developed considering the physical and mechanical geotechnical behaviour of the soil i.e. drained, undrained or mixed. Therefore, for a single seismostratigraphic unit, more than one geotechnical unit may be assigned to describe the soil behaviour.

An example of seismic interpretation revision through geotechnical integration is shown in Figure 5-4 and Figure 5-5. In this location, the top of Unit IIIa was reassessed and refined to have a consistent phase picked that aligned with the interpreted geotechnical markers. The previously interpreted H20 reflector was refined and the 'Chalk_UL' geotechnical marker confirmed that the once top of till was in fact the top of unlithified chalk. This was observed across the site. Additionally, the geotechnical data provided some (limited) lithified chalk top marks. Where the seismic data showed a coinciding reflector, the H35 reflector was interpreted. The reflectors listed in Table 5-1 were refined based on the methodology above.

To summarise, the seismic units discussed in section 6.2 were correlated with 12 interpreted geotechnical units. The relationship between these interpretations is shown in Table 5-2. Statistics intended to quantify reliability of interpretation on the correlation between seismic units and geotechnical tops are presented in section 6.6, with a more detailed table showing the integration in Table 6-2.

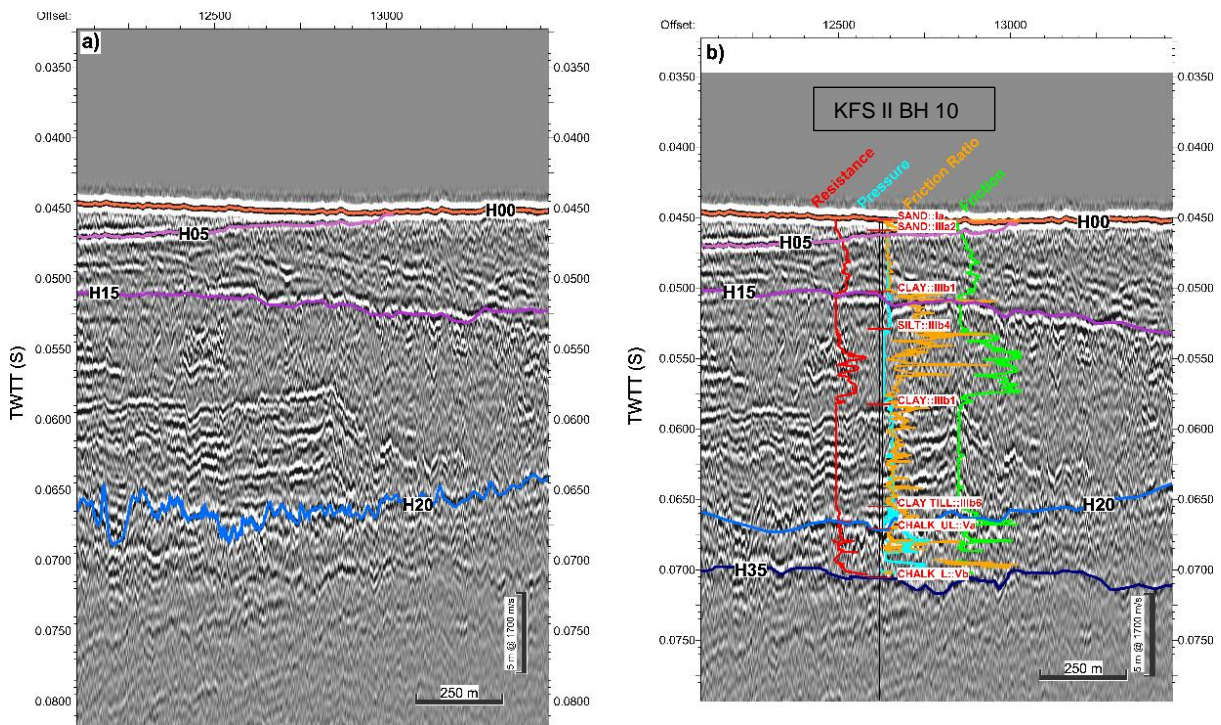


Figure 5-4 - Comparison of pre (a) and post (b) geotechnical interpretation integration UHRS line L020

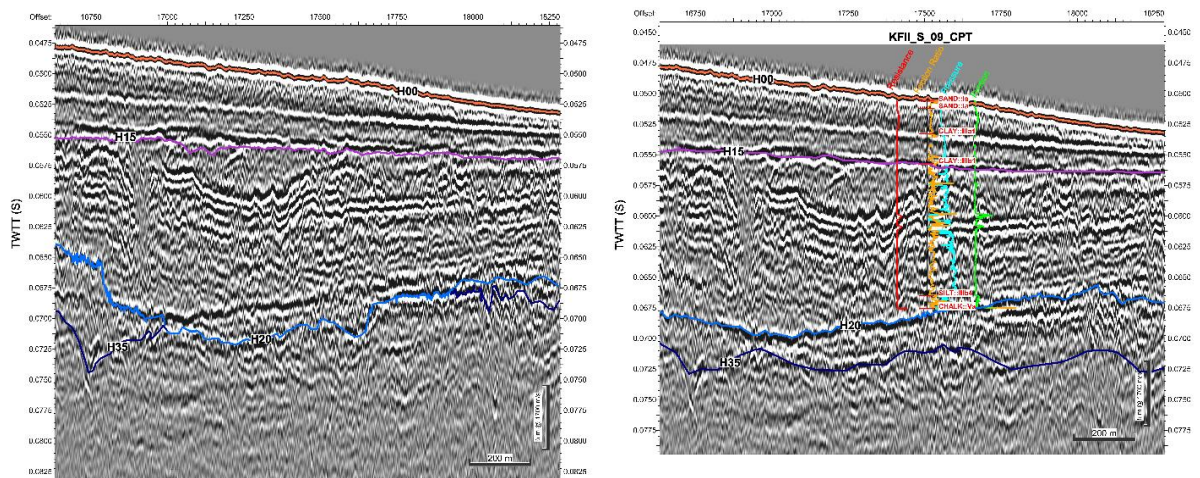


Figure 5-5 Comparison of pre (a) and post (b) geotechnical interpretation integration UHRS line L02

Table 5-2 - Correlation between seismic and geotechnical tops

Correlation between seismic and geotechnical tops	
Seismic Top	Geotechnical Unit
Seafloor/ Top Unit I	Ia
Top Unit IIIa	IIIa1
Top Unit IIIb	IIIb1
Top Unit Va	Va
Top Unit Vb	Vb

* Notes: The seismic and geotechnical units are described in Table 6-2

The geotechnical data are not always perfectly co-located with a corresponding seismic line (UHRS or SBP). During the integration, the geotechnical data were projected onto the nearest seismic lines. For larger distances between the geotechnical data and the seismic, there is a greater chance of uncertainty, and as such, inconsistencies remain when correlating the geotechnical tops with the geophysical interfaces. A summary of the distance between each geotechnical location and the closest UHRS seismic line is provided in Table 5-3.

Table 5-3 - UHRS line offsets from geotechnical locations

Geotechnical and Seismic Data Offsets						
ID	Easting (m)	Northing (m)	Type	Penetration (m)	Line Name	Line Offset (m)
KFII_S_01_CPT	368742.4	6087640.0	SCPSEA	15.45	A_KS_L018_UHR_T_MIG_STK	4.8
KFII_S_03_BH	370021.8	6087050.0	Borehole Hybrid	31.8	A_KS_L022_UHR_T_MIG_STK	2.1
KFII_S_03_BH_A	370027.5	6087038.0	Borehole Sampling	66.3	A_KS_X019_UHR_T_MIG_STK	3.8
KFII_S_03_CPT	370023.6	6087045.0	SCPSEA	9.7	A_KS_L022_UHR_T_MIG_STK	4.0
KFII_S_03_CPT_A	370025.8	6087049.0	SCPSEA	12.84	A_KS_L022_UHR_T_MIG_STK	1.1
KFII_S_04_CPT	358325.7	6087032.0	SCPSEA	15.76	A_KS_L006_UHR_T_MIG_STK	0.5
KFII_S_05_CPT	366865.4	6086955.0	SCPSEA	17.62	A_KS_X016_UHR_T_MIG_STK	4.1
KFII_S_07_CPT	362767.6	6086524.0	SCPSEA	15.17	A_KS_X012_UHR_T_MIG_STK	4.0
KFII_S_08_BH	359695	6086195.0	Borehole Hybrid	45.8	A_KS_L011_UHR_T_MIG_STK	3.3
KFII_S_08_CPT	359693	6086202.0	SCPSEA	2.76	A_KS_L011_UHR_T_MIG_STK	3.6
KFII_S_08_CPT_A	359694.8	6086206.0	SCPSEA	25.44	A_KS_L011_UHR_T_MIG_STK	6.8
KFII_S_09_CPT	369342.9	6085997.0	SCPSEA	14.02	A_KS_X018_UHR_T_MIG_STK	1.6
KFII_S_10_BH	365152.3	6085799.0	Borehole Hybrid	71.3	A_KS_L020_UHR_T_MIG_STK	6.3
KFII_S_10_SCPT	365161.1	6085801.0	SCPSEI	20.04	A_KS_X014_UHR_T_MIG_STK	0.4
KFII_S_12_CPT	357900.7	6085282.0	SCPSEA	18.56	A_KS_X007_UHR_T_MIG_STK	2.4
KFII_S_13_CPT	360207.3	6084793.0	SCPSEA	21.51	A_KS_X009_UHR_T_MIG_STK	2.3
KFII_S_14_CPT	362427	6084540.0	SCPSEA	8.06	A_KS_L021_UHR_T_MIG_STK	7.1
KFII_S_14_CPT_A	362429.4	6084544.0	SCPSEA	6.66	A_KS_L021_UHR_T_MIG_STK	10.3
KFII_S_15_CPT	364562.6	6084519.0	SCPSEA	20.99	A_KS_L024_UHR_T_MIG_STK	6.2
KFII_S_16_CPT	356108.6	6084361.0	SCPSEA	18.47	A_KS_X005_UHR_T_MIG_STK	3.8
KFII_S_17_BH	360628.7	6083617.0	Borehole Hybrid	71.3	A_KS_L022_UHR_T_MIG_STK	0.6
KFII_S_17_CPT	360635.1	6083620.0	SCPSEA	10.15	A_KS_L022_UHR_T_MIG_STK	0.8
KFII_S_19_BH	356537.8	6083182.0	Borehole Hybrid	72.9	A_KS_X005_UHR_T_MIG_STK	7.3
KFII_S_19_SCPT	356535.8	6083188.0	SCPSEI	13.76	A_KS_L018_UHR_T_MIG_STK	1.3
KFII_S_20_CPT	358670.2	6083169.0	SCPSEA	24.22	A_KS_X007_UHR_T_MIG_STK	5.6
KFII_S_21_CPT	357049.6	6081779.0	SCPSEA	22.92	A_KS_X005_UHR_T_MIG_STK	5.1
KFII_S_22_CPT	355087.6	6081329.0	SCPSEA	34.34	A_KS_L023_UHR_T_MIG_STK	0.6

5.4 VELOCITY MODEL REVISION

Initial velocity model proposed by GeoXYZ relied on a constant velocity of 1600 m/s in the sub-seabed, for the SBP dataset. For the 2D UHRS dataset, constant velocities of 1600 m/s for units above GeoXYZ Unit III “shallow Quaternary sediments” and 1800 m/s to GeoXYZ Unit III “relatively ancient rock” were applied for the Time-Depth (T-D) conversion of the interpreted horizons. According to GeoXYZ report (GEOxyz, 2024), the T-D conversion of SEGY data was performed accounting for water column velocity, constant velocity for the SBP dataset and a two-layer model, with constant velocities, for the UHRS dataset. Upper and lower limits of the interval velocities correspond to grids in TWTT.

Following reception of the datasets, new T-D charts were implemented for the northern and southern sites. For the display of geotechnical markers in the seismic section in time, initial TD charts used a constant velocity of 1700 m/s.

Along with the progress of the seismic interpretation, a more detailed velocity model using constant interval velocities has been introduced to account for the variable lithologies. Based on literature and geological knowledge, intervals of possible empirical velocities were attributed to each lithology (Table 5-4).

Table 5-4 - Velocity model parameters

Velocity Model Parameters		
Lithologies	Inferred Velocity Value (m/s)	Possible Range (m/s)
Shallow (marine) sand	1650	1600 - 1650
Shallow (marine) silt	1650	1550 - 1650
Post-glacial sand	1700	1600 - 1700
Post-glacial clay	1700	1650 - 1750
Till (clay, sand, silt)	1800	1700 - 1900
Chalk	2200	2000 - 2500

Following continuous revision of the seismic interpretation against geotechnical marker in time domain, constant interval velocities in the different lithologies were revised for each location (Figure 5-6).

MD
 TVD
 TVD Seismic
 Subsea
 |
 Interval Velocity
 Average Velocity

Formation Tops

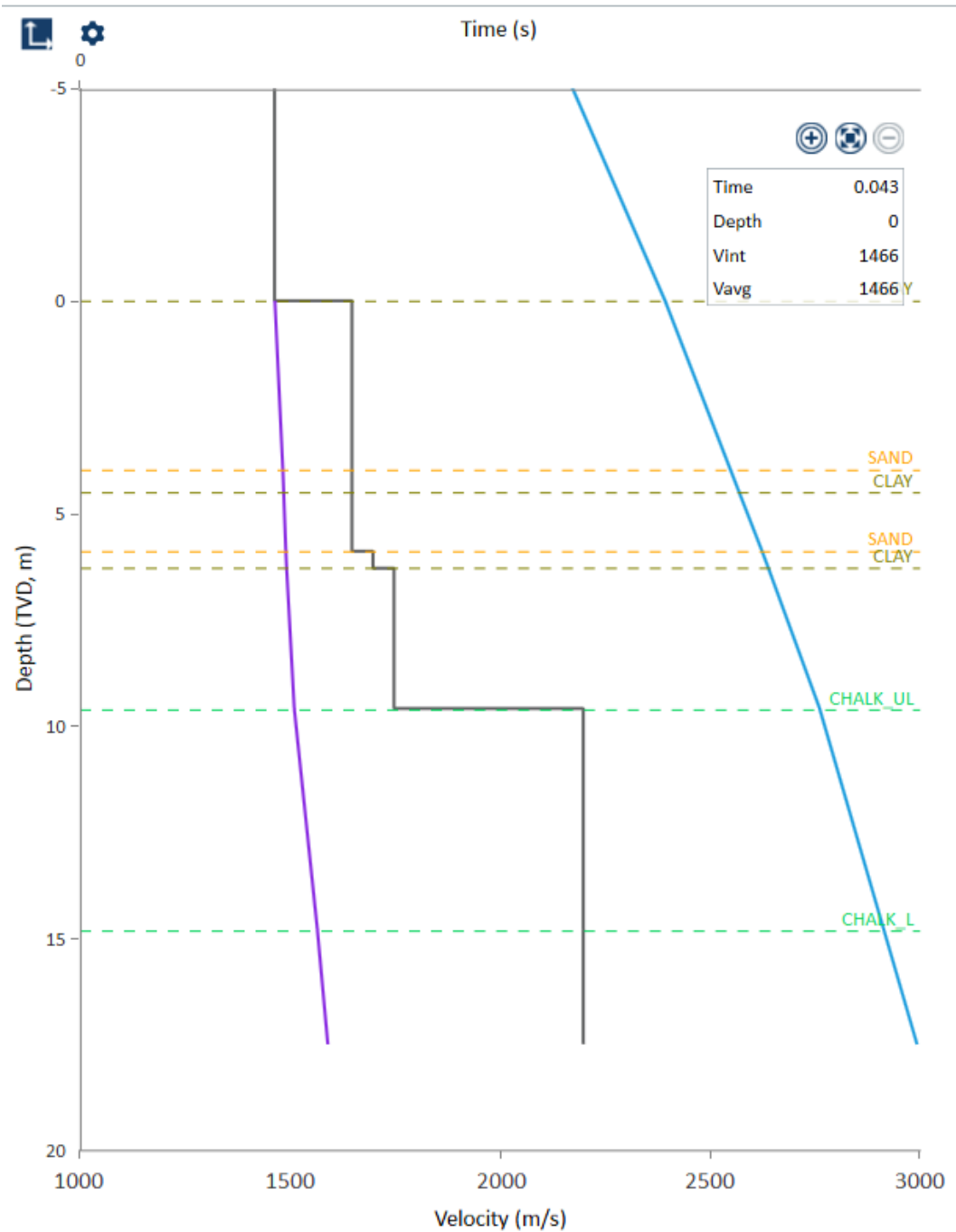


Figure 5-6 - Seismic unit velocity model

The final velocity model is based on the integration of the different lithologies per seismic units and the tie between the interpreted seismic horizons and geotechnical markers. For units with a single lithology and/or relatively homogenous sediments, a constant interval velocity was defined. For complex seismic units displaying multiple lithologies, spatially variable but constantly vertical, interval velocities were calculated based on the tie between seismic and geotechnical markers. Because of vertical uncertainties between the seismic and geotechnical markers, the calculated interval velocities for such units were rounded to nearest quarter. The

resulting spatially variable constant interval velocities were gridded and imported as a velocity grid to be used during the gridding process (section 5.5.1).

For the southern site, constant interval velocities were used for seismic units I, IIIa and V. For Unit IIIb, a spatially variable constant interval velocity grid was calculated with values ranging from 1650 to 1800 m/s (Table 5-5).

Table 5-5 - Final velocity model

Final velocity model	
Unit	Velocity (m/s)
Marine unit – Unit I	1650
Upper Glaciolacustrine – Unit IIIa	1650
Lower Glaciolacustrine – Unit IIIb	Velocity grid; 1650 to 1800
Chalk – Unit V	2200

5.5 GRIDDING AND DEPTH CONVERSION

5.5.1 GRIDDING

Following the integration of the geotechnical interpretation and the completion of seismic reinterpretation, in Kingdom, the following methodology was employed:

- a. Picked horizons, in TWTT, for all seismic units were gridded using the Flex Gridding algorithm in Kingdom, with Minimum Curvature (with a value of 0) and Smoothness set to Midway (with a value of 0.6). Extrapolation distance was set to 260 m for the coarsely spaced UHRS lines (at 250 m) and 60 m for finely spaced SBP lines, so that gaps in between lines and the site boundary were filled. Grids cell size was set to 5 m.

Several parameter variations were tested. Those selected were found to provide the best results once the whole gridding process had taken place – minimising unrealistic artefacts in the data and allowing unit trends that were extrapolated between lines to be more realistic. The cell size enabled high resolution grids to be calculated, retaining almost all horizon undulations, without processes being significantly time intensive. The extrapolation distance needed to be significant to account for line spacing gaps (250 m for the UHRS and 60 m for the SBP) and gaps between the lines and the site boundary.

- b. The Two-Map calculator in Kingdom was used to calculate the top of each seismic unit that originally had its base picked, and the base for each seismic unit that originally had its top picked such that each unit had grids representing its top and base. Through this process the grids were also trimmed against shallower unit interfaces.
- c. The Depth Conversion Tool ‘Compute Isochron Map’ in Kingdom was then used. This takes the top and base grids for each unit and calculates Isochrons, which represent the thickness of each seismic unit in TWTT.
- d. The Isochron grids were then reviewed. If the Isochron grids revealed unrealistic straight edges with a sudden, impossible, drop in unit thickness, then a copy of the original picked horizons were created and edited such that their subsequent grids provided consistent isochrons. This is typically done by adding false picks to adjacent lines to prevent abrupt grids truncations in the extrapolated area between lines, hence

allowing the grid surface to be smoothed. This can take several iterations to ensure consistent Isochrons.

- e. With consistent and realistic isochrons, the Depth Conversion Tool ‘Compute Isochore Map’ in Kingdom was then used. This takes the Isochron (thickness in TWTT), and the Interval Velocity Grid from the velocity modelling of each unit and creates an Isochore (thickness in metres). These were reviewed against the associated Isochrons to ensure processing was as expected. These Isochores were exported for charting unit thicknesses.
- f. The Depth Conversion Tool ‘Depth Map by Isopach Maps’ was then used to calculate grids representing the depth, in mBSF, of each seismic unit base. This required intermediate calculations to ensure that the extent of each successive unit was maintained. These mBSF grids were exported for charting unit depths.
- g. With Depth mBSF grids for the base of each seismic unit calculated, the ‘Depth Map by Isopach Maps’ tool was reused with the interpreted seafloor grids to calculate the Depth mMSL grids for each unit. These mMSL grids were then exported for charting unit depths, relative to datum (MSL).

In Kingdom, updated horizon picks are only present in Time domain. In depth domain, grids can be displayed in depth converted seismic sections (see section 5.5.2). Selection of the time or depth domain constrains the display of data coverage on the Base Map or in seismic sections.

5.5.2 SEG Y DEPTH CONVERSION

The time to depth conversion of the UHRS dataset SEG Ys was performed using the Dynamic Depth Conversion (DDC) tool in Kingdom. Unit tops calculated during the gridding process were used as constraints to setup the velocity model. Velocities used in T-D conversion were the same as the ones used in the T-D conversion of the grids.

Seismic velocities in the water column were assessed based on the T-D conversion of MBES bathymetry data and the tie with the seabed reflector in UHRS data.

Because of the limited penetration of SI in the south-western part of the site, velocities in the unit above bedrock were only constrained by one location. Therefore, in comparison with the rest of the site, uncertainty in the velocity model is higher in the southern-western part of the site. This uncertainty is propagated to the T-D converted SEG Ys and visible in the south-western part of the site, as a slight vertical offset between the top of bedrock reflector and the associated grid (maximum 1.8 m in the most southwestern part of the site) (Figure 5-7).

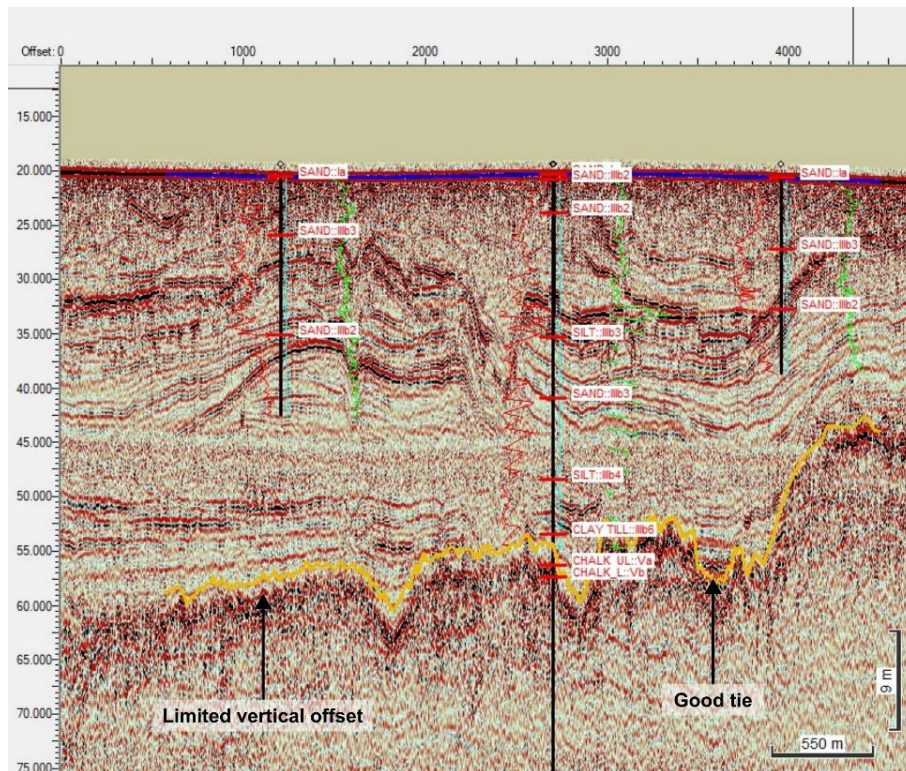


Figure 5-7 - Example of the transition between well constrained velocity model (right) and interpolated model with limited vertical offset (left)

In the DDC tool, no particular framework rule was applied as the unit truncations, onlaps, etc. were already accounted for in the unit tops.

Then, the T-D conversion was processed as follows:

1. Using the DDC tool, a constant interval velocity model was implemented and saved as a temporary attribute for each UHRS seismic line.
2. Using the T-D conversion tool in Kingdom, the DDC model implemented was applied to the T-D conversion of SEGYS.
3. Resulting SEGYS converted to depth are stored as attributes for each line.
4. Seismic sections converted to depth were quality checked against T-D converted grids and geotechnical markers.

Uncertainties associated with the T-D conversion of the SEGYS includes uncertainties in the bathymetry, which was used as the vertical reference layer. Additionally, because of extrapolation outside the site boundaries, more uncertainties exist for the velocity model used in the T-D conversion of seismic sections extending outside the site boundaries. Uncertainties are summarized in section 6.3.

In the Kingdom project, SBP and UHRS seismic sections converted to depth domain by GEOxyz and stored in attribute “Amplitudes Depth” (Depth data type) were retained. As part of this study, only the depth converted UHRS seismic section were updated. The updated UHRS seismic sections in depth domain are stored in attribute “Converted Depth” (Depth data type).

6 DISCUSSION OF SPATIAL INTEGRATED 3D GEOMODEL

6.1 SEAFLOOR INTERPRETATION

6.1.1 MULTIBEAM ECHOSOUNDER BATHYMETRY AND SLOPE

Bathymetry data with a 0.25 m resolution, shown in Figure 6-1, reveals that the seafloor dips from southwest to northeast, generally consistently, with elevations ranging from -18.5 m to -41.9 mMSL. The shallowest and almost flat areas were observed in the western part of the site. The elevation deepens towards the northeast; approximately at the site midpoint the seabed becomes more inclined and is gradually deepening to the eastern corner, where it reaches the maximum depth of -41.9 mMSL.

Variability in seabed morphology is best observed when a hill shade raster is derived from MBES data and applied as a semi-transparent layer. This allows the identification of more subtle changes in the seabed morphology.

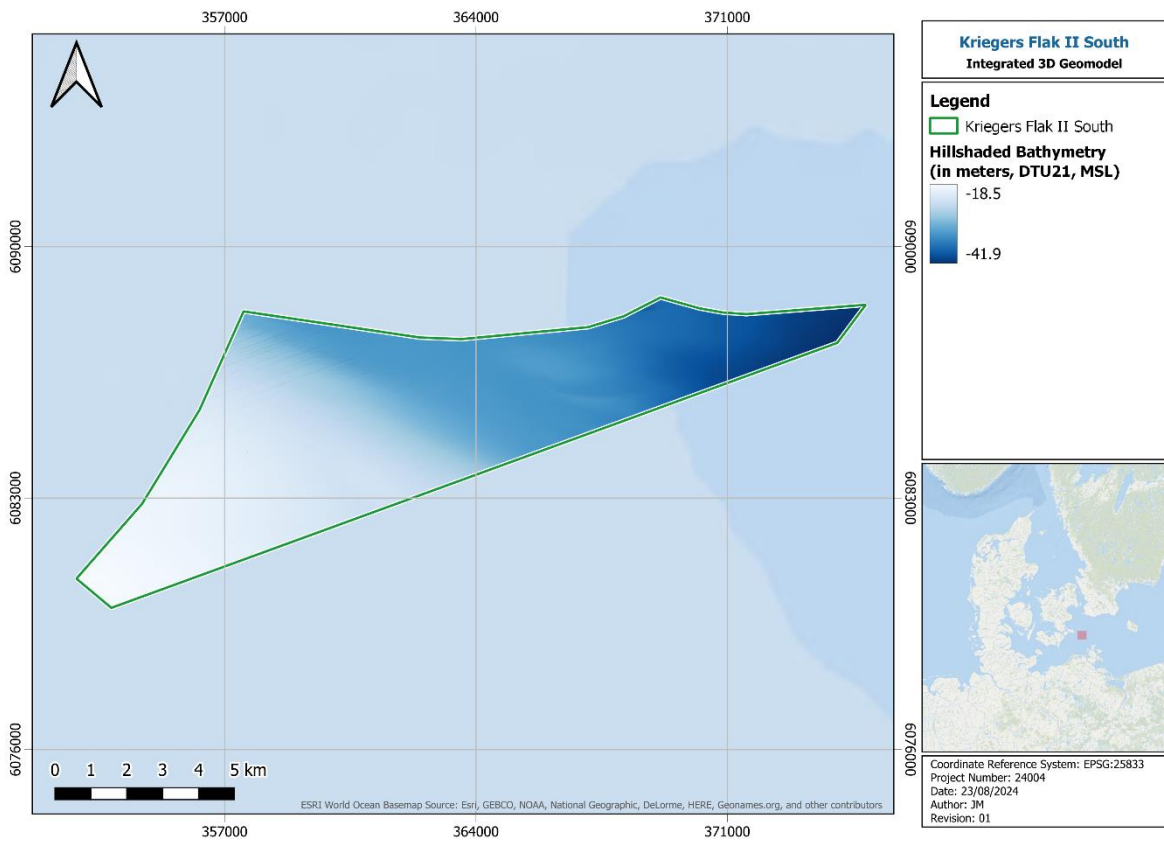


Figure 6-1 – Hillshaded MBES bathymetry

Slope, calculated from the bathymetry data, is presented in Figure 6-2. The average slope of the site is 0.30° and a profile across the site, west to east produces a dip of 0.13°. Localised areas with steep slopes (up to 32°) were reported within seafloor depressions, scars or associated with scouring around seafloor features.

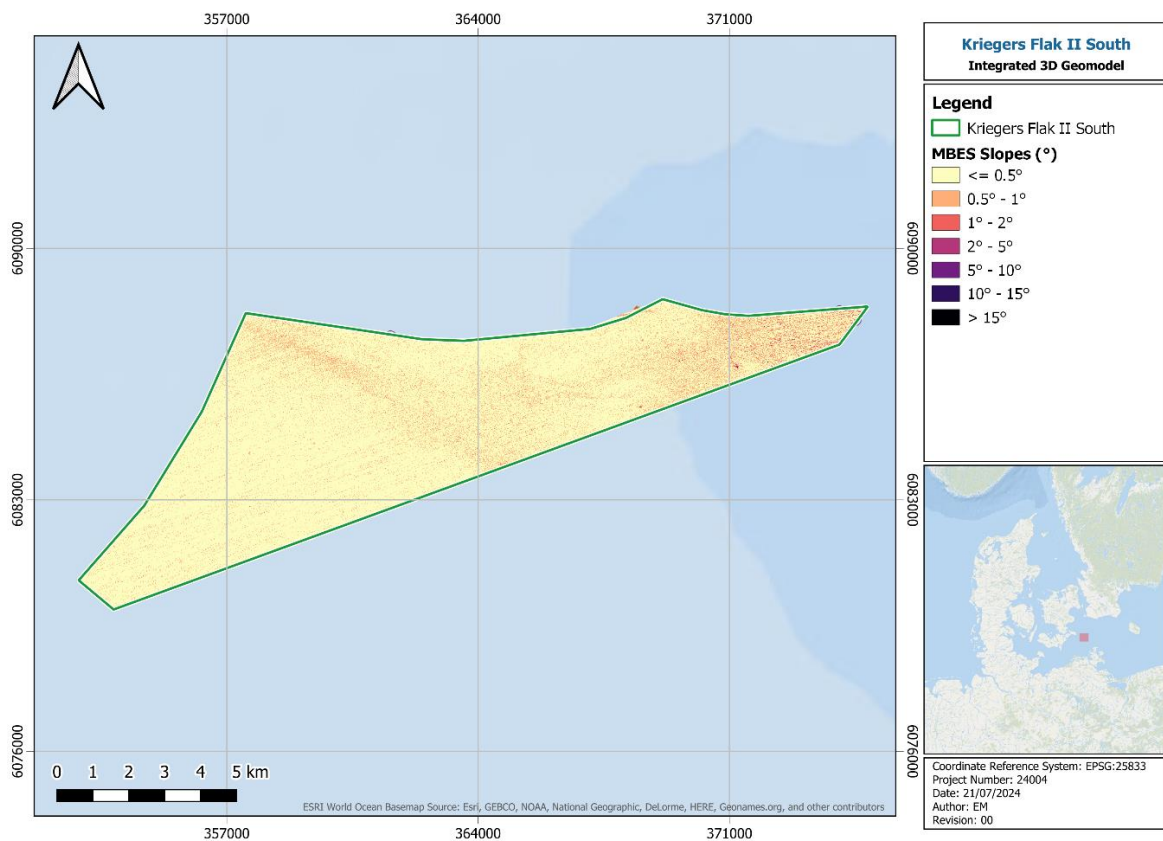


Figure 6-2 - MBES derived slope

Variations from the relatively flat seafloor are reported across the site. In the western part of the site there are no areas of any local increased slopes, the seabed slopes are generally gentle. The steepest slopes were reported in areas of seabed scars. The seabed features in the northeastern corner are mostly anthropogenic and are associated with different fishing operations in the area. The eastern and central areas are significantly scarred.

Figure 6-3 and Figure 6-4 showing the: 1) Pitted seabed or area of small depressions; 2) Bottom scarring associated with the fishing operations; 3) Anchor scars associated with the fishing operations in the area; 4) Raised area with increased slope values potentially related to the presence of a rock exposure.

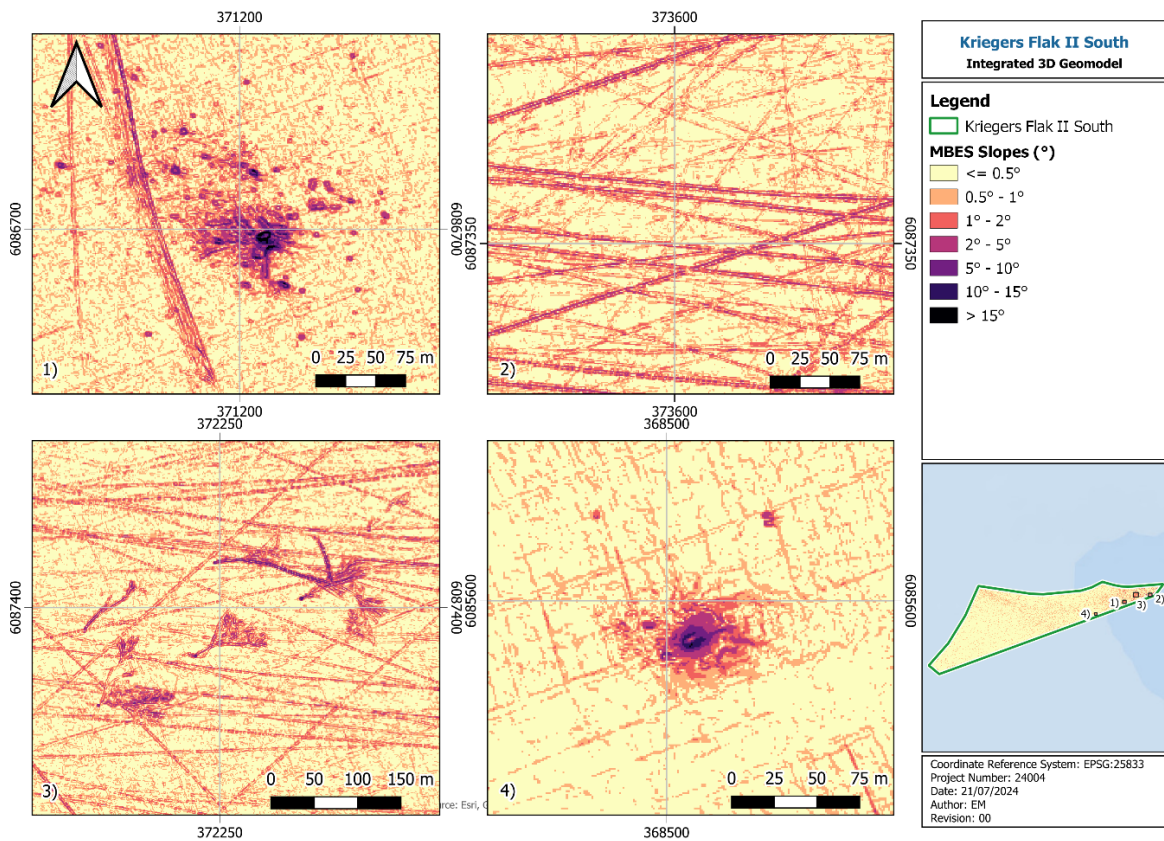


Figure 6-3 - Areas of increased slope angle

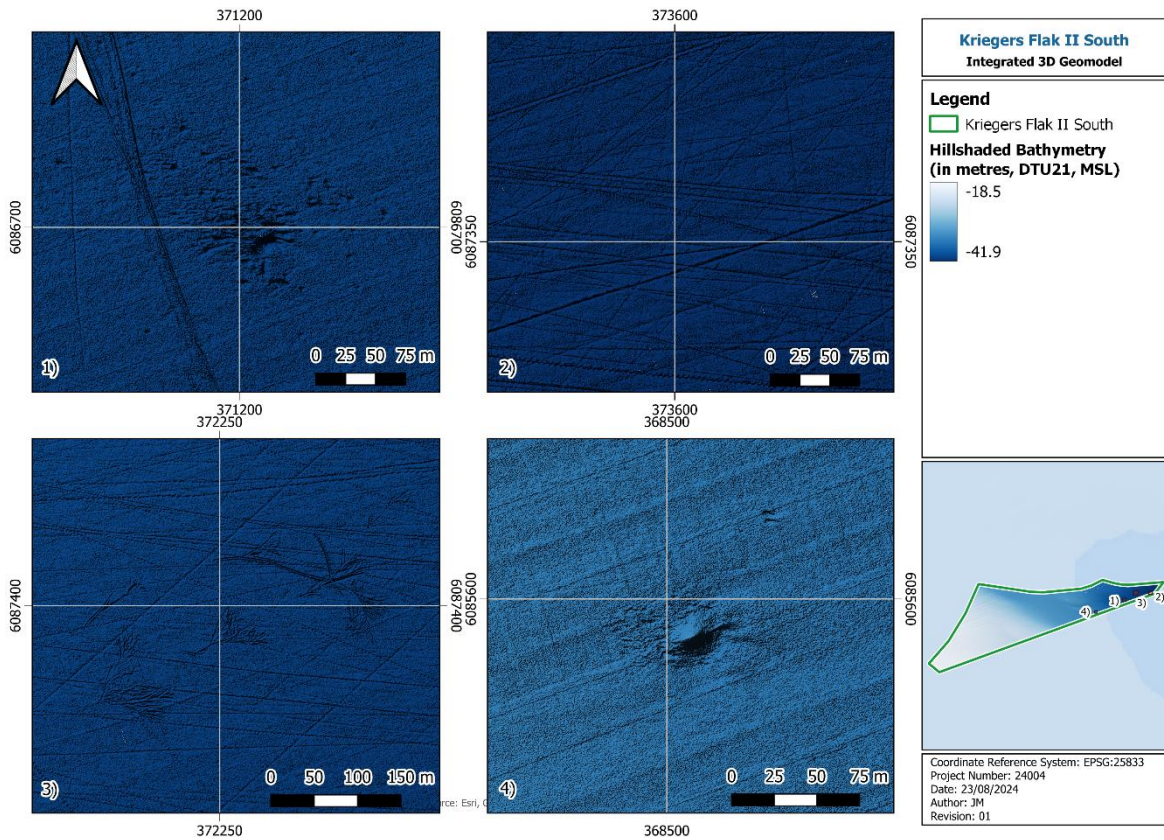


Figure 6-4 - Bathymetry with hillshade

The increase in slope values in the southern part of site was interpreted as seabed scars, which are associated with the fishing operations in the area. In the eastern and southern part of the site, a number of elevated areas were observed.

6.1.2 SIDE SCAN SONAR

The records of the side scan sonar and bathymetric data were used by GeoXYZ to identify seabed targets. The features identified on the SSS data correlate with those interpreted on the MBES grid.

Many features identified on SSS data were interpreted to be boulders (Figure 6-5). In general, the seabed across the site is homogenous, with only slight grain size changes, and occasional boulders.

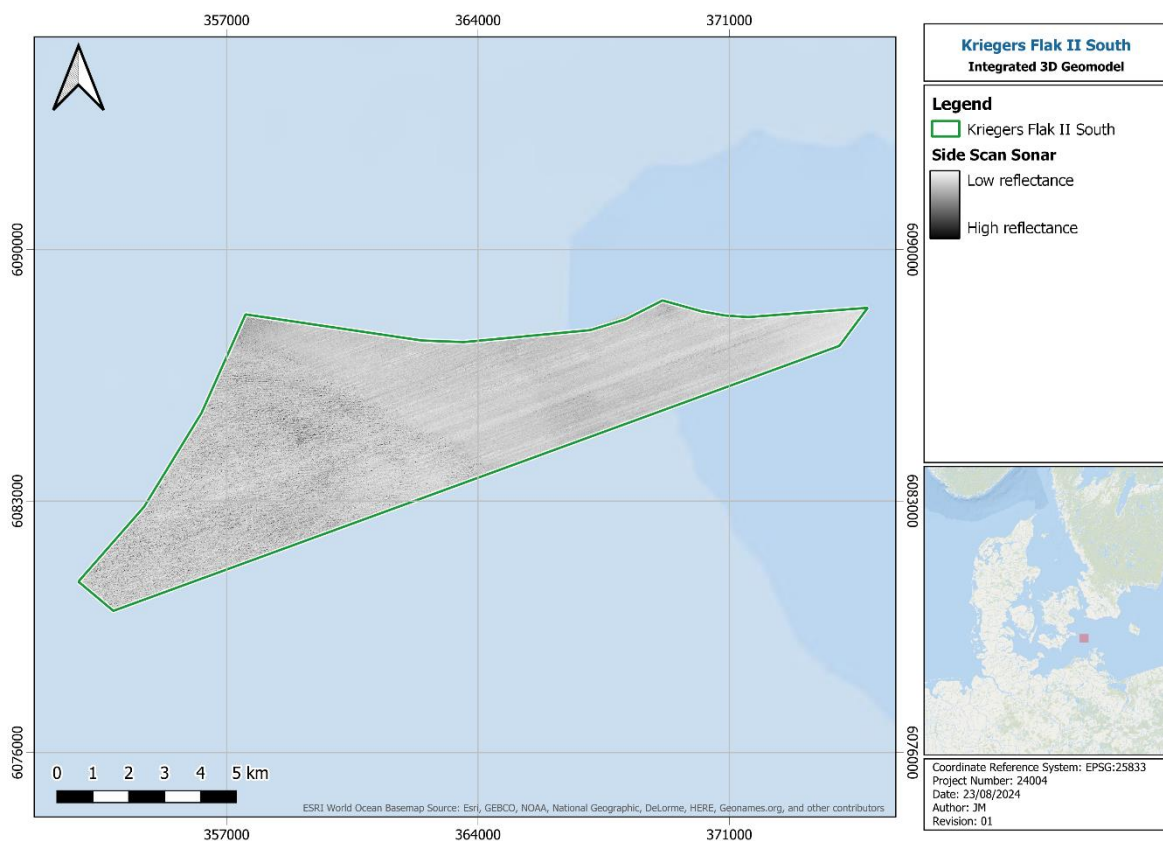


Figure 6-5 – Side scan sonar (GeoXYZ, 2023)

Figure 6-6 showing the: 1) a single feature potentially correlated with a wreck and its associated debris (see section 8.1.5). There are no public records of shipwrecks in this area, therefore further investigation would be needed to confirm this; 2) a boulder and associated scour 3) unidentified features, potentially anthropogenic, likely to be remains of fishing equipment.

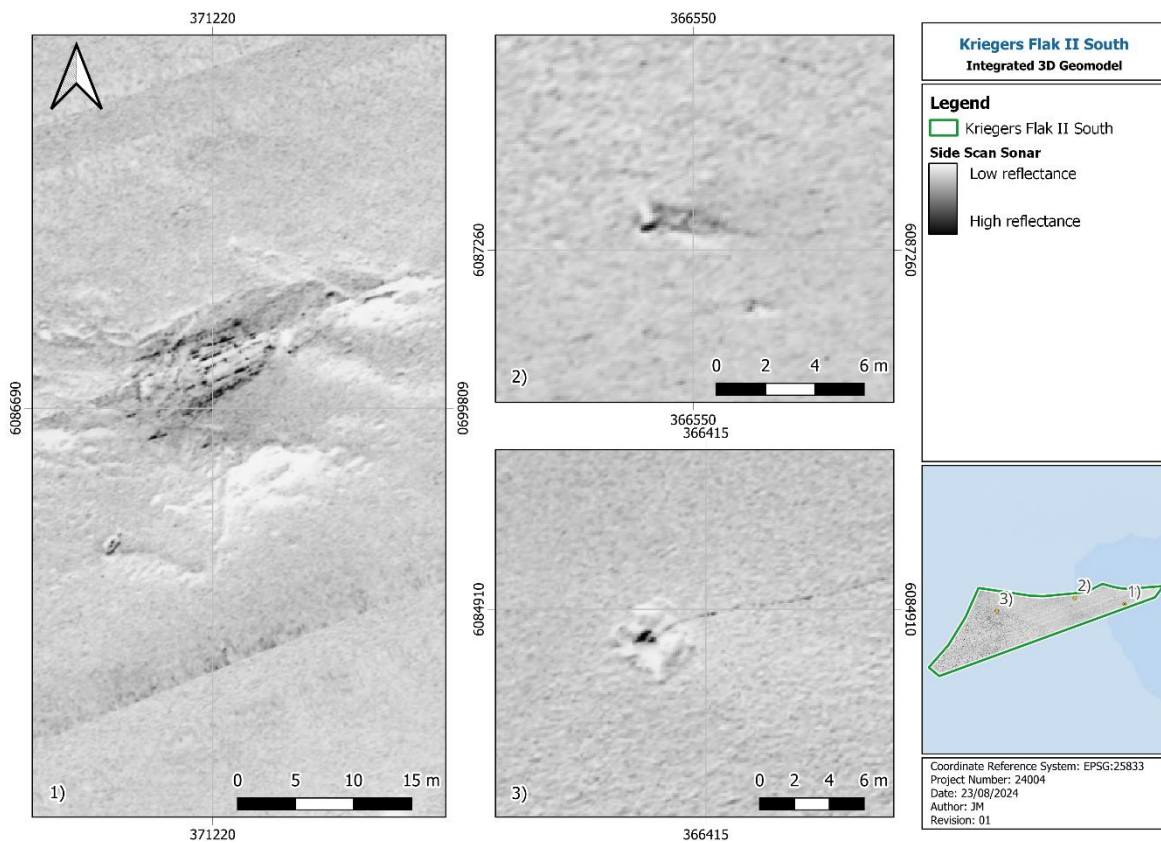


Figure 6-6 - Seafloor features identified on the SSS data (GeoXYZ, 2023)

6.1.3 SEAFLOOR LITHOLOGY

The seabed lithology data presented are based on the 2023 GeoXYZ geophysical survey and have been refined where deemed necessary. The seabed lithology was assessed based on the available bathymetry (Figure 6-1), backscatter (Figure 6-8), and low frequency (LF) and high frequency (HF) SSS data (Figure 6-5) to determine and define the sediment type and extents. Backscatter measures reflectance and can give indications of seabed texture and sediment grain size, as well as the seafloor relief and overall pattern. This was further constrained using grab samples obtained during the survey.

The seafloor sediment distribution across the site comprises of various types of sediments. In the western part of the site most of the seabed is covered with SANDs, in the centre of the site the composition changes to Muddy Sand. As the seabed deepens, the finer sediments in the northeastern corner of the site and comprise of MUD and sandy MUD, as seen by a change to darker reflectivity of the backscatter (Figure 6-8).

Examples of backscatter reflectivity data that were used during the assessment are provided in Table 6-1.

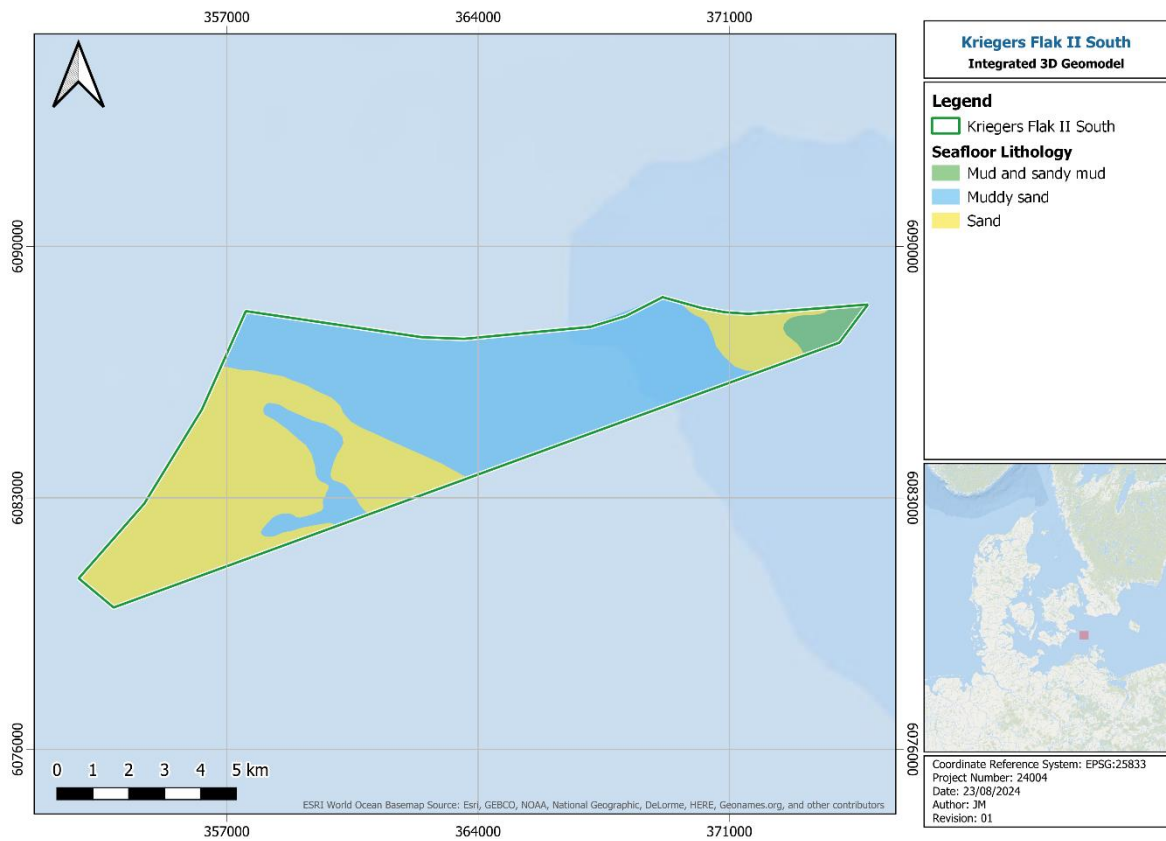


Figure 6-7 - Seabed lithology classification and extents (GeoXYZ, 2023; GDG, 2024)

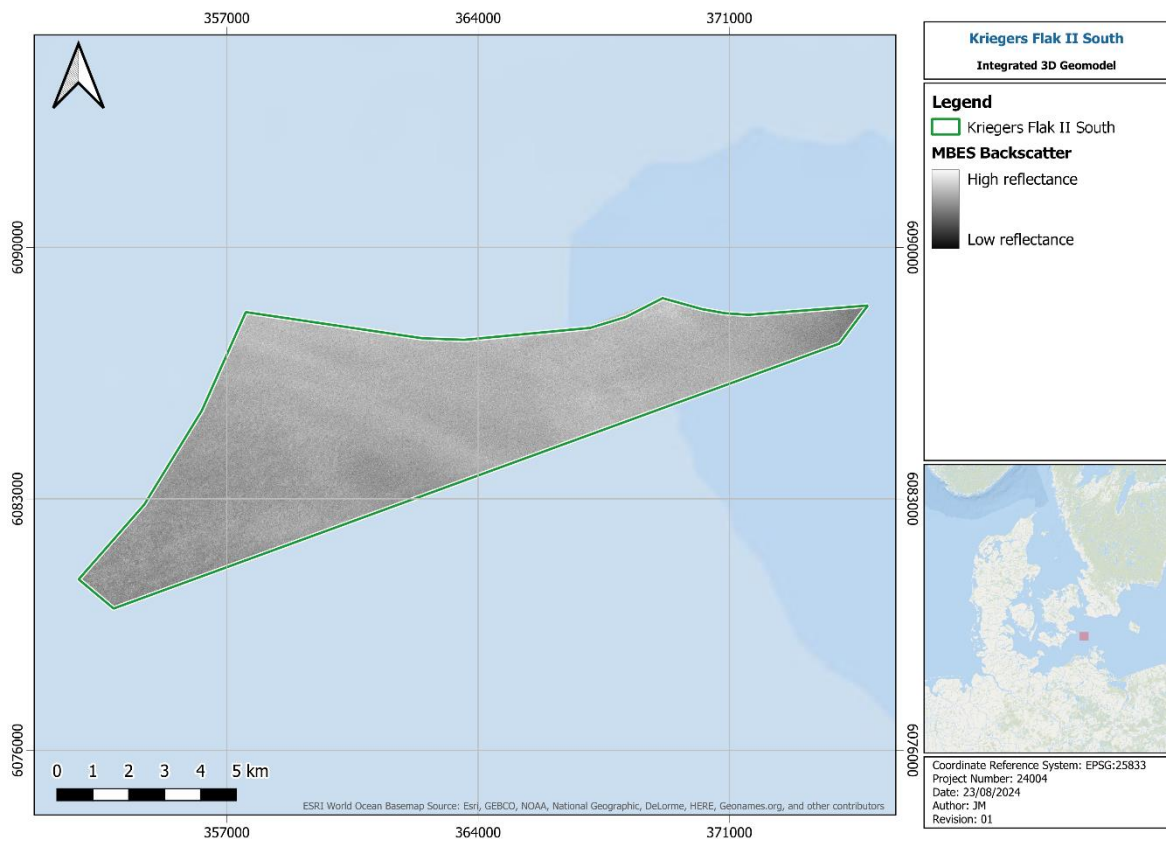
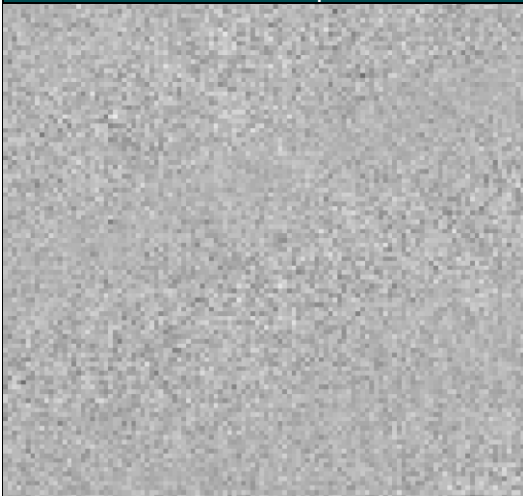
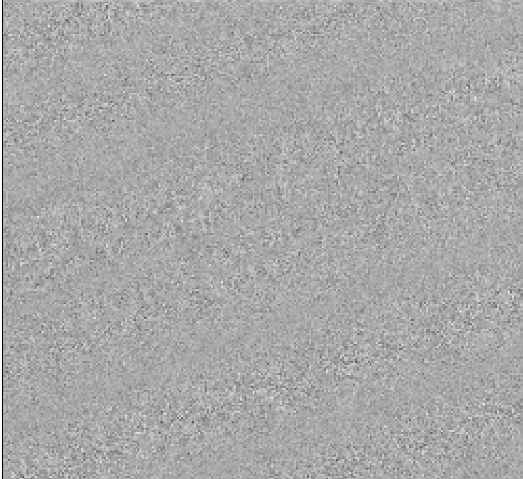
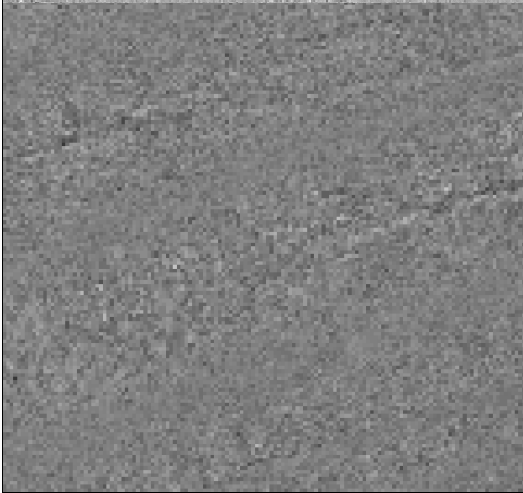


Figure 6-8 - MBES backscatter (GeoXYZ, 2023)

Table 6-1 - Sediment classification based on MBES backscatter analysis

Sediment classification based on MBES backscatter analysis		
Data Example	Description	Sediment Classification
	high reflectance; smooth texture	SAND
	medium reflectance; smooth texture	muddy SAND
	low reflectance; low/moderate texture	MUD and sandy MUD

6.1.4 SEAFLOOR MORPHOLOGY

The seabed across the site shows very little morphological change. It is generally flat and featureless with the only changes associated with biostructures, seabed depressions and pits, scars and trawl marks derived from fishing activities.

Extensive seabed scarring was found in the eastern section of the site as well as a larger area in the centre (Figure 6-9). These scars were interpreted to be associated with fishing activity and offshore operations in the area. In the east, these scars appear deeper and more erratic in their shape and positioning to other scars, compared to further west where the scars are more equally spaced and shallower with defined paths across a wider area.

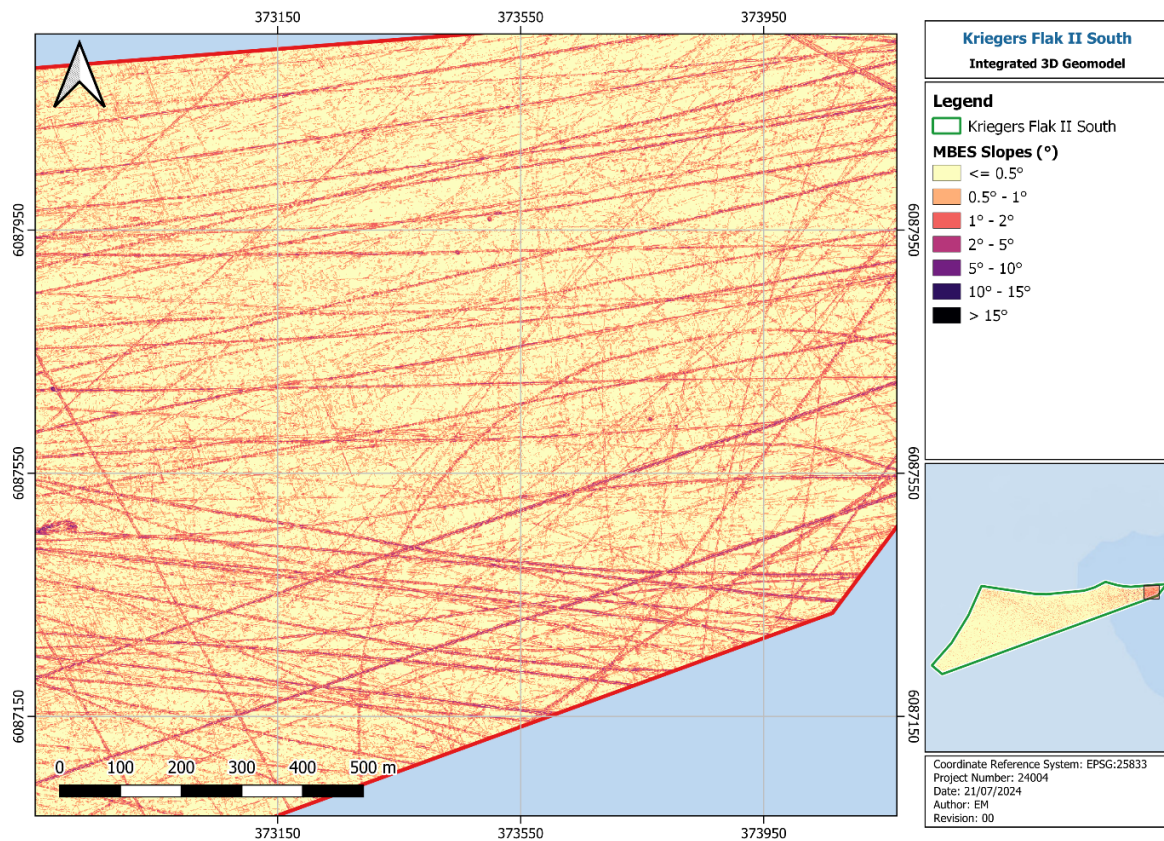


Figure 6-9 - Extensive scarring shown on the MBES slope

Small, isolated depressions, as seen on Figure 6-10, have been interpreted across the site. They occur most frequently in the northern and northeastern section as clusters of closely spaced depressions. These depressions are mostly 5-10 m in diameter, reaching up to 15 m maximum. They are rather shallow and gently sloped, the depth ranges between 0.4 - 0.6 m.

Given the nature of the underlying sediments these depressions can be interpreted as pockmarks. Possible gas blanking was observed on seismic data, which in combination with pockmarks might suggest shallow gas presence. Potentially, these pockmarks were created by gas escaping from beneath the seafloor.

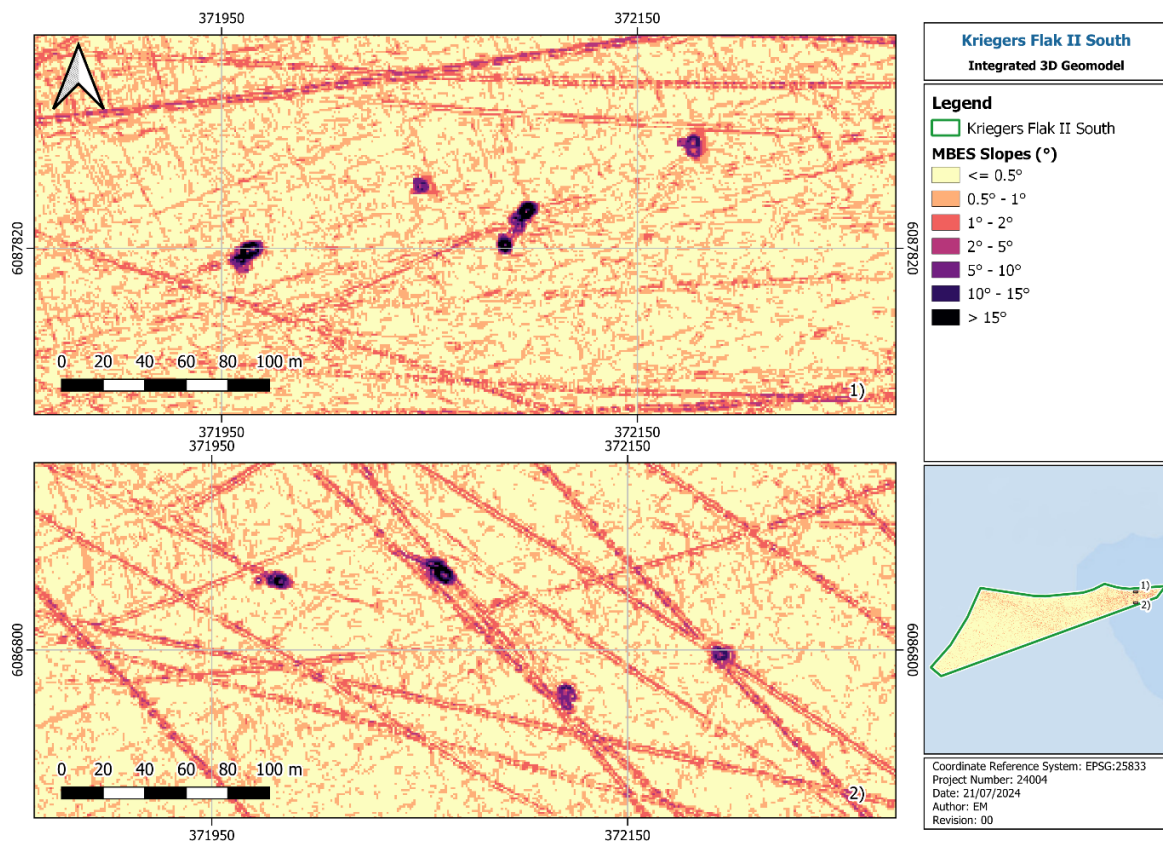


Figure 6-10 - Isolated depressions on MBES slope

6.1.5 SEAFLOOR OBJECTS

Seafloor contacts were picked by the survey contractor GeoXYZ using raw and processed data at a higher resolution in sensor specific software. The higher resolution enables more precise interpretation, but data are much denser and require sensor specific software to interrogate. Therefore, conventionally data are delivered as mosaics with a reduced resolution.

Venterra reviewed the positioning and correlation of the provided seafloor contacts to other datasets. A total of 479 seafloor contacts, shown on Figure 6-11, were picked on the SSS (323) and MBES (156) data and are classified as either boulders, debris, fishing equipment or unknown, with further comments on contacts potentially associated with known shipwrecks, or rock exposure.

Most of the seafloor contacts, 173 picked on the SSS and 70 picked on the MBES are classified as boulders.

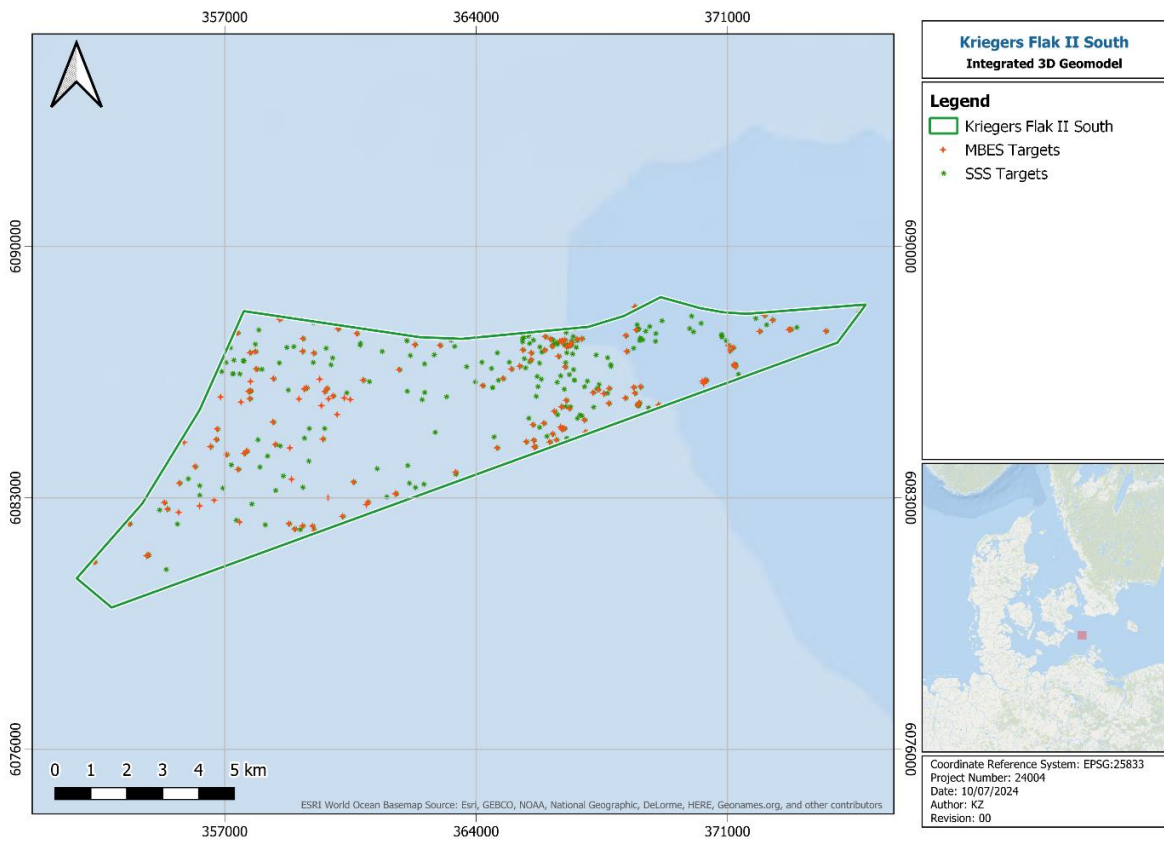


Figure 6-11 - Example of seafloor contacts picked on SSS and MBES bathymetry

6.1.6 MAGNETIC ANOMALIES

A total of 63 magnetic anomalies were interpreted within the site. These were classified as either generated by anthropogenic sources or related to geology. Interpreted magnetic anomalies are shown in Figure 6-12.

Several linear magnetic anomalies were identified in the immediate vicinity of known underwater cables and pipelines across the site.

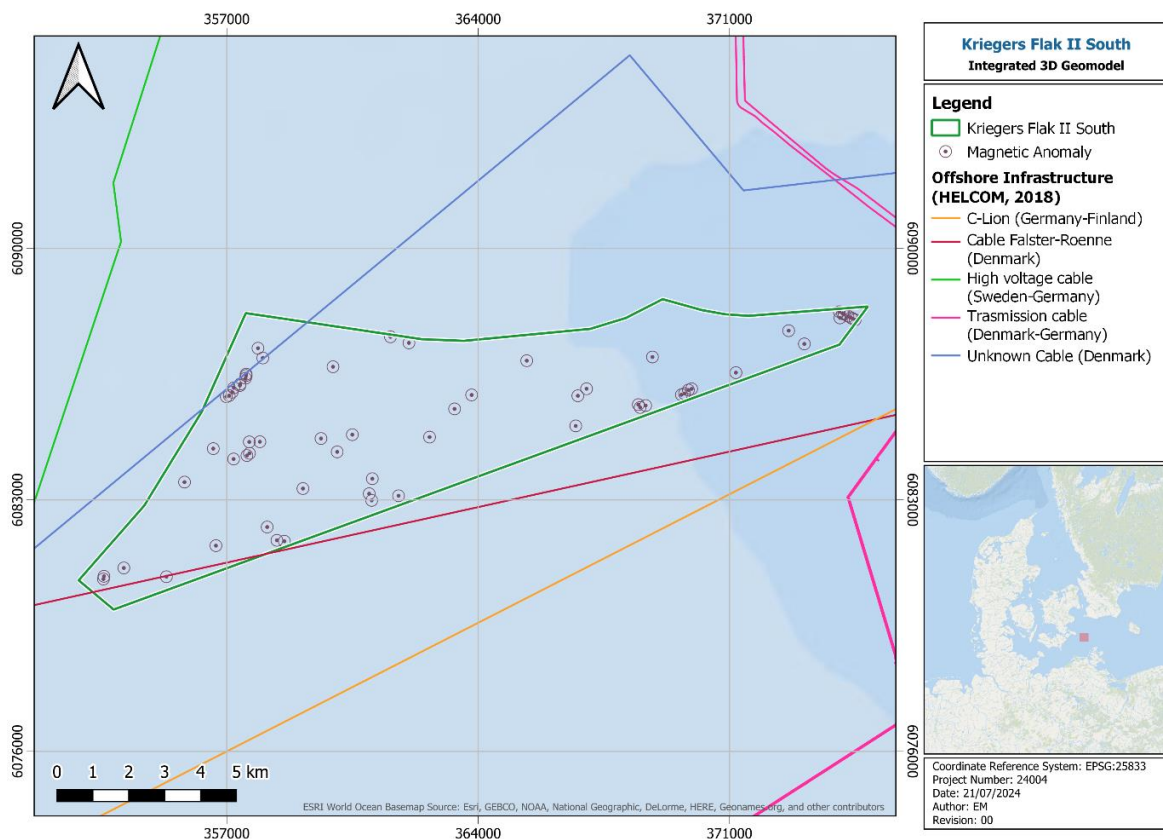


Figure 6-12 - Magnetic contacts and offshore infrastructure (Helcom, 2018)

6.2 SUB-SEAFLOOR INTERPRETATION

Any mention of “seismic unit” or simply “unit” refers to seismostratigraphic units.

Four horizons were interpreted in the seismic data, differentiating three seismic units. Two of the units were further subdivided into two subunits based on lithological and/or seismic facies variations. Table 6-2 shows a summary of the interpreted seismic units and horizons, their acoustic characteristics, age, lithology, and depositional environment (based on newly acquired geotechnical data and literature). A cross-sectional schematic diagram showing the approximate unit distribution across the width of the survey area, west to east, is presented in Figure 6-13. Detailed descriptions of each seismic unit are presented in sections 6.2.1 to 6.2.5. A summary of maximum and minimum elevations, depths, and thicknesses for each seismic unit can be found in Table 6-3. Description of additional elements identified during the seismic interpretation can be found in section 8.2.

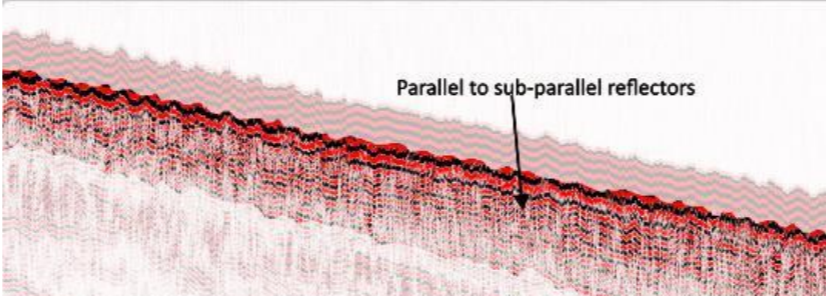
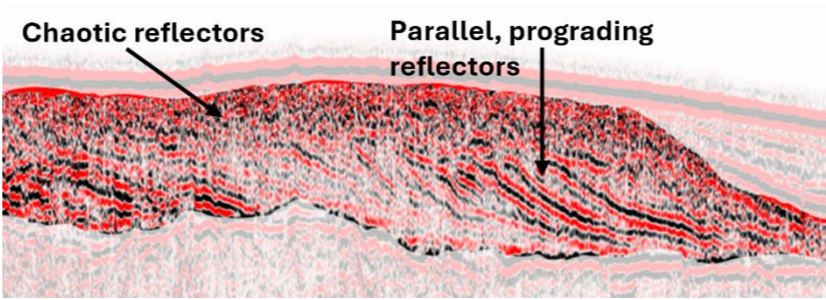
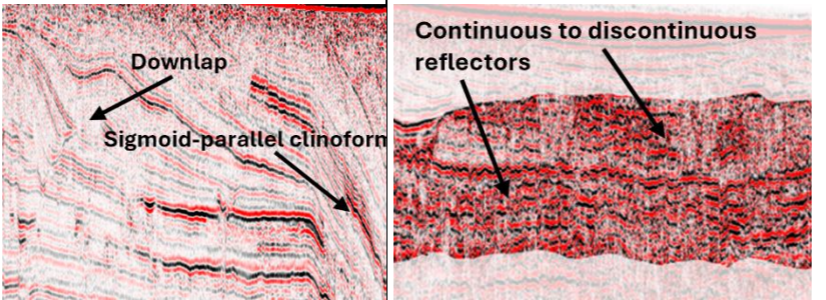
In addition to the figures shown in section 6.2, counterpart charts are also provided in Appendix A. Charts 24004-MSL-003-05-01 to 24004-MSL-003-09-01, show the elevations (mMSL) of the tops of seismic units I to IVa. Charts 24004-BSF-002-05-01 to 24004-BSF-002-08-01 show depths (mBSF) to the top of seismic units I to IVa. For the shallowest units, the charts displaying the top of the unit relative to depth below seafloor will be equal to zero as their unit top is the seafloor. Charts 24004-ISO-004-04-01 to 24004-ISO-004-06-01 show isochores (vertical thickness in metres) for seismic units I to IIIb. Charts with interpreted seismic cross sections are shown in Appendix B (Charts 24004-PRO-006-13-00 to 24004-PRO-006-24-00).

The seismic unit numbering takes into account the two units that have not been interpreted in the seismic data as it was not part of the remit of this study. These consist of:

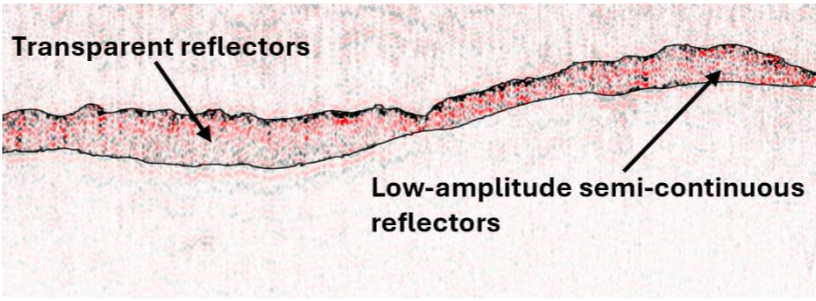
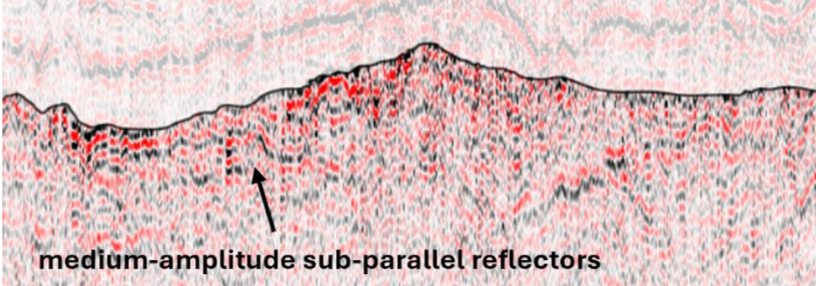
- Unit II (post-glacial transition) was only partially observed in some of the SBP lines and so a seismic unit could not be interpreted. This unit is believed to be a transitional layer between Unit I and Unit III, sharing similar geotechnical properties with both Geotechnical Unit (GU) Ib and GU IIIa1. It was considered to have limited impact on design, because its geotechnical properties are captured by the overlying (GU Ib) and underlying (GU IIIa1) sub-units.
- Unit IV, glacial till, which was identified in some of the borehole locations was not observable within the seismic datasets. Where this unit was interpreted geotechnically, there was no significant change to the associated seismic facies and no clear reflector was present to allow a separate unit to be picked. Therefore, this unit was not included within the seismic unitisation, but the numbering accounts for it given its presence within the geotechnical data. This remains an uncertainty in the IGM for its position at the H20 interface with unlithified chalk and has been included in the IGM uncertainty Table 6-6.

Table 6-2 - Overview of the interpreted units

Overview of the interpreted units

Seismic Unit	Geotechnical Unit	Seismic Dataset	Top Horizon	Base Horizon	Seismic Facies Description	Seismic Facies Example	Age	Geotechnical Description	Depositional Environment
Unit I (SU I)	Ia	SBP	H00 Seafloor	H05	Medium amplitude, chaotic reflections displayed in the upper part, with medium amplitude, subparallel to parallel semi-continuous reflectors seen in the mid-section. The lower part displays lower amplitude, transparent reflectors		Holocene	loose to medium dense SAND	Marine
	Ib							Very low to low strength CLAY	
Unit IIIa (SU IIIa)	IIIa1	UHRS	H00 H05	H15	The upper parts show chaotic reflectors directly below the seabed and overlying Unit 1, with parallel, prograding reflectors seen. Lower part shows high amplitude sigmoid to oblique-tangential clinofoms. Areas of medium to high amplitude sub-parallel semicontinuous reflectors observed		Pleistocene (Weichselian)	Medium to high plasticity, very low to low strength CLAY	Late glacial/ glaciolacustrine
	IIIa2							Dense to very dense silty SAND	
Unit IIIb (SU IIIb)	IIIb1	UHRS	H00 H05 H15	H20	<p>The upper section typically shows medium to high amplitude, subparallel semi-continuous reflectors. The lower section shows high amplitude, continuous reflectors of sigmoid-parallel clinofoms. Local downlap observed.</p> <p>Areas of medium to high amplitude prograding and continuous, parallel reflectors were also observed.</p>		Pleistocene (Weichselian)	Silty to very silty, slightly sandy, medium to high plasticity, very low to low strength, CLAY	Late glacial/ glaciolacustrine
	IIIb2							Very dense, sorted to well sorted, micaceous, slightly calcareous fine to medium, SAND with trace to rare organic matter	
	IIIb3							Medium dense to dense silty SAND with closely to widely spaced thin beds of clay	
	IIIb4							Slightly to very sandy, medium to high slightly clayey to clayey SILT/ Interbedded sandy CLAY	
	IIIb5							sandy, slightly gravelly, medium to extremely high strength CLAY	

Overview of the interpreted units

Seismic Unit	Geotechnical Unit	Seismic Dataset	Top Horizon	Base Horizon	Seismic Facies Description	Seismic Facies Example	Age	Geotechnical Description	Depositional Environment
	IIIb6							CLAY TILL, very silty, very sandy, slightly gravelly, low plasticity, micaceous, highly calcareous (Very high to extremely high strength), sand is fine to medium, gravel is fine, of mixed lithology	
Subunit Va (SU Va)	Va	UHRS	H20	H35	Low to medium amplitude, subparallel semi-continuous reflectors, locally contorted. In addition, locally high-amplitude dipping reflectors were identified in channel-like incision features.	 <p>Transparent reflectors</p> <p>Low-amplitude semi-continuous reflectors</p>	Upper Cretaceous	CHALK (Dm/Dc), unlithified (H1), very light grey to white (N8-N9), highly calcareous, with fine to medium gravel sized fragments of chalk (A1), slightly indurated (H2), white (N9), highly calcareous	Marine (sedimentary bedrock)
Subunit Vb (SU Vb)	Vb	UHRS	H35	N/A	The upper parts show multiple Low to medium amplitude, subparallel semi-continuous reflectors. The lower part is of low amplitude and transparent.	 <p>medium-amplitude sub-parallel reflectors</p>	Upper Cretaceous	CHALK (A1-B4), slightly indurated (H2), slightly fractured (S2), white (N9), highly calcareous (Very weak), interbedded with thin laminations to very thin beds of marl, medium grey (N5), highly calcareous and with rare medium gravel to stone sized fragments of chert, very strongly indurated (H5), dark grey to black (N3-N1), non calcareous (Very strong to extremely strong)	Marine (sedimentary bedrock)

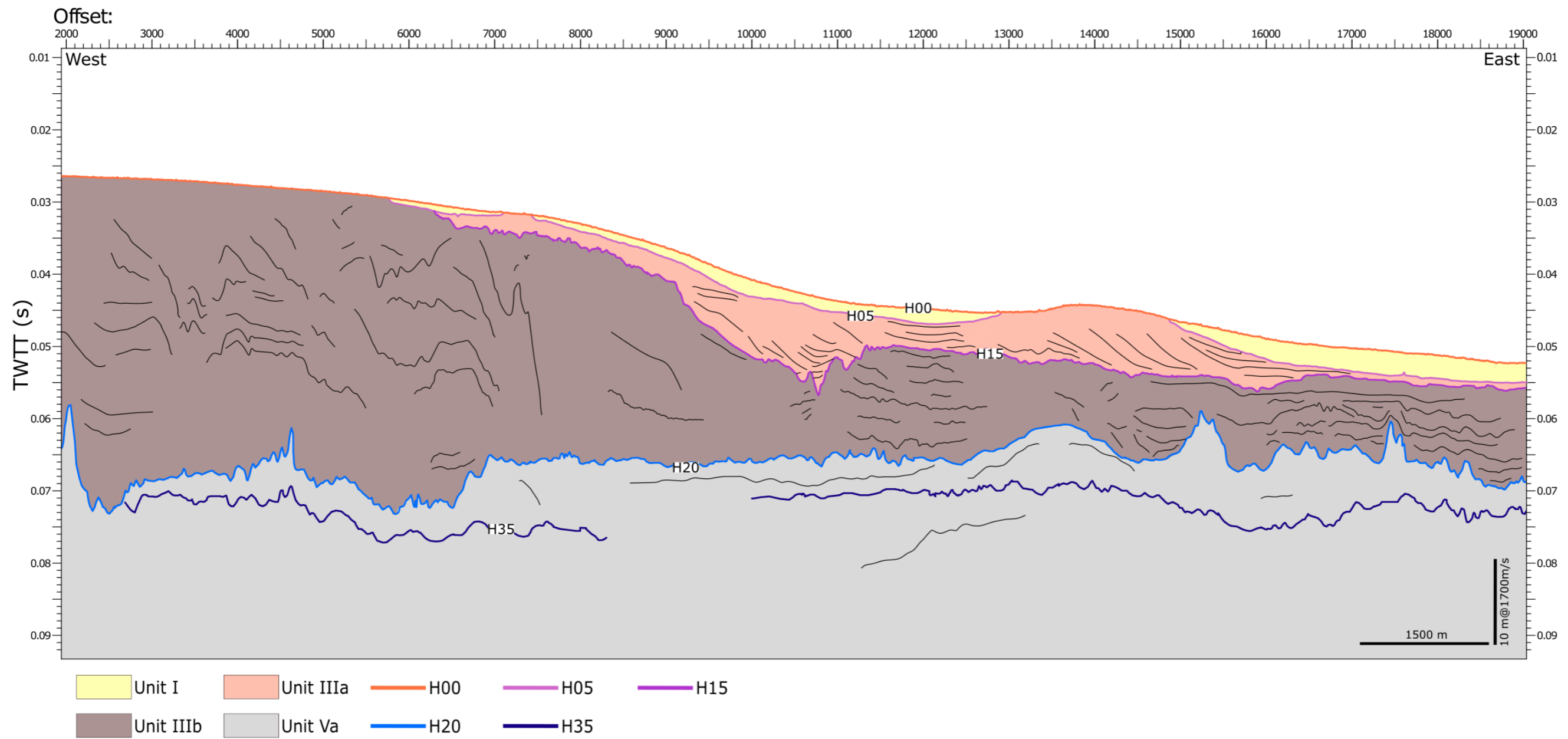


Figure 6-13 - Schematic diagram of unit distribution in the survey area

6.2.1 SEISMIC UNIT I (SU I) - MARINE SEDIMENTS

6.2.1.1 GEOPHYSICAL DESCRIPTION

The top of Unit I corresponds to the seafloor, which is represented by a high amplitude reflection across the entirety of the site. The upper section of the unit displays medium amplitude, chaotic reflections, with medium amplitude, sub-parallel to parallel semi-continuous reflectors observed in the mid-section. Often the unit is represented as lower amplitude, and transparent seismic facies. Seismic horizon H05 corresponds to the base of Unit I H05 represents the interface between seismic units I and IIIa, though in some areas, where H05 becomes shallower and truncates against the seabed, there is some evidence of an underlying unit (Unit II), though the visibility and occurrence of these reflectors are low such that a corresponding unit/reflector was not picked. It is believed this may correspond to Unit II, post-glacial transition (section 6.2, non-interpreted units summary).

H05 was solely mapped on the SBP, with minimal reflectors seen within the depth range of the unit within the UHRS data.

6.2.1.2 SPATIAL DISTRIBUTION

Unit I was interpreted across most of the site, except for areas in which the unit is truncated against the seabed or is not seen within the seismic data. This corresponds to a north-south trending gap that spans the width of the site in the eastern-central area and four smaller gaps spread across the north and southern site boundary of the western-central area. In the southwest of the site the unit has not been interpreted (refer to section 6.2.1.4 for further detail). The top of the unit corresponds to the seabed and its elevation varies between -21.3 to -41.8 mMSL (Figure 6-14).

The unit is present as a relatively thin layer of up to 2.8 m thick, as shown in the isochore map (Figure 6-15), with the highest thicknesses observed in the central and eastern parts of the site. The unit is at its thinnest in the centre of the site, alongside areas in which the unit is pinching out against the seabed (Figure 6-15).

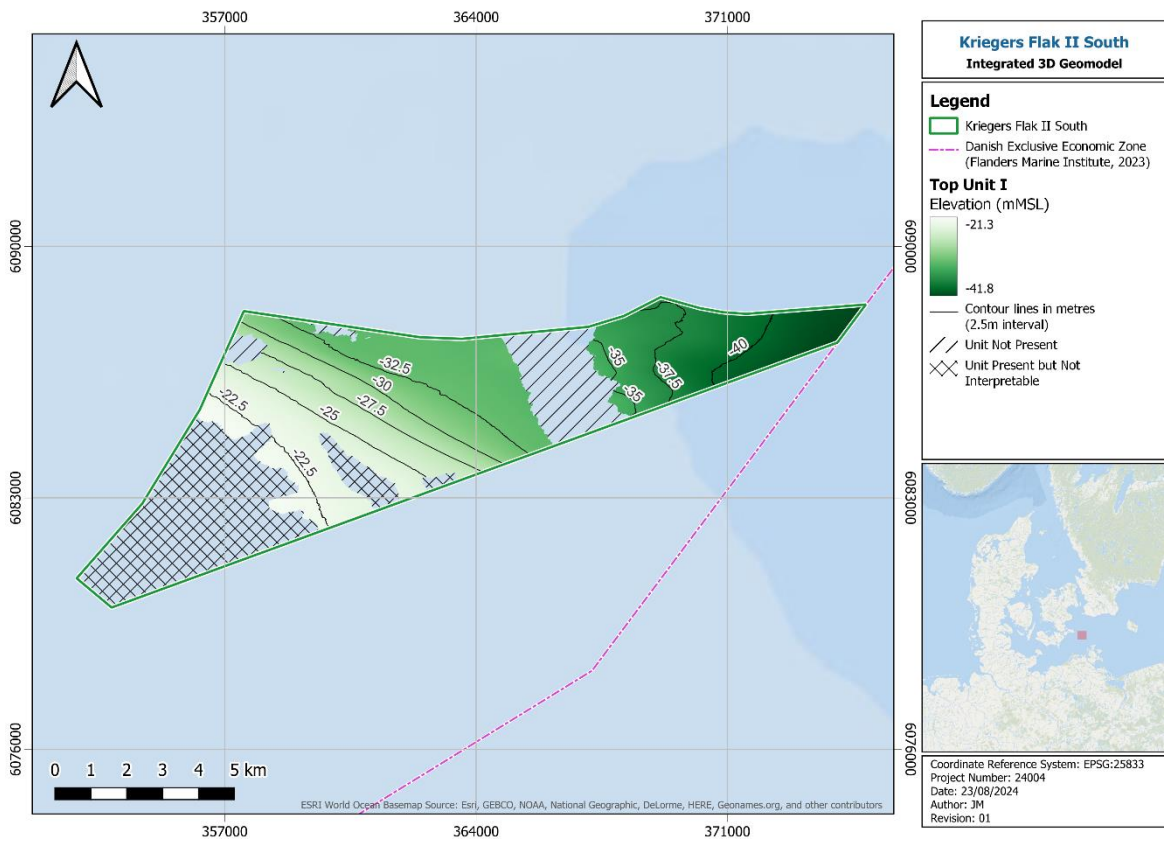


Figure 6-14 - Top of Unit I elevation (mMSL)

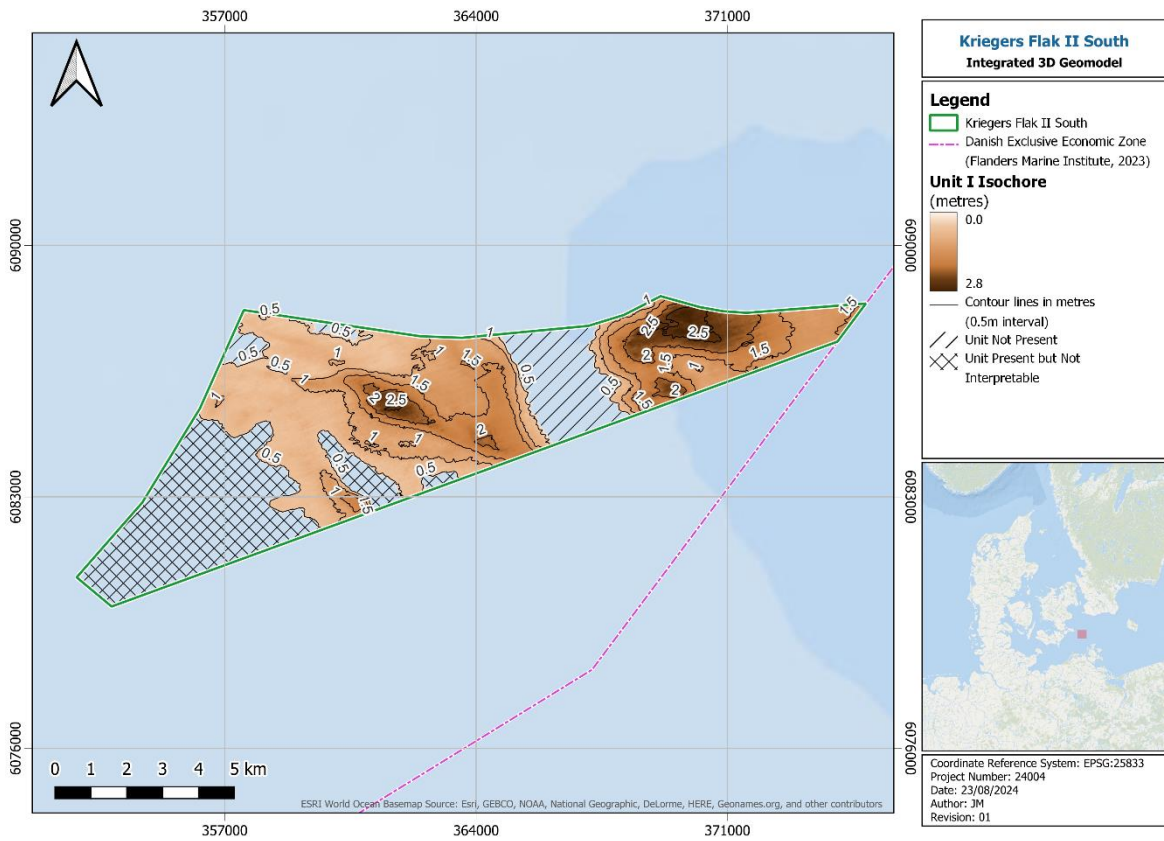


Figure 6-15 - Unit I vertical thickness isochore

6.2.1.3 GEOTECHNICAL DESCRIPTION

Unit I is described based on seismic as medium amplitude, chaotic reflections displayed in the upper part, with medium amplitude, subparallel to parallel semi-continuous reflectors seen in the mid-section. The lower part displays lower amplitude, transparent reflectors.

The geotechnical properties for this unit were described from CPT data to determine the appropriate geotechnical unitisation. Unit 1 was split into two geotechnical units:

- GU Ia described as a medium to loose sand.
- GU Ib described as very low to low strength clay.

6.2.1.4 INTERPRETATION

Seismic horizon H05 is a continuous reflector, corresponding to the base of Unit I. Locally this represents the top of Units IIIa and IIIb where each respective unit is underlying Unit I. This reflector marks the transition from the mostly transparent lower facies of Unit I and the reflectors of increased amplitude of Unit IIIa and Unit IIIb. Where the unit is truncated against the seabed it is not possible to fully trace H05 up to the H00 (seabed) reflector due to the width of the ringing signal of the seabed reflection (Figure 6-16). Due to this, pseudo picks were applied to force the horizon up to and above the seabed for gridding purposes. The effect of the pseudo pick is visible within the final grids, though this is the current limitation of the methodology at this iteration of the IGM. An example of the seismic and geotechnical integration is presented in Figure 6-17 (GI locations are imported to UHRS seabed levels and so there is a slight vertical offset when displayed on SBP lines).

During this interpretation, the Unit I extents have been refined and revised based on the original extents provided by GeoXYZ (GEOxyz, 2024). The original H05 interpretation (GEOxyz, 2024) had a much more extensive coverage of the site, with the main difference being the coverage in the southwest part of the site. In the southwest of the site, the original H05 pick extended into the ringing component of the seabed and it was not clear as to where the true H05/base of Unit I was. The decision was made to remove all affected areas and the current extents reflect this. It is likely that a thin layer of surficial sediments corresponding to Unit I are present, though they are not distinguishable from the seabed ringing of the current SBP dataset.

The SBP dataset had an inconsistent tidal reduction applied during the original data processing stage (GEOxyz, 2024). This adds difficulty to establishing a consistent H05 pick and tie-in across a large dataset when working in Two-Way Travel Time (TWTT). Every effort has been made to reduce offsets between lines using mistie analysis, though there may be some remnant evidence of this in the final grids.

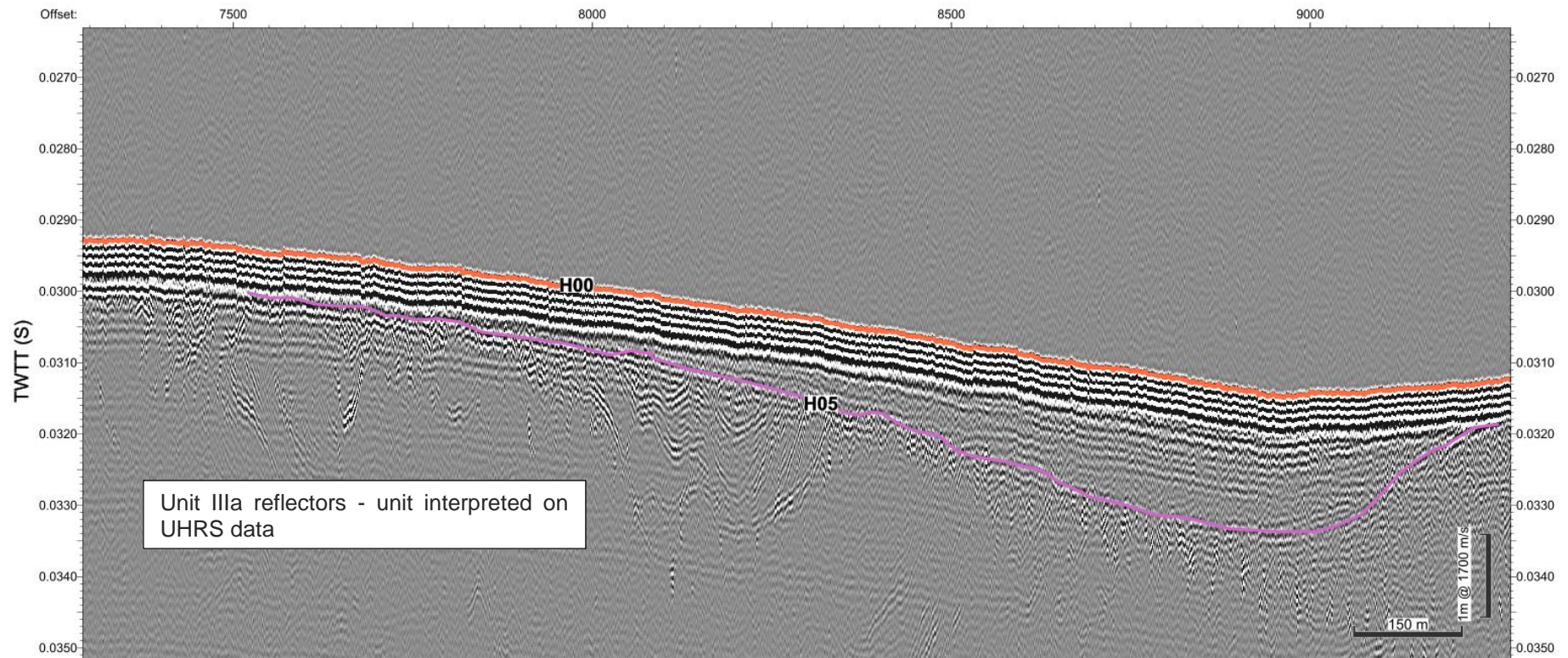


Figure 6-16 - Interpretation of SBP line 1755

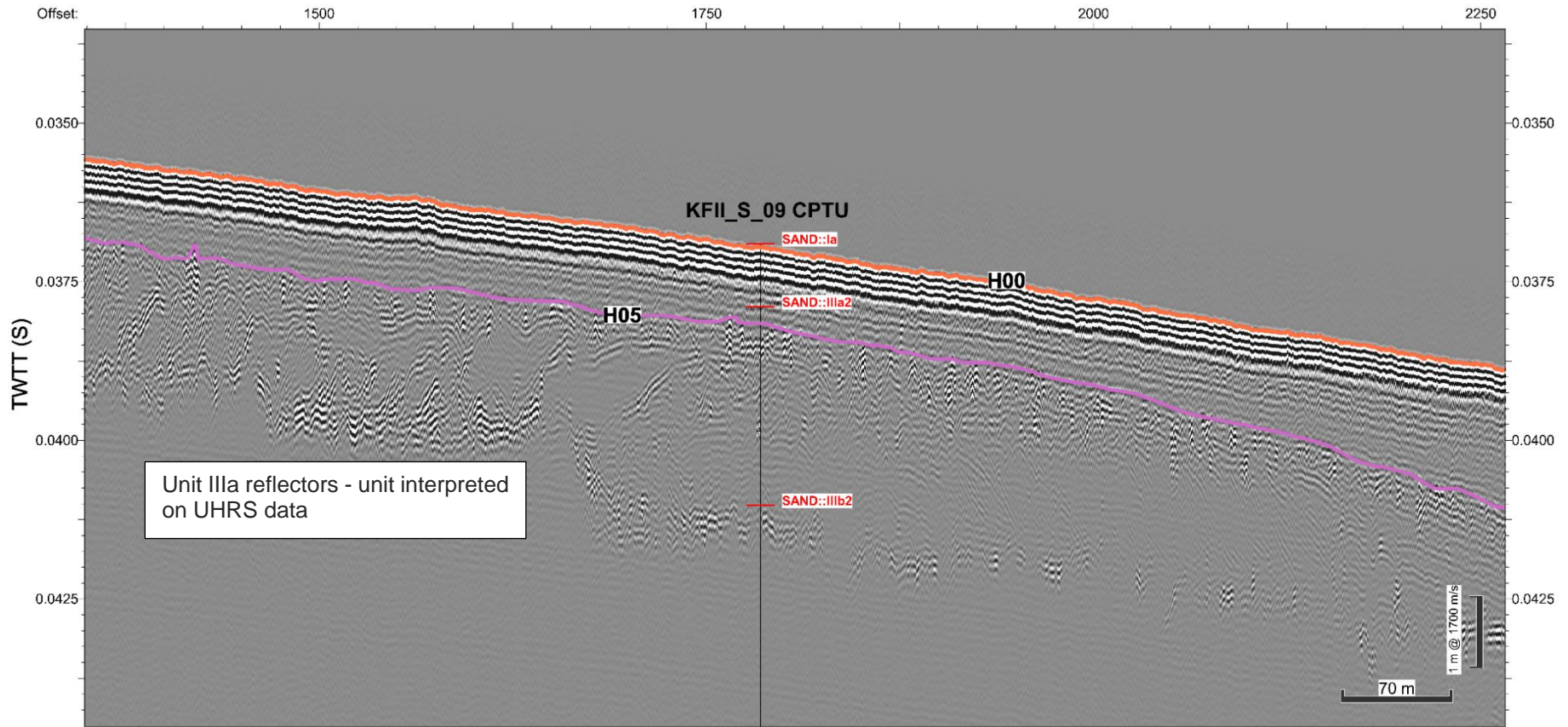


Figure 6-17 - SBP line X011 integration

6.2.2 SEISMIC UNIT IIIA (SU IIIA) - UPPER GLACIOLACUSTRINE

6.2.2.1 GEOPHYSICAL DESCRIPTION

Unit IIIa is bounded by H05 and H00 at the top and H15 at the base. The internal seismic facies consist of medium to high amplitude chaotic reflections at the top of the unit where it is bounded by H00. The lower part shows high amplitude sigmoid to oblique-tangential clinoforms and occasionally medium to high amplitude, sub-parallel semicontinuous reflectors. The unit typically demonstrates more structured reflections (either prograding or sub-parallel) in comparison to the units both above and below it. The base of the unit corresponds to H15. This is a medium to high amplitude, continuous reflector marking the transition between the subdivision of Unit III. The prograding reflectors observed at the lower part of Unit IIIb downlap onto the H15 reflector, and clearly highlight the transition to the sub-unit below.

6.2.2.2 SPATIAL DISTRIBUTION

Unit IIIa was mapped on the UHRS data, though where it was shallow enough it was constrained by the SBP dataset. The Unit is present across the central and eastern parts of the site, and is absent from the southwest, where it truncates against the seabed. The unit elevation varies from -21.4 mMSL to -43.4 mMSL across the site and is deepest in the east and at its shallowest in the western extent of the unit interpretation (Figure 6-18). The vertical thickness (shown in Figure 6-19) shows areas of increased thickness in the centre of the site, sub-cropping the seabed where Unit I is absent. The unit thickness varies from 0.1 m to 8.4 m.

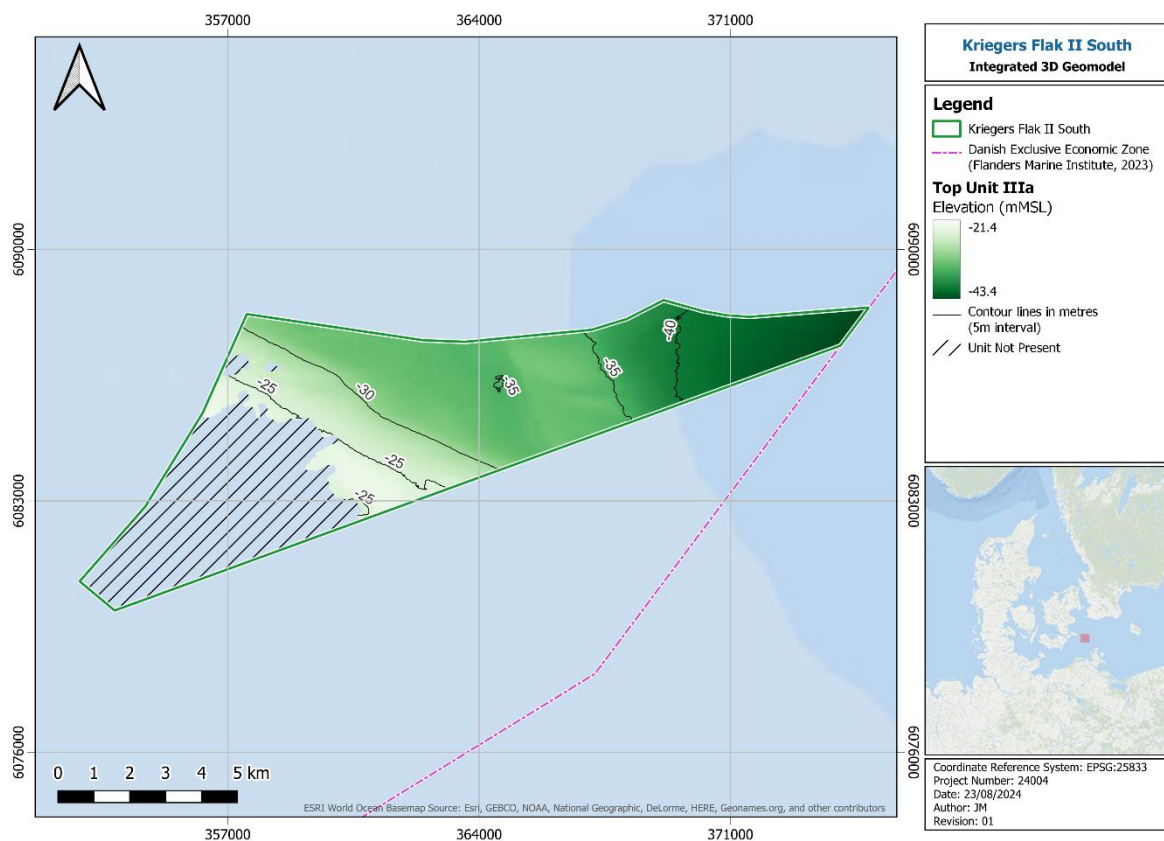


Figure 6-18 - Top of Unit IIIa elevation (mMSL)

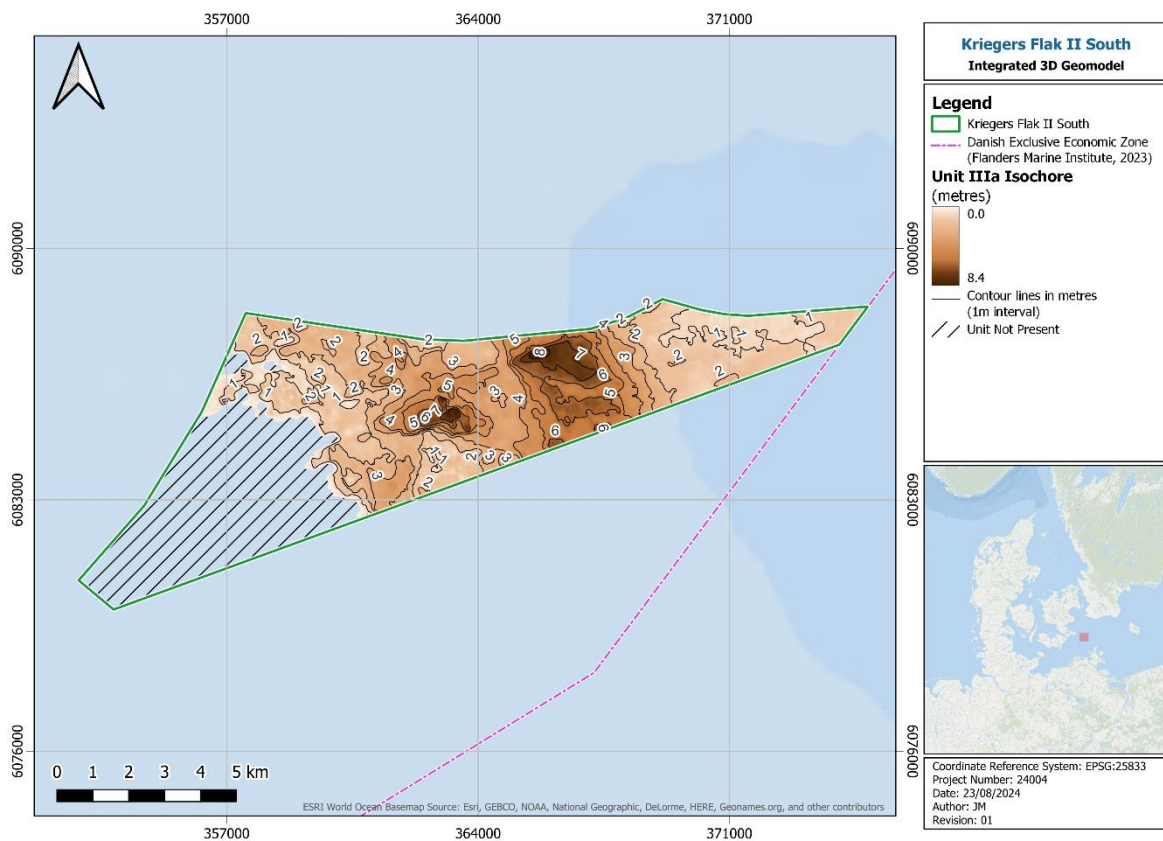


Figure 6-19 - Unit IIIa vertical thickness isochore

6.2.2.3 GEOTECHNICAL DESCRIPTION

Unit IIIa is described based on seismic as having a lower and upper. The upper parts show chaotic reflectors directly below the seabed and overlying Unit 1, with parallel, prograding reflectors seen. Lower part shows high amplitude sigmoid to oblique-tangential clinoforms. Areas of medium to high amplitude sub-parallel semicontinuous reflectors are observed.

The geotechnical properties for this unit were described from CPT data, PSD and Atterberg limit test data to determine the appropriate geotechnical unitisation . Unit 3a was split into two geotechnical units:

- GU IIIa1 described as medium to high plasticity, very low to low strength clay
- GU IIIa2 described as dense to very dense silty sand

6.2.2.4 INTERPRETATION

The internal prograding reflectors of Unit IIIa are described by (Jensen, et al., 1997) in their documented E3 sequence, and were reported to reduce in thickness to 10 m towards the east of the Arkona Basin, conforming with the results presented in the Unit IIIa isochore (Figure 6-19). These deposits, of ice-lake origin during the late glacial period (Jensen, et al., 1997).

The H15 reflector (base of Unit IIIa) was interpreted on the UHRS data. This provided sufficient resolution at depth where the base of the unit extended deeper below the seabed. The SBP data provide improved shallower resolution for the unit, though in the SBP dataset the base is often not seen within the attenuated component of the seismic signal. For this reason, the H15 reflector was interpreted using the UHRS data, however, the SBP dataset was used to

constrain the unit base where is became shallower and the base became more difficult to interpret within the UHRS dataset. An example of seismic and geotechnical data integration is presented in Figure 6-20.

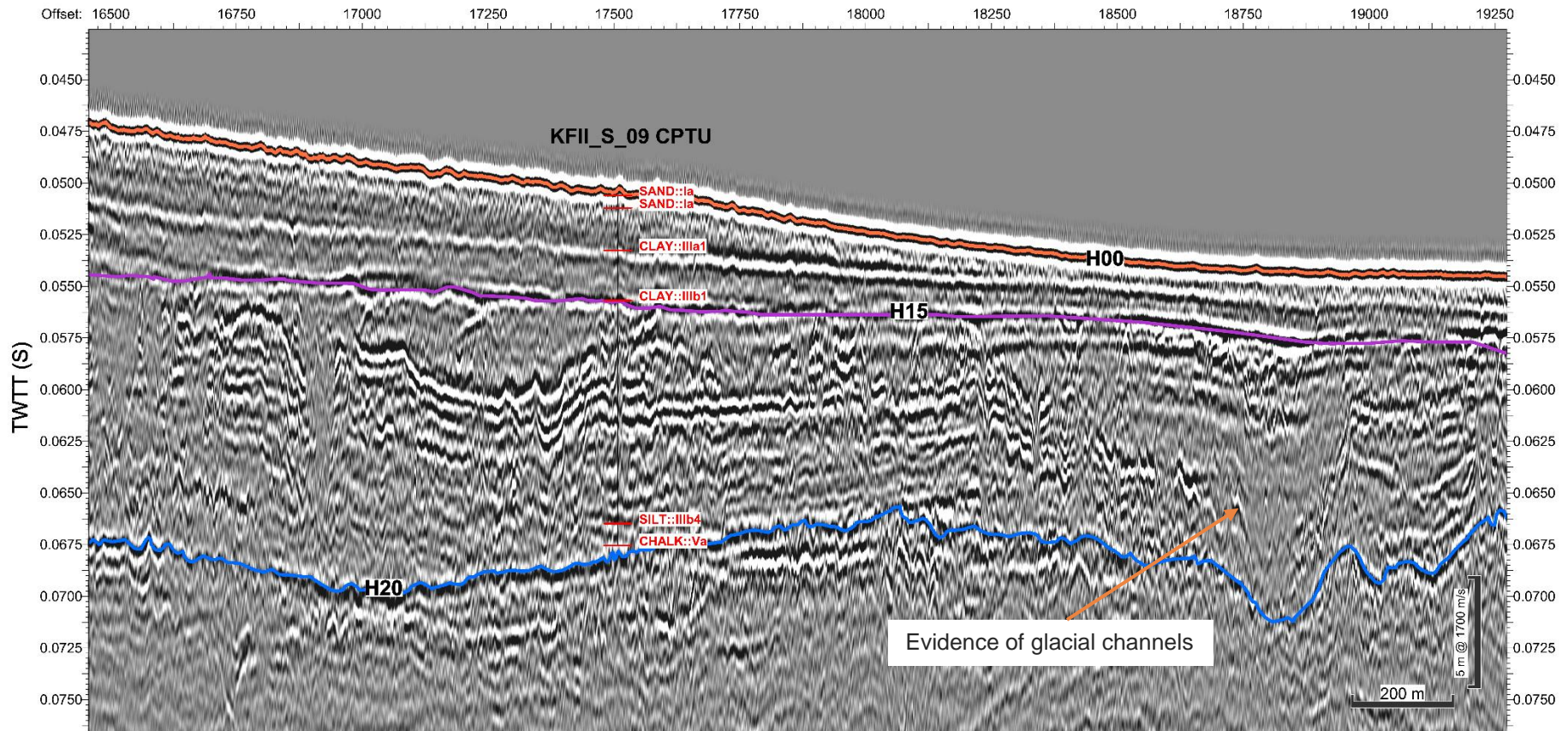


Figure 6-20 - UHRS line L025 integration

6.2.3 SEISMIC UNIT IIIB (SU IIIB) - LOWER GLACIOLACUSTRINE

6.2.3.1 GEOPHYSICAL DESCRIPTION

Unit IIIb is bounded by H00, H05, and H15 at the top and by H20 at the base. The internal seismic facies of this unit varies laterally across the site, due to the change in unit composition from the varied historic depositional environments that the proposed site extents cover. In the west of the site, the seismic facies show medium to high amplitude, continuous reflectors of sigmoid-parallel clinofolds with localised reflector downlap (Table 6-2).

In the centre of the site, these facies transition to medium to high amplitude, subparallel semi-continuous reflectors in the upper section, Areas of medium to high amplitude prograding and continuous, parallel reflectors were also observed. The lower section shows more reflector variability with reflectors of medium to low amplitude that are semicontinuous to continuous as well as chaotic close to the H20 horizon.

Areas of low amplitude, transparent reflectors have been observed site-wide within Unit IIIb (as well as the shallower Unit IIIa). Within these areas, although continuous reflectors may be disrupted, there is still visibility of some reflectors within and below the reduced amplitude region, indicating that this is not necessarily a gas-blanking related effect, but the presence of gas at the site cannot be fully ruled out (section 8.2.2).

6.2.3.2 SPATIAL DISTRIBUTION

Unit IIIb has been interpreted across all the proposed site extents. The top of the unit displays a variable elevation ranging from 0 - <-20 mMSL in the southwest where the unit is present at the seabed (or beneath a suspected thin surficial layer of Unit I), to -30 to -40 mMSL in the centre of the site, to -40 mMSL in the eastern part of the site (Figure 6-21). The highest thickness of Unit IIIb occurs in the southwest, where the unit is observed to be at the seabed, whereas the remainder of the site, the unit is covered by either Unit IIIa, Unit I or a combination of the two units (Figure 6-22).

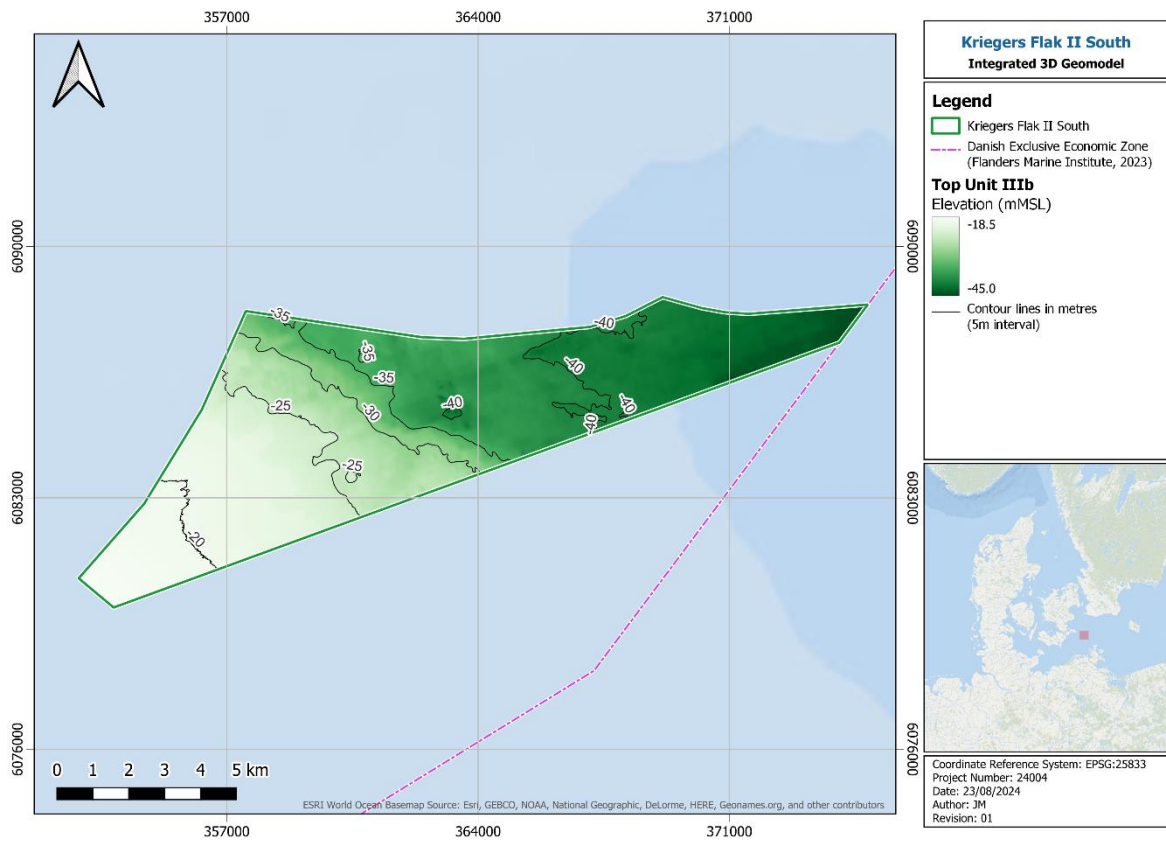


Figure 6-21 - Top of Unit IIIb elevation (mMSL)

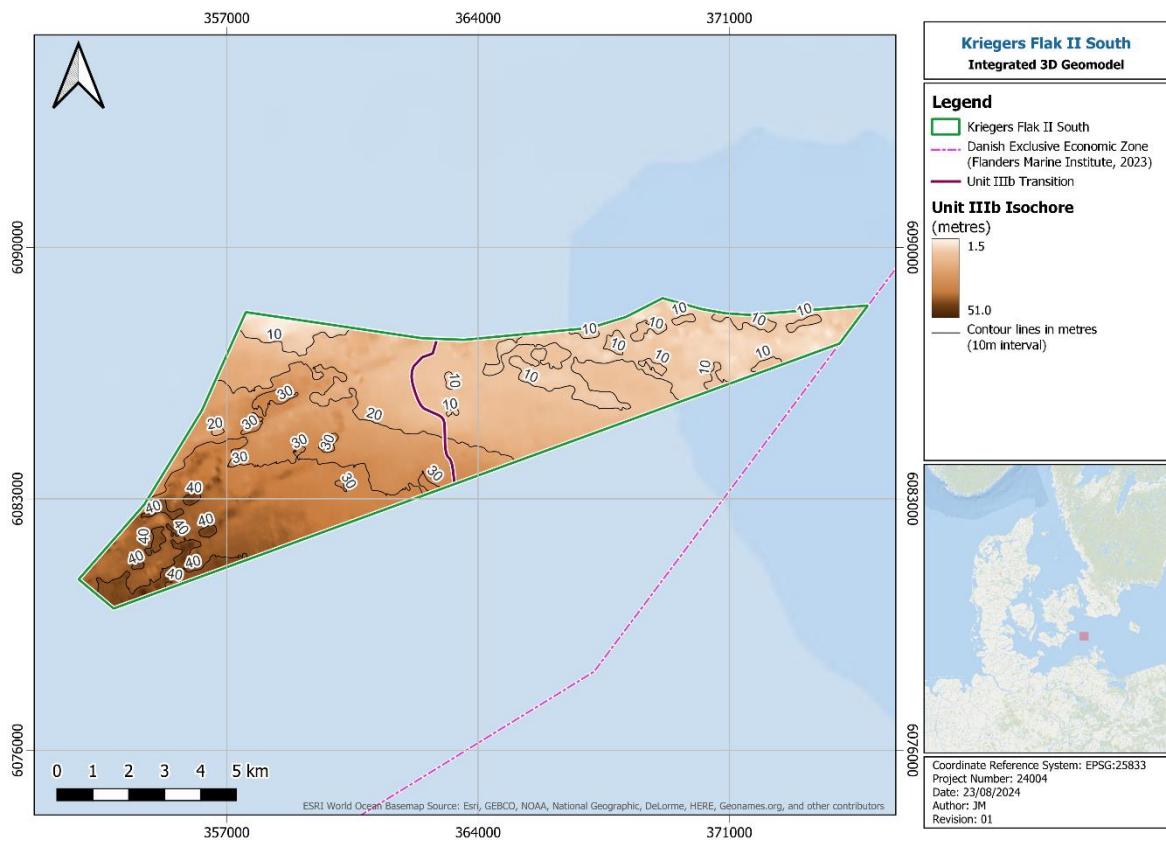


Figure 6-22 - Unit IIIb vertical thickness isochore

6.2.3.3 GEOTECHNICAL DESCRIPTION

Unit IIIb is described based on seismic as having an upper section typically consisting of medium to high amplitude, subparallel semi-continuous reflectors. The lower section shows high amplitude, continuous reflectors of sigmoid-parallel clinofolds. Local downlap observed. Areas of medium to high amplitude prograding and continuous, parallel reflectors were also observed. This indicates that Unit IIIb is very variable consisting of a mix of sand, silt and clay.

The geotechnical properties for this unit were described from CPT data, classification and advanced lab test data to determine the appropriate geotechnical unitisation. Unit 3b was split into six geotechnical units to enable characterisation of similar geotechnical properties.

- GU IIIb1 described as silty to very silty, slightly sandy, medium to high plasticity, very low to low strength, Clay
- GU IIIb2 described as very dense, sorted to well sorted, micaceous, slightly calcareous fine to medium, Sand with trace to rare organic matter
- GU IIIb3 described as medium dense to dense silty Sand with closely to widely spaced thin beds of clay
- GU IIIb4 described as slightly to very sandy, medium to high slightly clayey to clayey Silt/ Interbedded sandy Slay
- GU IIIb5 described as sandy, slightly gravelly, medium to extremely high strength Clay
- GU IIIb6 described as Clay Till: very silty, very sandy, slightly gravelly, low plasticity, micaceous, highly calcareous (Very high to extremely high strength), sand is fine to medium, gravel is fine, of mixed lithology.

6.2.3.4 INTERPRETATION

Based on the available literature (GEUS, 2023; Jensen, et al., 1997; Mathys, et al., 2005), Unit IIIb is interpreted as late glacial to glaciolacustrine in origin. The available literature and previous studies in the surrounding basins report of a prograding sand wedge at the western extents of the Arkona basin (GEUS, 2023; Jensen, et al., 1997). The seismic profiles interpreted as part of the GEUS studies (GEUS, 2023) conform to the newly acquired seismic data, displaying similar stratigraphy originally derived from those studies. The Jensen et al., 1997 study defined an E2 sequence in the Arkona basin, which describes the interpreted sand wedge as the product of a prograding delta system during late-glacial ice lake periods. The seismic facies described conforms with the results of this study and the sand wedge is observed at its maximum thickness in the southwest of the site (up to the seabed), with internal facies indicating an eastwards trend of progradation (Figure 6-23). In the centre of the site, the Unit IIIb seismic facies (and geotechnical data) show a distinct change from the thicker, prograding sand deposits, to comprise more clay sediments and display a more layered seismic reflector pattern. This area of transition is illustrated in Figure 6-22 and in a seismic cross section in Figure 6-23 and Figure 6-24.

Moving eastwards from the area of transition, the unit shows some evidence of possible incision/channel features, though these are variable between UHRS lines and do not present

large-scale features that can be tracked. Evidence of this is visible in Figure 6-23, with dedicated examples presented and discussed in section 8.2.3.

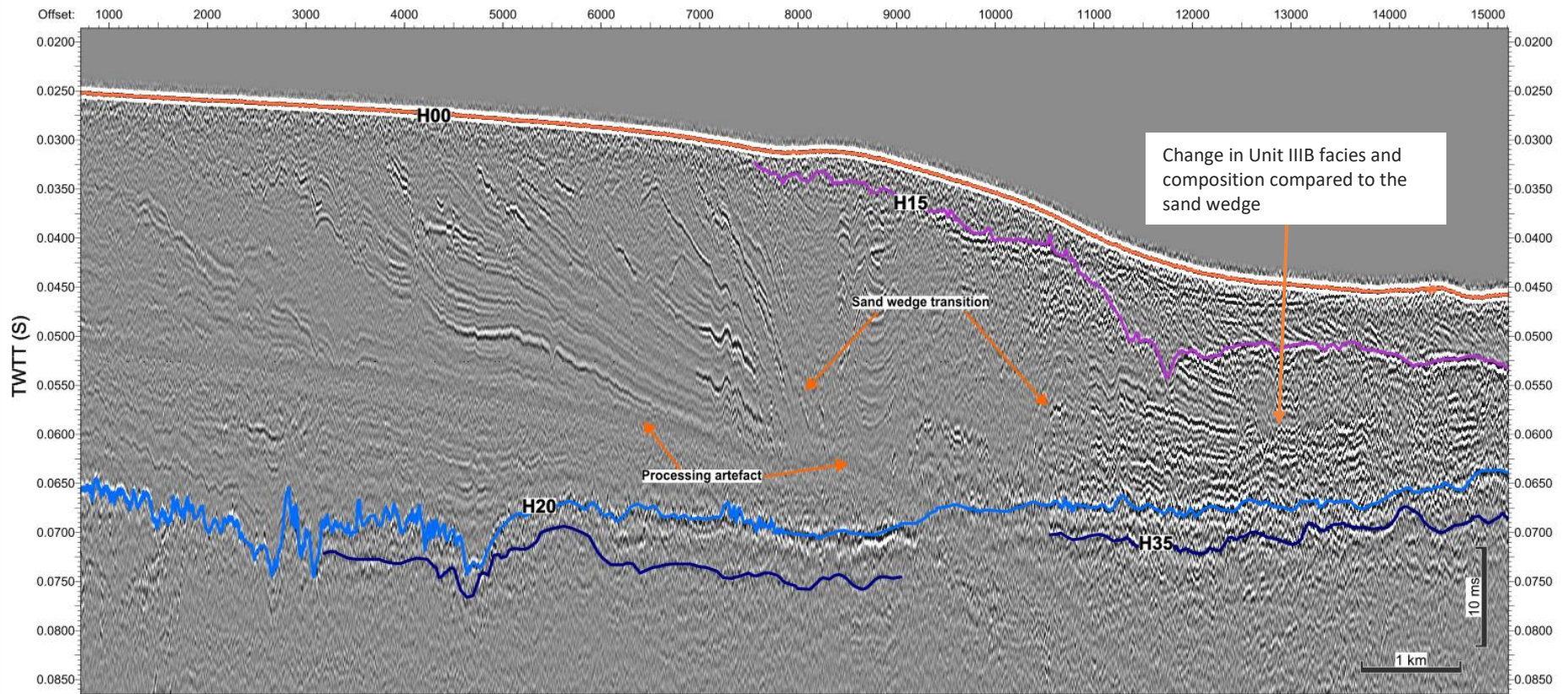


Figure 6-23 - Interpretation of UHRS line L021

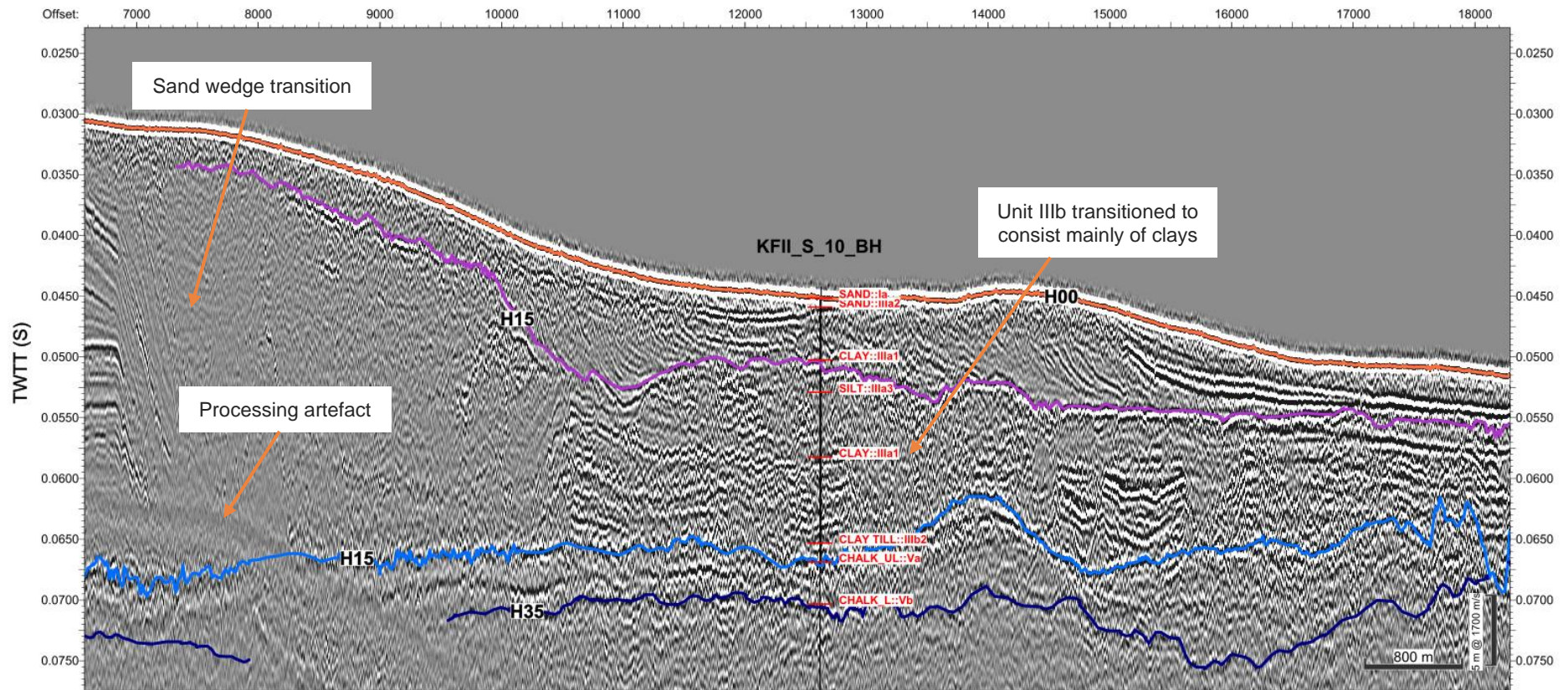


Figure 6-24 - UHRs line L20 integration

(GEUS, 2022) describes the observed transition of the glaciolacustrine unit deposits from comprising sand (coastal derived) sediments in the southwest, to clay deposits moving eastwards towards the centre of the Arkona Basin. It was also reported that a clay layer is present at the base of the glaciolacustrine unit in the Arkona basin. CPT's from the recent campaign have identified clay marks that coincided with the base of the unit (not to be interpreted as till given the continuous and parallel facies). A preliminary interpretation was produced, though it was decided by the client not to proceed with this reflector.

The available studies from GEUS on the proposed site report that from the limited available geotechnical data at the time, their conclusion was that the prograding deposits of the sand wedge are positioned on top of a clay/Till of glacial origin. Unit IV, Till, has not been interpreted within this study due to a lack of visibility of till within the seismic data (GEUS, 2022; 2023).

Limited geotechnical investigation sites (Gardline, 2024) have confirmed a presence of till derived from CPT measurements and recovered borehole samples, though there was insufficient evidence of a till surface reflector within the seismic data to distinguish it from the internal reflectors of lower Unit IIIb. Figure 6-24 shows a clay till top marker (corresponding to the recovered material in borehole KFII_S_10_BH, shown on seismic data in Figure 6-24) positioned above the unlithified chalk surface (H20) with a thin layer thickness. This example alongside occurrences elsewhere across the site, show no significant changes in the seismic facies that would correspond to a distinct till layer. This may be due to the thickness of the till in relation to it overlying unlithified chalk (Figure 6-25) and as such the difference in acoustic impedance and seismic resolution may not be optimal for separation of the two interfaces. With this, Unit IIIb is presented as transitional at its base given the presence of till within the geotechnical data (Figure 6-25) and supporting literature.



Figure 6-25 - KFII_S_10_BH example of till to chalk interface

There is a degree of uncertainty associated with the base of Unit IIIb/ Top of unlithified chalk surface. The exact thickness of the till unit is unknown and not possible to interpret from the current geophysical data. In the west of the site, this interface is affected by the seabed multiple removal artefact and the continuity of the reflector is broken. Targeted geotechnical data alongside appropriate seismic data are required to constrain the base of Unit IIIb from the unlithified chalk in this region and confirm the presence of till. Future data acquisition (both seismic and geotechnical) alongside re-processed UHRS data would be able to better constrain the Unit IIIb / Unit IVa interface in this region to understand if it represents the top of unlithified chalk, till or other units.

6.2.4 SEISMIC UNIT VA (SU VA) - UNLITHIFIED CHALK

6.2.4.1 GEOPHYSICAL DESCRIPTION

The top of Unit Va corresponds to H20 (base of Unit IIIb). It represents the top of Unlithified chalk (UL) and has been interpreted on UHRS seismic data. The top of the unit is bounded by the high amplitude, continuous H20 reflector. Internally, the unit displays low to medium amplitude, subparallel semi-continuous reflectors, locally contorted. In addition, locally high amplitude dipping reflectors were identified in possible incision features. The unit is bounded at its base by H35 (top of Unit Vb - lithified chalk) where it can be interpreted. In the current seismic data, the H35 reflector is not continuously visible and therefore cannot be fully relied upon to produce a true thickness of Unit Va.

6.2.4.2 SPATIAL DISTRIBUTION

Unit Va has been interpreted across the entire proposed site in the UHRS dataset. The top of the unit has a variable elevation based on the thickness of the overlying Unit IIIb and shallower deposits. It ranges from -35.2 mMSL to -70.1 mMSL (Figure 6-26). The top of the unit is deepest in the southwest of the site, where the overlying Unit III sand wedge extends up to the seafloor where it reached its largest thickness. The unit top elevation reduces from the centre to the east of the site, as well as in the far north of the site where unit top reaches its shallowest elevation of -35.2 MSL.

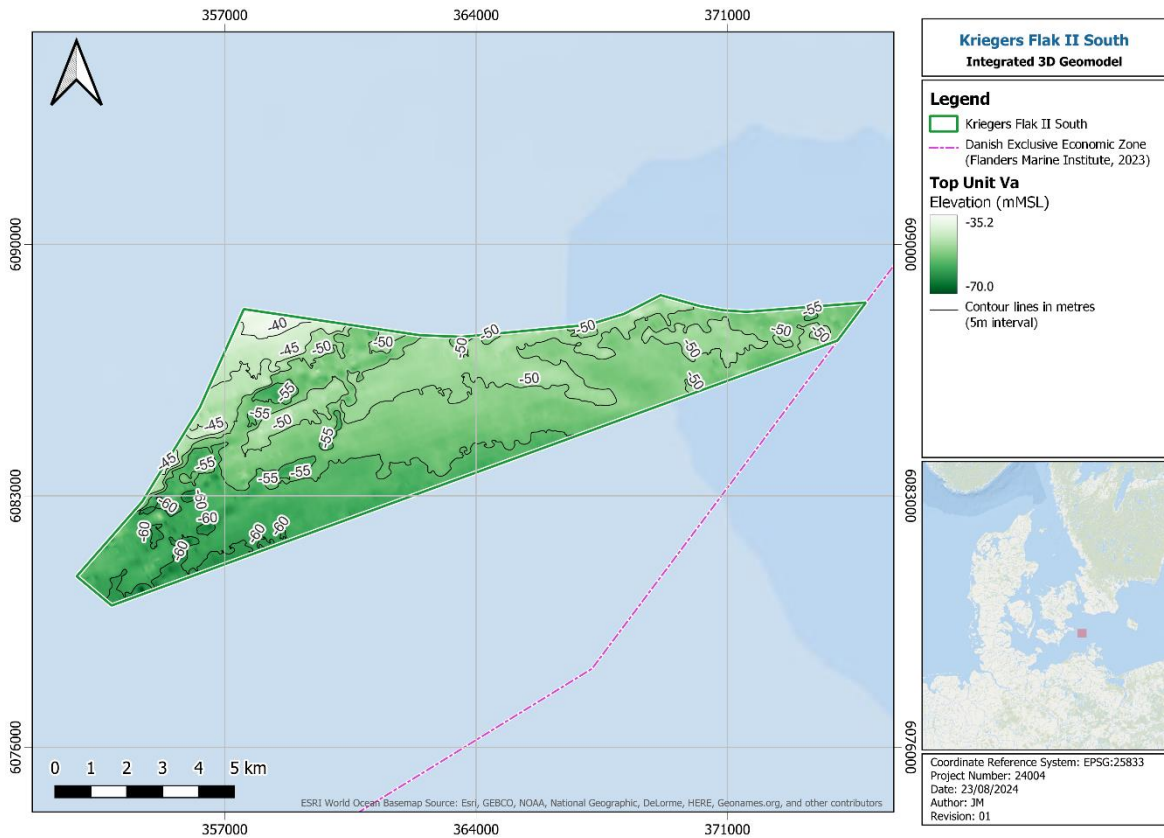


Figure 6-26 - Top of Unit Va elevation (mMSL)

6.2.4.3 GEOTECHNICAL DESCRIPTION

Unit Va is described based on seismic as Low to medium amplitude, subparallel semi-continuous reflectors, locally contorted. In addition, locally high-amplitude dipping reflectors were identified in channel-like incision features. This unit is generally described as the top on the chalk unit and identified as unlithified (structureless) Chalk.

Geotechnical unitisation within this unit was identified from CPT data, sampling and laboratory test data. It should be noted that where CPT data only was performed, top of the unlithified chalk was not always picked with certainty. This led to review and reprocessing of some of the top of the unlithified chalk with geophysical seismic points.

Unit Va was characterised as GU Va which is described as Chalk (Dm/Dc), unlithified (H1), very light grey to white (N8-N9), highly calcareous, with fine to medium gravel sized fragments of chalk (A1), slightly indurated (H2), white (N9), highly calcareous.

6.2.4.4 INTERPRETATION

Unit Va has been interpreted to be the class D, unlithified chalk (of upper Cretaceous age) identified on the recovered boreholes (Gardline, 2024) across the site. As discussed in section 6.2.3, this interface and its interaction with the base of Unit IIIb presents some uncertainty across the site due to the till surface that has not been interpreted within the seismic but identified in the geotechnical results. In the west of the site the processing artefacts present in the data add more complexity to the interpretation of deeper reflectors and affects their continuity. In addition to processing artefacts, in the southwest corner of the site, there are higher amplitude, dipping reflectors indicating a possible channel incision in the rock (Figure 6-27). For context, an example of geotechnical integration is provided in Figure 6-28. From the seismic lines that extend away from the site extents, this feature can be seen to extend both south and west of the site boundary. This possible incision appears to have multiple infill events; however, it was decided by the client that these would not be picked or provided as part of this study. High-level extents of the features are provided in Figure 6-29

With H20 marking the Top of UL chalk, the current interpretation strategy would not allow this infill to be glacial in origin. Given the complexity in identifying the till at the UL chalk interface, it may be possible that in this incision infill, the till dominates in multi-infill patterns, with the UL chalk absent or not resolved in the current seismic data resolution/penetration. In this case the current H20 reflector may represent a top of till surface, though targeted geotechnical investigations are required in this area to identify the origin of the infill material as there is currently no geotechnical investigation locations close enough to constrain this uncertainty.

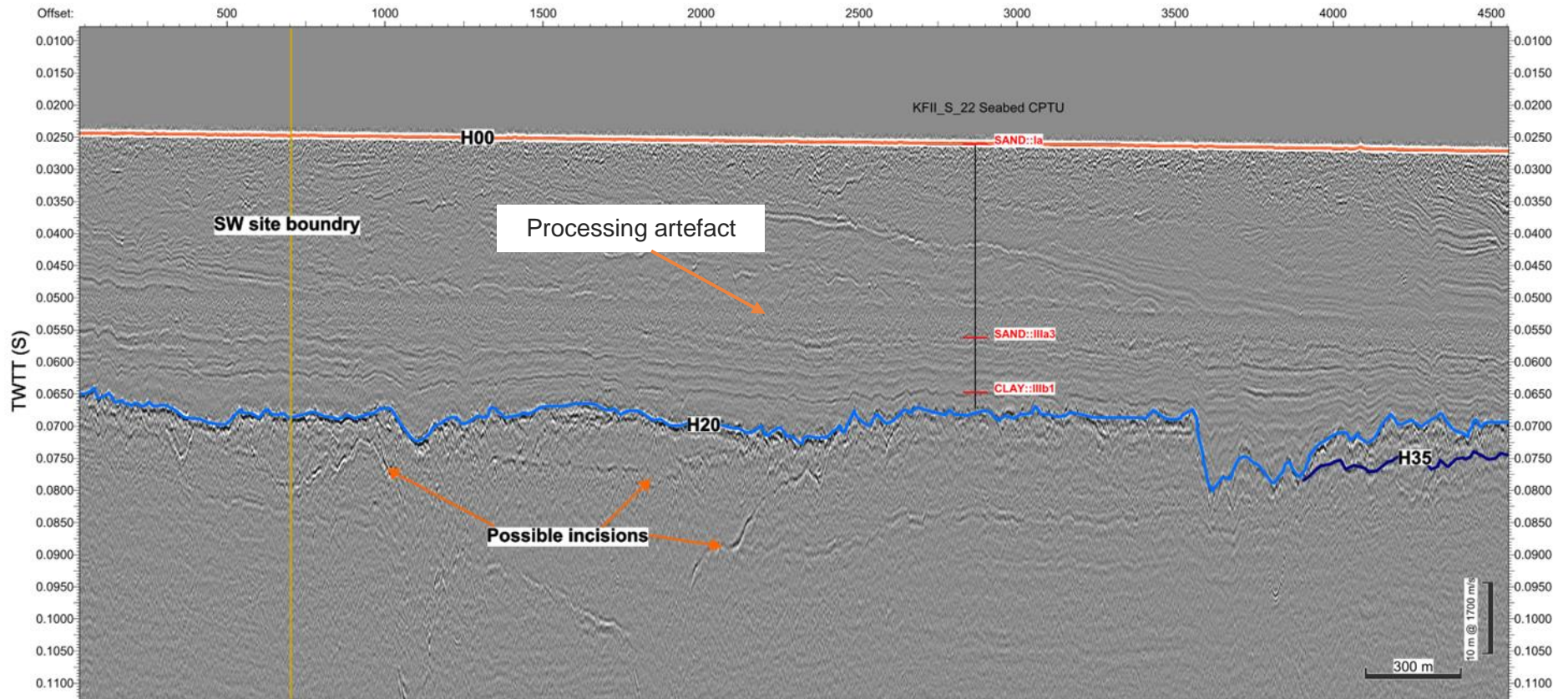


Figure 6-27 - Interpretation of UHRs line L023

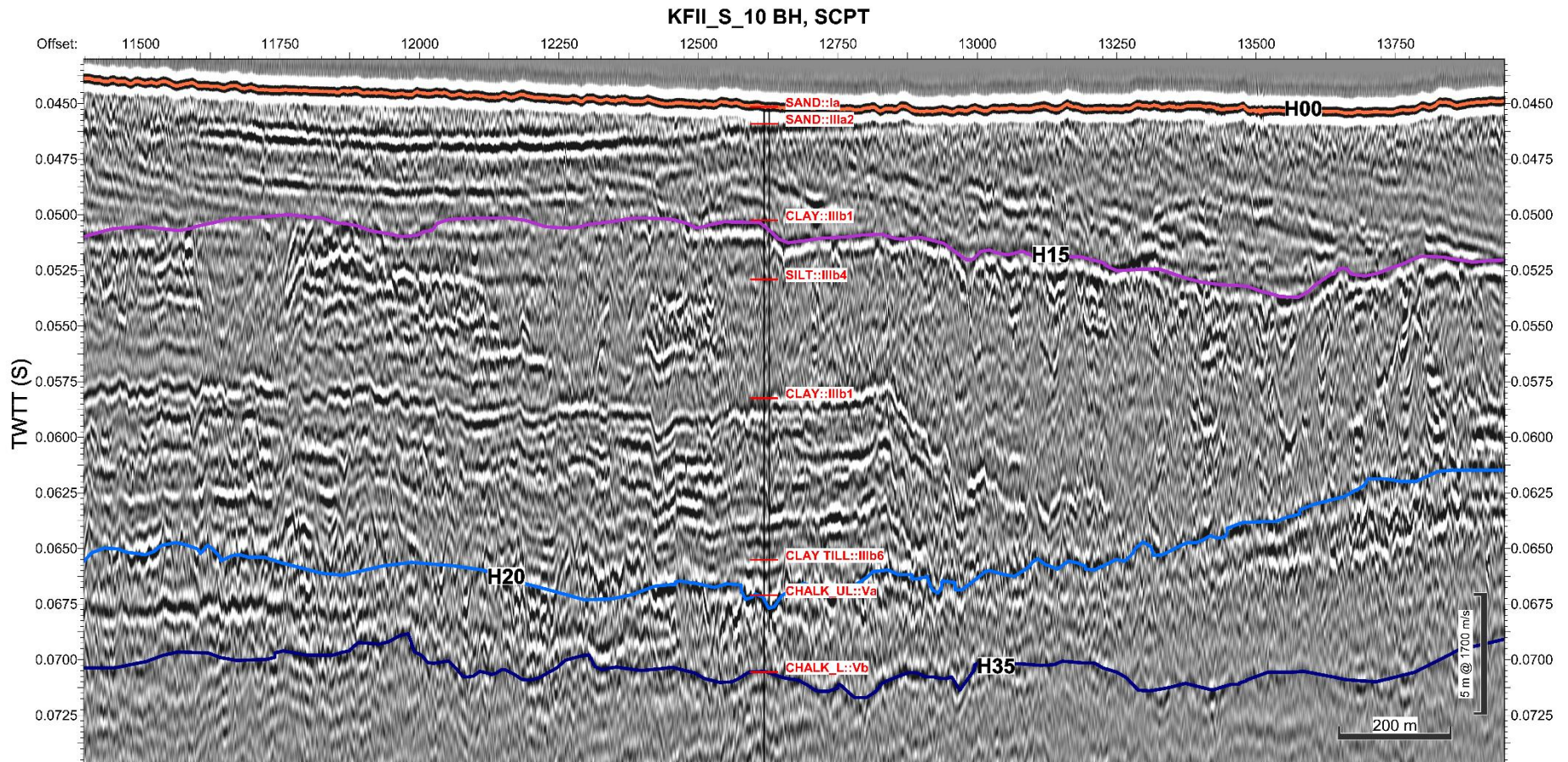


Figure 6-28 - UHRS line L020 integration

6.2.5 SEISMIC UNIT VB (SU VB) - LITHIFIED CHALK

6.2.5.1 GEOPHYSICAL DESCRIPTION

Unit Vb is bounded by reflector H35 at its top. The reflector is of low to medium amplitude, semi-parallel, discontinuous. Internally the seismic facies consist of low amplitude and semi-transparent with incoherent reflection patterns that are often sub-parallel. This reflector was interpreted based on where it coincided with geotechnical markers and extending as far either side as possible based on the visibility of the reflector. It does not serve as a fully interpreted horizon as per the previous sections and should only be used to inform on the possible lithified chalk interface.

6.2.5.2 SPATIAL DISTRIBUTION

Extents of the pick have been plotted in Figure 6-29, alongside areas of uncertainty. The horizon has been interpreted across most of the site, with gaps in the interpretation present along the eastern edge, in the centre of the site (attributed to a processing artefact), and in the southwest corner of the site where a possible channel feature (dipping reflectors) were observed (sections 6.2.3 and 6.2.4). In the centre of the site, an area of no interpretation, caused by a processing artefact extends from the southern site boundary northwest through the site. The processing artefact covers a wider area and often areas of interpretation. Given the uncertainty in the top of the lithified chalk pick (section 6.2.5.1), this unit was not gridded as part of the work performed on the shallower units.

6.2.5.3 GEOTECHNICAL DESCRIPTION

Unit Vb is described based on seismic as low to medium amplitude, subparallel semi-continuous reflectors changing to low amplitude and transparent at lower depths. This unit was geotechnically classified based on the BH log descriptions. Unit Vb was characterised as GU Vb which is described as CHALK (A1-B4), slightly indurated (H2), slightly fractured (S2), white (N9), highly calcareous (Very weak), interbedded with thin laminations to very thin beds of marl, medium grey (N5), highly calcareous and with rare medium gravel to stone sized fragments of chert, very strongly indurated (H5), dark grey to black (N3-N1), non-calcareous (Very strong to extremely strong).

6.2.5.4 INTERPRETATION

There is uncertainty as to the exact depth of the lithified chalk surface across the site. Limited borehole data means that the top cannot be defined with confidence given that the seismic facies exhibit multiple strong reflectors, of parallel, medium to high amplitude below H20, meaning that it is often difficult to determine a continuous reflector for the top of the surface. In conjunction with this, the seabed de-multiple process has a remnant artefact in the UHRS data which is illustrated in Figure 6-23 and Figure 6-24. This blanking of the seismic signal interrupts the H20 and H35 reflectors (as well as the internal reflectors of the respective units), meaning that it is not possible to track a reflector across the affected area. In the extreme case, this has greater impact where the seabed has a higher degree of slope which is carried forward to the artefact. This provides additional difficulty for interpretation when the H20 and H35 reflectors demonstrate vertical variability (Figure 6-24).

Extents of this affected area (processing artefact) alongside areas where H35 has not been interpretable within the data, are presented in Figure 6-29. An example of the geotechnical and seismic integration is provided in Figure 6-30.

It is recommended that a sitewide extensive geotechnical campaign is conducted, alongside additional seismic data acquisition, to provide samples across the site to determine the top of lithified chalk.

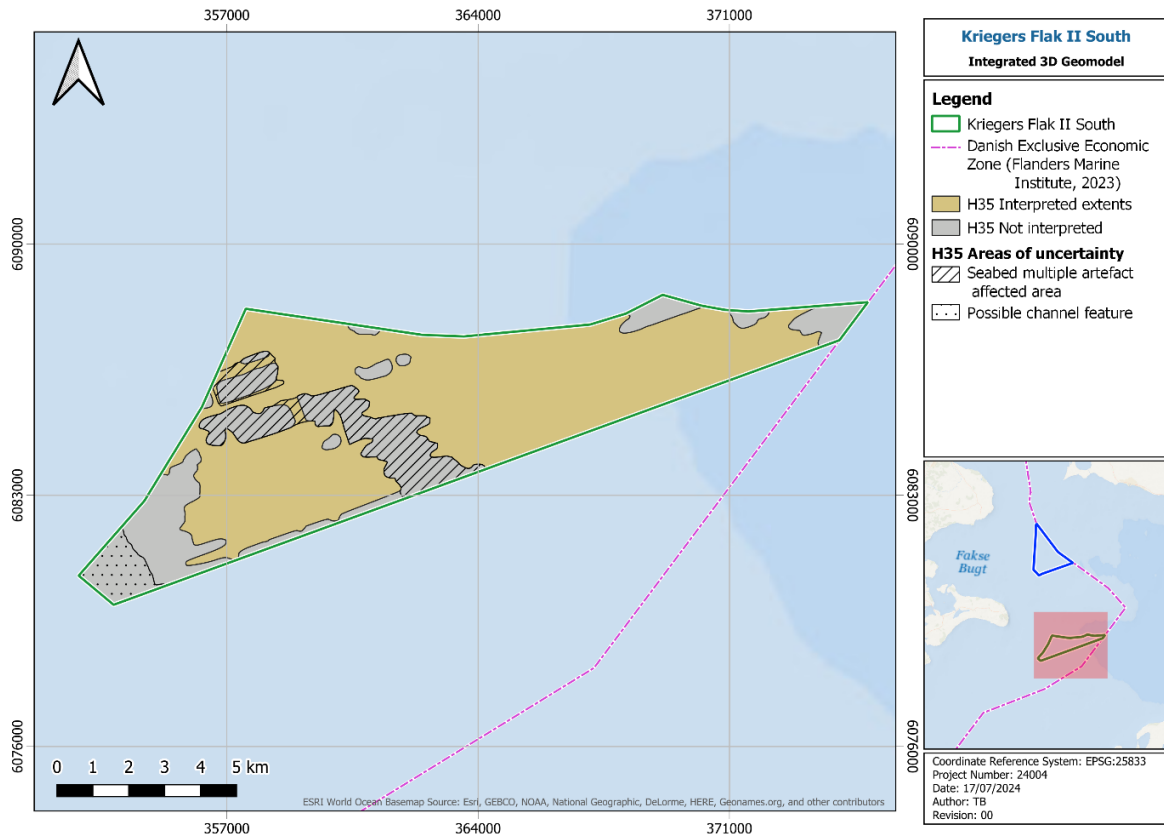


Figure 6-29 - H35 lithified chalk pick overview

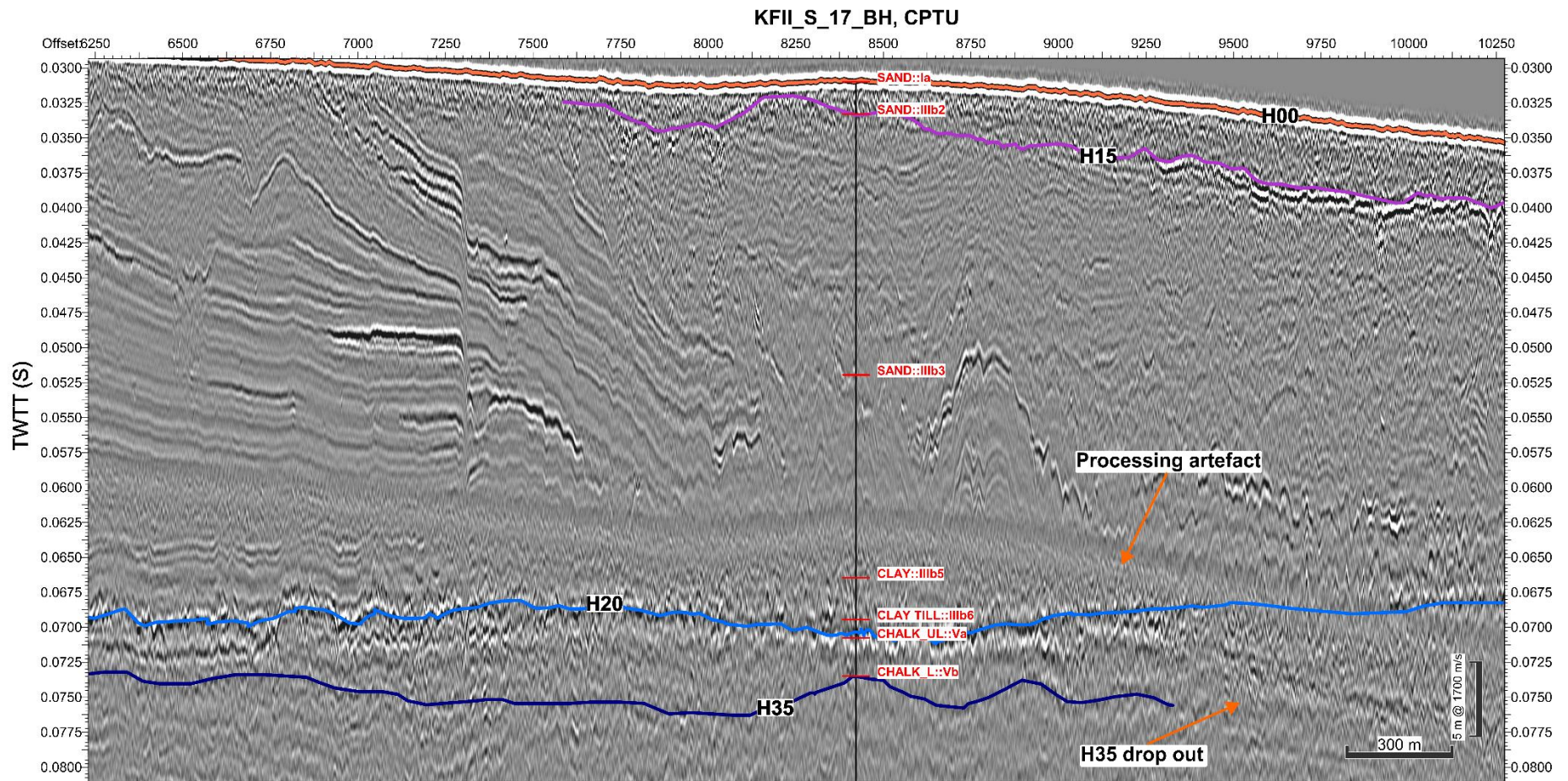


Figure 6-30 - UHRs line L022 integration

6.2.6 GEOLOGICAL UNITS SUMMARY

A summary of the interpreted geological units, their minimum and maximum elevations in mMSL and depths in mBSF, and their thicknesses is presented in Table 6-3.

Table 6-3 - Geological units summary

Geological units summary									
Seismic Unit	Top	Base	Distribution	Top Min. Elevation (mMSL)	Top Max. Elevation (mMSL)	Top Min. Depth (mBSF)	Top Max. Depth (mBSF)	Thickness (m)	Geotechnical Unit
I	H00	H05	Present across most of the site, except for where it has not been interpreted in the southwest, gaps along both the northern and southern site, and a large gap in the centre of the site that spans the width of the site boundary. The thicket deposits occur in the centre and east of the site.	-21.3	-41.8	0.0	0.0	<0.1 – 2.8	Ia/ Ib
IIIa	H00 H05	H15	Present in the eastern and central part of the site. The thickest deposits occur in the centre of the site.	-21.4	-43.4	0.0	2.9	<0.1 – 8.4	IIIa1, IIIa2
IIIb	H00 H05 H15	H20	The unit is present across the entire site. The highest thicknesses occur in the southwest, where the unit is present at the seabed (or sub cropping a thin veneer of Unit I).	-18.5	-45.0	0.0	9.5	1.5 – 51.0	IIIb1, IIIb2, IIIb3, IIIb4, IIIb5, IIIb6
Va	H20	H35	The unit is present across the entire site. The maximum depths occur in the southwest of the site where the Unit IIIb thickness is greatest. Thickness for the unit is not available due to the uncertainty associated with the H35, top of Unit Vb pick.	-35.2	-70.0	3.8	51.0	N/A	Va
Vb	H35	N/A	The unit is present across the site, though not interpreted fully. The unit is not seen in the southwest of the site as well as a central section affected by the processing artefact and several areas along the eastern boundary where it was not seen at depth.	N/A	N/A	N/A	N/A	N/A	Vb

6.3 SOIL ZONATION

Soil zonation (provinces) across the site highlights the horizontal and vertical variability in ground conditions. Soil provinces were defined following the subseafloor interpretation, seismic unitisation, geotechnical unitisation, integration of the available geophysical and geotechnical data.

Soil provinces were initially defined based on the geophysical seismostratigraphic units across the site based on the IGM. The soil zonation was further refined based on the geotechnical unitisation considering the available geotechnical data as well as the engineering drivers influenced by the zone of interest for structures/ foundations being considered such as depth to top of rockhead, channels across the site where geotechnical features may vary both laterally and axially etc.

Four main provinces were defined across the site. Table 6-4 summarises the 4 geotechnical provinces defined.

Table 6-4 - Defined provinces

Defined provinces	
Province	Definition
1	Depth to top of Chalk, 0 – 10 m
2	Depth to top of Chalk, 10 – 20 m
3	Depth to top of Chalk, 20 – 30 m
4	Depth to top of Chalk, greater than 30 m

Figure 6-31 illustrates the soil provinces at the north site. Appendix E presents the cross sections along the site. The cross sections are presented to understand the geological and geotechnical profiles across the site. It should be noted that some boreholes were offset from some cross sections and there may be an apparent misfit of the boreholes with the cross sections. However, the boreholes are representative of the location data.

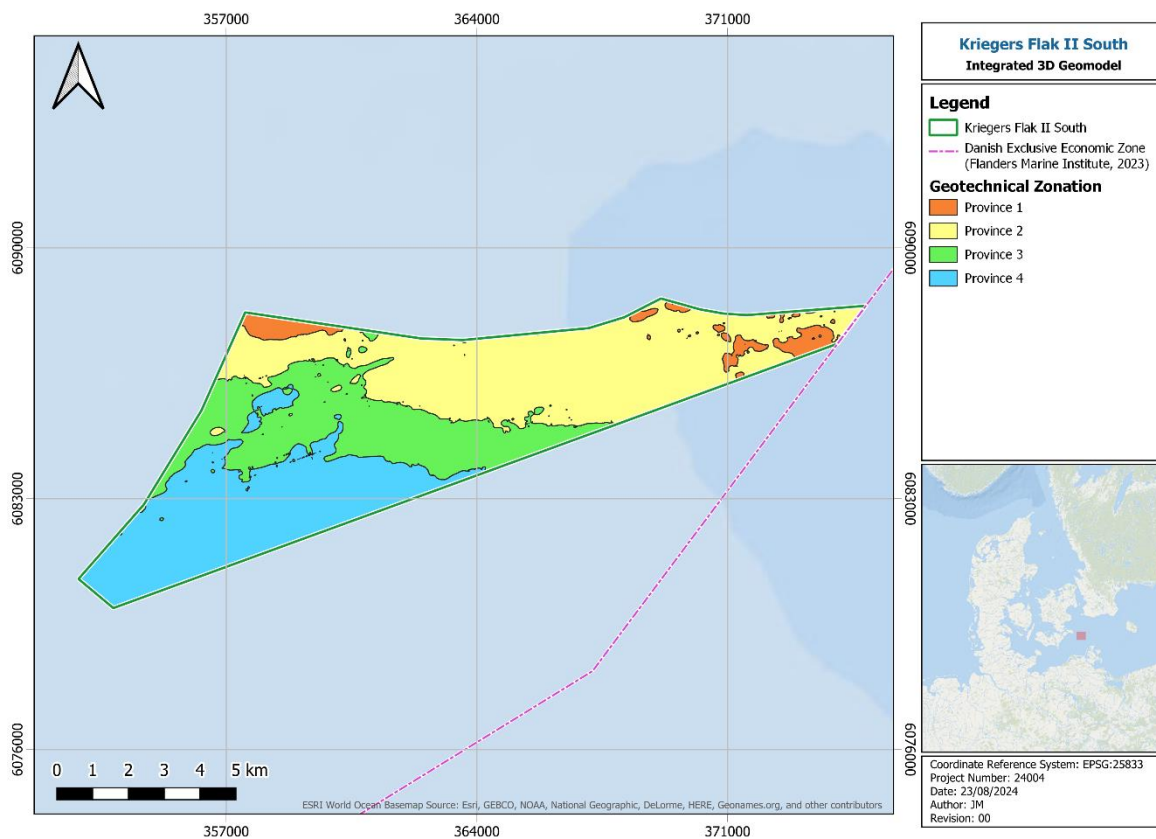


Figure 6-31 Geotechnical zonation provinces

The site is characterised by shallow bedrock consisting of Chalk and a thick seismic unit (SU) III. The provinces were defined based on the depth to top of bedrock and SUIII thickness which are the main engineering drivers. The following should be considered when design and installing foundations in Chalk:

- Uncertainty in chalk properties can lead to excessively long monopiles which can increase the overall weight of the monopiles.
- The chalk is observed to be within the foundation depth across most of the site. Hence, there may be potential damage of the piles during installation or specialised installation methods maybe required such as drive-drill-drive or drill and grouting. These can have cost impact to foundation installation.
- Competent (strong) Chalk layers are present within the structureless and structured Chalk which may lead to premature refusal during foundation installation or foundation damage.
- Flint beds or layers maybe present within the structureless and structured Chalk which may lead to premature refusal during foundation installation or foundation damage.
- The behaviour of Chalk can be affected based on different installation methods and loading conditions. Therefore, design of foundation (monopiles) in chalk need to consider latest findings such as ALPACA JIP (Jardine et al 2022).

It should be noted that the soil province map represents incorporation of a wide distribution of similar geotechnical units to aid in the understanding of the formations that may influence

geotechnical foundation design. However, the soil province map should be viewed with caution as it does not incorporate the substrata data and only considers a wide spread of geotechnical data. Hence, the geotechnical unitisation which represents the vertical and lateral variability of the substrata should be reviewed alongside the soil province map.

Appendix E presents the zonation map for the site and various cross-sections across the site. It should be noted that the soil profiles presented with the zonation map are representative of the seismic unitisation. Table 6-5 summarises the ground conditions within each province and probable foundation design and installation challenges in general.

6.4 GEOTECHNICAL UNITISATION

Geotechnical soil unitisation was performed based on the factual geotechnical data and considering the seismostratigraphic unitisation presented in the IGM and understanding of the geotechnical and geological conditions across the site.

The geotechnical units identify ground conditions with similar geotechnical properties. Therefore, a single seismic unit could be broken down into different geotechnical units e.g. SU IIIb is defined as GU IIIb1, IIIb2, IIIb3, IIIb4, IIIb5, IIIb6, to define different geotechnical properties. Table 6-2 summarises the different geotechnical units identified at the site.

6.5 INTEGRATED 3D GEOMODEL UNCERTAINTY

The remaining uncertainties for the site for this iteration of the IGM are presented in Table 6-6.

Table 6-5 Ground conditions and design challenges at each Province

Ground conditions and design challenges at each Province		
Province	Ground Conditions	Foundation Design and Installation Challenges
1	<p>Chalk is encountered less than 10 m BSF</p> <p>Low strength sediments overlying the Chalk bedrock. Low strength sediments consist of very loose to loose Sand and very low to low strength Clays</p>	<ul style="list-style-type: none"> • Low strength sediments may result in jack-up installation challenges such deep leg penetration, rapid leg penetration etc • Most foundation types likely to encounter Chalk • Design of piles in Chalk may lead to excessively long piles or piles with larger wall thicknesses • Installation of piles in Chalk may result in premature refusal, damage to pile tip due to hard competent layers of Chalk or layers of flint
2	<p>Chalk is encountered between 10 m and 20 m BSF</p> <p>Sediments consist of loose to very dense Sand overlying very low to extremely high strength Clays</p> <p>Very dense Sand is observed at shallow depths close to seafloor.</p>	<ul style="list-style-type: none"> • Most foundation types likely to encounter Chalk • Design of piles in Chalk may lead to excessively long piles or piles with larger wall thicknesses • Installation of piles in Chalk may result in premature refusal, damage to pile tip due to hard competent layers of Chalk or layers of flint • The very dense Sands at shallow depths may result in shallow design penetrations of foundations and installation challenges for foundations.
3	<p>Chalk is encountered between 20 m and 30 m BSF</p> <p>Sediments consist of loose to very dense Sand becoming medium dense to dense overlying very low to extremely high strength Clays</p> <p>Very dense Sand is observed at shallow depths close to seafloor.</p>	<ul style="list-style-type: none"> • The medium to very dense sands overlying very low strength Clays may result in design challenges such as punch through, excessive long piles. • Sandy Clays and Clay Till is observed overlying the bedrock. These clays should be considered with caution as they may behave like a transitional soil.
4	<p>Chalk is encountered greater than 30 m BSF</p> <p>Sediments consist of predominantly medium dense to very dense Sand overlying transitional soil consisting of Silt, Clay Till or Sand Till</p> <p>Very dense Sand is observed at shallow depths close to seafloor.</p>	<ul style="list-style-type: none"> • Dependent on depth of the foundation type, Chalk may not be encountered. • The very dense Sands at shallow depths may result in shallow design penetrations of foundations and installation challenges for foundations. • Transitional soils should be considered with caution by the designer as they may behave as either cohesive and cohesionless dependent on the design condition.

Table 6-6 - IGM uncertainty

IGM uncertainties						
Item	Associated Uncertainty	Data Type	Horizon	Seismic Unit	Geotechnical Unit (s)	Extents
Seabed ringing	The SBP data supplied from the survey contractor have a component of seabed ringing at the seabed interface for the entire dataset. This influences the capability of identifying the true extent of the shallowest unit (Unit I), where it's corresponding reflector (H05) pinches out against the seabed. Pseudo picks were generated for the H05 reflector to allow for a correct gridding process, though there remains some uncertainty because of this.	SBP	H05	I	N/A	Site-wide
Tide reduction	The tidal reduction applied to the SBP dataset is inconsistent between lines and across the site. When observing the cross lines, there is a significant variability in elevation between the crossing in-lines. This means that all SBP are not accurately reduced to a correct MBES level and therefore any result in time relative to MSL, are not reliable.	SBP	H00, H05	I	N/A	Site-wide
Processing artefact	The processing techniques applied to the UHRS data for the removal of the seabed multiple have left a remnant area of blanking within the data, which follows the path of the seabed multiple, at depth. Unfortunately, this blanking cuts through the H20 and H35 reflectors and breaks their continuity. As a result, there are parts of the site where there is uncertainty in the H20 pick (Figure 6-23)	UHRS	H20, H35	IIIb, Va, Vb	N/A	For coverage see Figure 6-29
Geotech and seismic correlation	On affected CPT locations (for example, CPT 05), where 'end of logging' was provided as a description, the geotechnical description is given as chalk due to refusal and recovery of equipment. Often the seismic reflector for the chalk is seen slightly shallower and does not tie in perfectly. Recovered borehole samples are recommended to gain additional verification on this interface.	UHRS	H20	IIIb, Va	Va, Vb	Site-specific
Geotech	Transitional soil units: Silt, very sandy Clay, very clayey Sand. The geotechnical behaviour of these soils needs to be reviewed with caution dependent on the foundation type, loading conditions etc.	GEO		IIIb	IIIb4, IIIb6	Site Wide
Geotech	Chalk: Chalk was encountered at the site. Unlithified (structureless) Chalk was observed overlying Lithified (structured) Chalk. The behaviour of chalk needs to be considered with caution by the foundation designer.	GEO		Va, Vb	Va, Vb	Site wide
Till extents and thickness	Till has been identified within the recently acquired geotechnical campaign, though within the seismic data it has not been possible to fully resolve a clear till reflector interface (sections 6.2.3 and 6.2.4). This is a remaining uncertainty in the current model and will require direct efforts to reduce in future studies.	UHRS	H20	IIIb, Va	IIIb6	Site-wide
SW channel features	In the southwest of the site there is a possible channel/incision feature below the current H20 reflector. There is no available geotechnical data in this region to confirm if the current H20 reflector still represents the top of unlithified chalk. Preliminary extents of this have been provided (Figure 6-29), though it was decided by the client to not proceed with interpreting this feature. The available data outside of the site boundary suggests that the feature extends both to the south and to the west of the site.	UHRS	H20, H35	Va, Vb	Va	Southwest corner
Unit II interpretation	Unit II corresponds to a transitional unit between Unit I (marine) and Unit III (glaciolacustrine). This unit was only partially visible on few SBP lines, and a consistent unit could not be interpreted. Geotechnically the unit shares properties with GU IIIa1 and has been amalgamated into that unit, considered to be transitional.	SBP	H05	I, IIIa	Ib, IIIa1	Site-wide
Possible gas	Across the site, areas of seismic signal blanking have been observed, though unlike typical signal blanking associated with gas, the seismic signal is still visible both below, within and above areas of reduced amplitude/transparency. It is possible that this may be related to an acquisition set up issue, though the possibility of gas on the site cannot be fully ruled out.	SBP, UHRS	H05, H15, H20	I, IIIa, IIIb	N/A	Site-wide
Lithified Chalk	The H35 reflector for lithified chalk that has been supplied is only to inform on the likely position of the lithified chalk only. There is greater confidence in the pick in the areas surrounding GI locations with a lithified chalk top marker, with confidence continually reducing laterally away from these points. In some instances, multiple reflectors were observed beneath the unlithified chalk interface, though these varied laterally and often a continuous reflector could not be traced. The extents shown in 6-19 illustrate the associated uncertainty with areas the reflector was not seen but also the large area in the centre of the site in which H35 (top of lithified chalk - Unit Vb) was directly impacted by the processing artefact. In this area it was not possible to infer or track a reflector to understand its true change in elevation and therefore understand if the reflectors either side of the affected area were associated with each other. This remains a large uncertainty in this revision of the IGM and forms the basis of future investigation requirements.	UHRS	H20, H35	Va, Vb	Va, Vb	For coverage see Figure 6-29
Gridding parameters	The gridding parameters used were required to fully interpolate seismic data interpretation between mean line spacings of 250 m (see Figure 5-2) and extrapolate to fill the site boundary with 3D interfaces. Gridded surfaces lose reliability away from the survey lines. This is particularly noticeable when the picked horizon shows greater spatial variation than the line spacing (i.e. if a picked horizon is steeply dipping or highly textured the gridding process is unable to capture the full detail and gridding artefacts are more significant). Because of the parameters used to account for the large line spacing on the UHRS data, the values that intersect the interpretation (on the track lines) have good confidence levels (subject to outstanding interpretation uncertainty); interpolated and extrapolated areas (away from or between the track lines) are where the depth and elevation values are not as accurate and must be treated with extreme caution.	UHRS	H15, H20	IIIa, IIIb, Va	N/A	Site-wide

IGM uncertainties						
Item	Associated Uncertainty	Data Type	Horizon	Seismic Unit	Geotechnical Unit (s)	Extents
Time-Depth conversion of SEGYS	<p>Bathymetry data was used as the vertical reference layer for the T-D conversion of SEGYS. Differences between the bathymetry and the UHRS seabed picks varies between 0 and 1.5 m at maximum, with an average of 0.18 m (99% of values below 0.40 m difference). Maximum differences are observed where seabed features occur, which are not visible in the UHRS seabed picks because they fall in between lines.</p> <p>Second source of uncertainties is related with the grid extent being limited to the site boundary and some seismic lines extending outside the site boundaries. Within the site boundaries, the T-D conversion model is constrained by the seismic unit grids. However, outside the site boundaries (17.4% of total UHRS dataset line distance), T-D conversion model layers have been extrapolated by the DDC tool to allow the T-D conversion of the full seismic sections. Because of the absence of geotechnical markers and seismic interpretation outside the site boundaries, uncertainties related with the extrapolated T-D conversion model cannot be quantified.</p>	UHRS	X	X	N/A	Site-wide

6.6 STATISTICAL CORRELATION OF GI WITH GEOPHYSICAL DATA

Correlation between the interpreted unit boundaries from geophysical data and geotechnical markers was assessed by quantifying the differences in depth. Statistics have been calculated on absolute differences, with minimum, maximum and average values, which are provided in Table 6-7.

Table 6-7 - Statistical correlation between GI and geophysical data

Statistical Correlation				
Unit Top	Minimum Difference (m)	Maximum Difference (m)	Average Difference (m)	Difference Standard Deviation (m)
Top Unit IIIa	0.07	0.50	0.27	0.11
Top Unit IIIb	0.01	0.61	0.22	0.19
Top Unit V	0.06	1.14	0.37	0.36

For the southern site, correlation between the GI and geophysical data was assessed for the top of Unit IIIa, Unit IIIb and V Chalk with average differences of 0.27 m, 0.22 m and 0.37 m, respectively.

For the correlation between Unit IIIa top and the geotechnical markers, all locations have been used in the statistical assessment. For this unit, the correlation at each location shows difference values consistently below or equal to 0.50 m. Most of those differences are related to with locations where the top of Unit IIIa has been picked at the seabed and where the veneer of modern marine sediments could not be observed other than in geotechnical data.

For the correlation between Unit IIIb top and the geotechnical markers, 8 locations have a geotechnical marker which can be correlated with the geophysical data. Out of the 8-locations used for testing the correlation, only location KFII_S_08_BH shows a difference greater than 0.50 m, with a value of 0.61 m. This difference can be explained by the sediment behaviour variability and the fact that the boundary between the two seismic units do not necessarily align with a change in geotechnical behaviour. It can also explain why the top of Unit IIIb could be correlated with a geotechnical marker at the 10 remaining locations.

For the correlation between Unit IV and the till markers, 8 out of the 18 locations have a geotechnical marker which can be used for correlation. Out of the 8-locations used for testing the correlation, only location KFII_S_05_CPT shows a difference of 1.14 m. This difference can be explained by the sediment variability and the fact that the boundary between the two seismic units do not necessarily correspond to a change in sediments and also by the fact that the top of chalk could only be assessed from CPT loggings without any samples to support its interpretation.

Overall, the correlation between the geotechnical units and the seismic units is fairly robust and the discrepancies are essentially explained by the intrinsic nature of the geotechnical and seismic data.

7 GEOTECHNICAL PARAMETERS

7.1 GENERAL

Geotechnical parameters were determined for each geotechnical unit identified at the site. The geotechnical unitisation was performed to capture the broad-based geotechnical properties identified based on the geophysical data, IGM and factual geotechnical data (Gardline, 2024). Table 7-1 summarises the geotechnical units and descriptions identified. It should be noted that different nomenclatures were used to differentiate between the seismostratigraphic units (e.g. SU I, SU II etc) and geotechnical units (e.g. GU Ia, GU Va etc).

7.2 GEOTECHNICAL SOIL PARAMETERS

This section presents the parameters included in this report that are relevant to foundation design. Soil parameters within different strata are graphically presented in Appendix C. Table 7-1 summarises the parameters presented in this report when characterising the geotechnical soil and rock properties.

Table 7-1 - Geotechnical soil and rock parameters determined

Geotechnical soil and rock parameters determined	
Soil Properties	Rock Properties
CPT measured parameters (q_c , f_s , u_2)	Unconfined compressive strength
CPT interpreted parameters (q_t , q_n , R_f , Q_t , B_q , F_r , I_c)	Young's modulus
Water Content	Poisson's ratio
Unit weight	RQD
Atterberg limits	
Particle density	
Chemical tests (CO_3 , Cl , SO_4 , pH , organic content)	
Undrained shear strength (undisturbed and remoulded)	
Soil sensitivity	
Relative density	
Friction angle (ϕ' , ϕ_{cs} , ψ)	
Interface friction angle (δ)	
Shear wave velocity	
Small strain shear modulus (G_0)	
Strain at half deviator stress (ϵ_{50})	
Preconsolidation stress	
Overconsolidation ratio (OCR)	
Lateral stress ratio (K_0)	
Thermal conductivity	

The strength, stiffness and cyclic behaviour of soil and rock were not derived as part of this IGM as outside the scope. However, cyclic test data has been presented by (Gardline, 2024) and should be considered by the geotechnical designer.

Unitised geotechnical parameters were derived from the available factual data. However, it should be noted that for certain soil and rock parameters, limited data was available in the individual units. In such units, the parameters for different units were compiled together to

provide representative derived parameters based on statistical and engineering judgement. Hence, this provided a general representation and characterisation of a broader group of units with similar properties.

7.3 RECOMMENDED PARAMETER BOUNDING FRAMEWORK

A bounding framework is commonly used to evaluate geotechnical soil parameters. Venterra adopted a best estimate (BE), lower estimate (LE), and high estimate (HE) approach, when applicable, to demonstrate data trends and quantify soil variability. The BE lines have been derived with due consideration of the soils and geotechnical parameters variability using statistical assessment and/or engineering judgement. The BE lines may be considered as characteristic values for engineering behaviour where ‘average’ properties are most relevant for the limit state under consideration. For independent parameters with sufficient data, the BE has been generally estimated as the mean of the measurements available for specific soil layers. Some additional conservatism on either side of the unbiased “Best Estimate” may be required in certain situation such as where localised behaviour governs (e.g. end bearing capacity of the pile).

Statistical assessment was performed following DNV-RP-C207 (2012) recommendations. Where statistical assessment was performed, outliers were identified and removed from the dataset. The statistical assessment was then performed on a revised dataset without outliers. Where few data were available (e.g. only two data points) statistical assessment could not be performed. Therefore, engineering judgement was adopted to determine the geotechnical bounds.

The LE and HE lines have been derived using engineering judgement to provide a credible indication of the low and high distribution of the parameters, respectively.

BE soil profiles for CPT measurements and interpreted data, that is, q_c , q_t , q_n , were determined considering the soil behaviour and adopting engineering judgement. In clay dominated soils, the BE may not consider the sand spikes with the profile biased towards the clay dominated units. In sand dominated units, thin to thick beds of clay may not be considered. The LE and HE profiles captured the peaks and troughs of the CPT measurements based on engineering judgement.

In some geotechnical units where varied soil properties were identified e.g. transitional soil units, GU IVa and GU IVb defined as clay and sand tills, variable soil units were observed consisting of predominantly sand or clay but also consisting of silt, sandy or clay, gravel. Engineering judgement was applied in determining the geotechnical bounds. The geotechnical behaviour of these units may vary and these units should be considered with extreme caution by the geotechnical designer.

The LE and BE parameter profiles maybe considered applicable for settlement analysis, axial and lateral capacity assessments. The HE parameter profiles maybe considered applicable to installation assessments. The geotechnical designer is ultimately responsible for determination of the applicable parameter profiles for design.

The proposed indicative recommended lines may be amended by the designer for specific design purposes reflecting the geotechnical problem considered, to provide a more detailed assessment and/or as a result of consideration of complex soil-structure interaction.

7.4 INTERPRETATION STRATEGY

An in-depth analysis of borehole logs, CPT data, and soil profiles was conducted to provide information about soil and rock layers at varying depths. Locations and depths of soil samples were identified, facilitating the correlation of laboratory test results with specific subsurface conditions. Laboratory test results were comprehensively evaluated to discern crucial engineering properties of the soil. The interpretive analysis of these laboratory test results forms a foundational element in the comprehensive understanding of the engineering properties of the soil. The following interpretation strategy was followed:

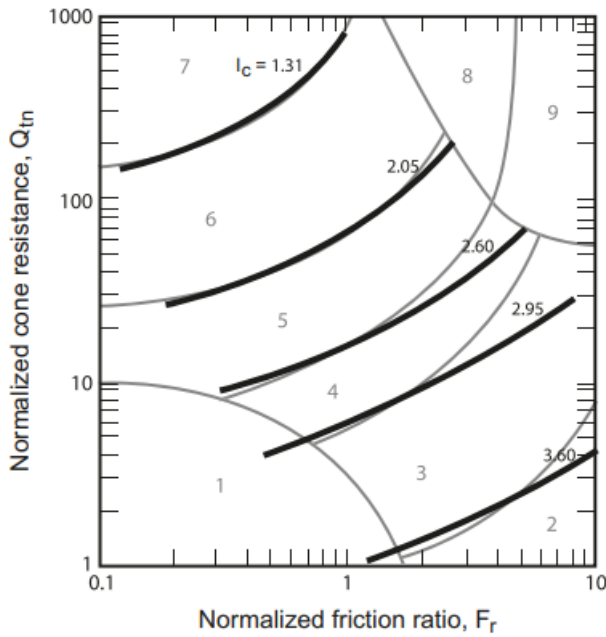
- Review of borehole information and any co-located CPT. Soil layer boundaries are established based on this review.
- Evaluation of the CPT measurements (tip resistance, sleeve friction, friction ratio, and excess pore pressure) to understand typical trends in soil response to CPT advancement.
- Confirm that variation in CPT trends match the initially established soil layer boundaries and adjust as needed.
- Review laboratory test results to corroborate the assigned soil classification and establish additional soil parameters.

Geotechnical units which were observed to behave as a transitional unit such as silt, both drained and undrained parameters have been presented.

7.5 SELECTION OF CPT CLASSIFICATION METHOD

7.5.1 GENERAL

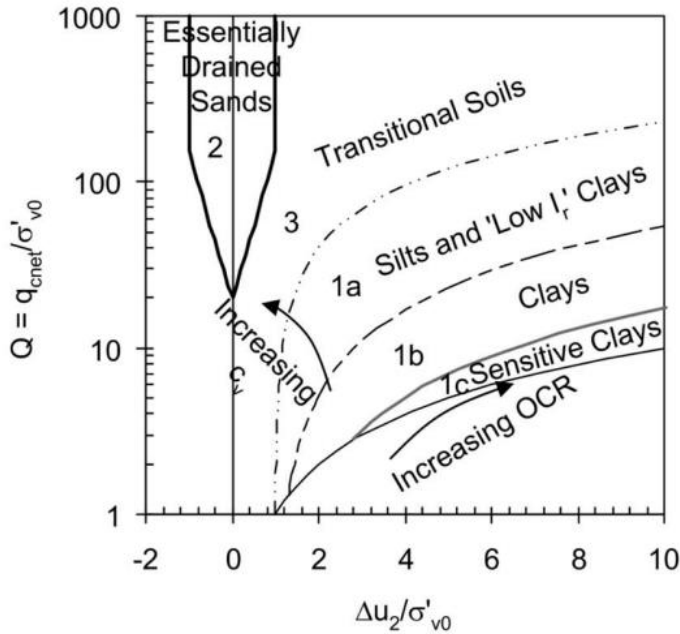
There are several CPT classification methods available. Each method was developed and calibrated for specific soil types and can have different degrees of precision in identifying all soil types. Venterra therefore compared the soil behaviour type methods by (Robertson, 2009) (Schneider, 2008) and (Robertson, 2016), which related more to soil behaviour than classification, to the soil classifications presented in the final borehole logs. Appendix C presents the CPT classification based on Robertson (2016).). Figure 7-1 shows the soil classification according to Robertson (2016) and Figure 7-2 shows the soil classification according to Schneider et al (2018) used to assess pore pressure response.



Zone	Soil Behavior Type	I_c
1	Sensitive, fine grained	N/A
2	Organic soils – clay	> 3.6
3	Clays – silty clay to clay	2.95 – 3.6
4	Silt mixtures – clayey silt to silty clay	2.60 – 2.95
5	Sand mixtures – silty sand to sandy silt	2.05 – 2.6
6	Sands – clean sand to silty sand	1.31 – 2.05
7	Gravelly sand to dense sand	< 1.31
8	Very stiff sand to clayey sand*	N/A
9	Very stiff, fine grained*	N/A

* Heavily overconsolidated or cemented

Figure 7-1 - Robertson (2016) classification



Zone	Soil Type
1a	SILTS and 'Low I _r ' CLAYS
1b	CLAYS
1c	Sensitive CLAYS
2	Essentially drained SANDS
3	Transitional soils

Figure 7-2 - Schneider et al (2018) classification

7.5.2 SOIL CLASSIFICATION BASED ON CPT DATA

Table 7-2 summarises the CPT classification for each geotechnical unit based on the classification charts from both Robertson (2009) and Schneider et al. (2008).

Table 7-2 CPT classification

CPT Classification			
GU	Robertson (2009) Chart Zone	Schneider et al. (2008) Chart Zone.	CPT Classification Description
Ia	5, 6	2,3	Silty sand to sandy silt
Ib	3, 4, 5	1b, 1a, 3	Clay to silty clay
IIIa1	3	1b	Silty Clay to Clay
IIIa2	6,7	2	Clean sand to silty Sand
IIIb1	4, 6	1b to 2	Clayey silt to silty Clay with clean sand to silty sand. This unit should be cautiously evaluated by a geotechnical engineer
IIIb2	6, 7	2	Clean Sand to gravelly Sand
IIIb3	6, 5	2	Clean sand to silty sand
IIIb4	6 to 4	2 to 1a	Silty Sand and to silty clay. This unit needs to be reviewed against lab data to ascertain its behaviour during design and should be assessed by a competent geotechnical engineer
IIIb5	5, 4	3	Sand mixtures to silty sand. this unit should be assessed similar to a transitional unit by a competent geotechnical engineer to ascertain its geotechnical behaviour depending on the loading conditions, foundation type etc
IIIb6	6, 5,4, 8, 9	3, 1a, 1b	Silty sand to very stiff fine grained
Va	6, 5	1a	Clean sand to silty sand. This may indicate that this chalk unit to behave as a cohesionless unit. This unit has been described as unlithified Chalk in the geotechnical logs. However, this will have to be further evaluated by a competent geotechnical engineer to ascertain its geotechnical behaviour depending on the loading conditions, foundation type, etc

7.6 SUMMARY OF LABORATORY TESTS

Table 7-3 summarises the types and number of tests that were available at the time of preparing this report as presented by (Gardline, 2024). The laboratory test quantities presented in Table 7-3 contain total quantities for the southern site as extracted from AGS data.

Table 7-3 - Types and number of tests available at time of reporting (Gardline, 2024)

Types and number of tests available at time of reporting ^a		
Classification Test Type	Lab	South Site
Water Content - Soil	Gardline	114
Water Content - Rock	Gardline	103
Bulk and Dry Density – Soil	Gardline	126
Bulk and Dry Density – Rock	Gardline	69
Particle Density	Gardline	46
Atterberg Limits (4 Point Method)	Gardline	19
Particle Size Distribution	Gardline	41
Angularity	Gardline	15
Maximum and Minimum Dry Density	Gardline	4
Carbonate Content	Gardline	12
Acid Soluble Sulphate	GEOLABS	12
Loss on Ignition	Gardline	7
Thermal Conductivity	Gardline	4
Acid Soluble Chloride	GEOLABS	12
Oedometer	Gardline	4
UUT	Gardline	13
UCS	GEOLABS	18
UCS with Young's Modulus	GEOLABS	15
Point Load ^b	Gardline	23
CIUc	GEO	3
CIDc	GEO	8
CAUc	GEO	2
CAUcyc	GEO	1
DSS	GEO	8
CSS ^c	GEO	3
Notes:		
a. The test quantities presented include total number for both North and South site		
b. Point load test numbers including tests conducted on cancelled UCS tests		
c. Each CSS allowed for a series of three tests		

7.7 CLASSIFICATION PROPERTIES AND UNIT WEIGHT

The soil and rock were classified in accordance with ISO 14688 and 14689 standards, respectively. The index testing used for classification of the soil samples included grain size distribution, Atterberg limits, moisture content, and unit weight. The summary of the results of these tests is tabulated in this section and presented graphically when applicable in Appendix C.

7.7.1 PARTICLE SIZE DISTRIBUTION

Particle Size Distribution tests (PSD) curves provide information about percentage of different grain sizes for a soil sample. The gradation characteristics of selected samples were estimated in general accordance with the sieve procedures of ISO 17892-4: 2016. The unitised PSD curves are presented in Appendix C.

The distribution of different soil fractions versus depth was analysed for the different geotechnical units. This parameter is important for understanding the composition of the subsurface and the likely engineering properties.

7.7.2 PLASTICITY

Atterberg Limits refer to specific moisture contents at which a soil undergoes changes in its physical properties. These limits are commonly used to classify fine-grained soils, such as silts and clays, based on their plasticity. The Atterberg limits include the following:

- Liquid Limit (LL): The moisture content at which the soil transitions from a plastic to a liquid state.
- Plastic Limit (PL): The moisture content at which the soil transitions from a plastic to a semi-solid state.

A plasticity chart divides soils into various zones or classes, each representing different engineering properties and behaviour. Atterberg's limits tests using the 4 point method were performed in accordance with ISO 17892-12: 2022 Standard. The plasticity chart is presented in Appendix C. The results demonstrate that all geotechnical units can be classified as predominantly low to medium plasticity.

The geotechnical parameter bounds were determined by statistical assessment and engineering judgement.

7.7.3 MOISTURE CONTENT

The moisture content, w , is a parameter typically used for soil classification, estimation of void ratio and correlations to other soil parameters. Plot of moisture content versus depth from offshore and onshore laboratory testing are presented in Appendix C.

The geotechnical parameter bounds were determined by statistical assessment and engineering judgement.

7.7.4 UNIT WEIGHT

Unit weight was determined from bulk density and CPT-data. CPT derived unit weights were determined in accordance with (Robertson, 2010) and compared to laboratory measurements (Appendix C). The CPT methods underestimate the unit weight especially for shallower soil layers where the overburden pressures are lower. This is not unusual as most unit weight correlations from CPT include a high degree uncertainty. CPT-derived values were not relied upon when calculating representative geotechnical profiles unless there was insufficient bulk density data within the unit.

7.7.5 PARTICLE DENSITY

Particle density is a measure of the mass of solid particles per unit volume within a soil or sediment sample and provides information about packaging and arrangement of soil particles.

Particle density (G_s) measurements were performed following the fluid pycnometer method. Due to the limited number of particle density tests, some of the units were combined to determine a statistical assessment. Appendix C presents the particle density profiles.

7.7.6 ORGANIC CONTENT

Organic content (OC) was measured by the loss on ignition method in accordance with BS1377-3:2018. Appendix C presents the parameter plots presenting the OC.

7.7.7 CARBONATE, SULPHATE, AND CHLORIDE CONTENTS

The carbonate content test was performed using the gasometric method. The results are reported as % CaCO₃ of soil dry mass.

The sulphate and chloride contents were performed using the acid and water-soluble method, whereas the chloride content tests were performed using the acid soluble method.

The carbonate, sulphate and chloride testing was performed following BS 1377-3:2018 recommendations.

7.7.8 THERMAL CONDUCTIVITY

Thermal conductivity (TC) tests have been performed using the transient heat method. TC was performed following ASTM D5334-22:2014 methodology. TC testing was performed on both undisturbed and reconstituted samples.

TC is highly influenced by saturation and dry density. An increase in either parameter will result in an increase in the soil's TC. Other factors of secondary importance include mineral composition, temperature, and time. Appendix C presents the TC profile versus depth.

7.8 ENGINEERING PROPERTIES

This section discusses the engineering properties of the sediments encountered during our field exploration program. The engineering properties are evaluated for each specific unit.

Section 7.3 discusses the bounding framework used to determine the engineering properties of fine-grained and coarse-grained sediments, respectively. Properties such as laboratory and field undrained shear strength (s_u), site-specific cone bearing capacity factor, derived S_u from cone data, epsilon 50 (ϵ_{50}), consolidation properties and compressibility, and interpretation of stress history are discussed. The state of consolidation from laboratory and in-situ testing of fine-grained sediments is discussed. The state of consolidation of clayey soils was determined from incremental load consolidation tests, and empirically from correlations with CPT data. This coefficient is used to determine the depositional history of sediments and is used to predict the relative density and OCR.

7.9 CONE PENETRATION TEST PARAMETERS

7.9.1 GENERAL

The following cone penetration test (CPT) parameters are presented for each geotechnical unit.

- Measured cone resistance (q_c)
- Total cone resistance (q_t)
- Net cone resistance (q_n)

- Measured sleeve friction (f_s)
- Measured pore-water pressure (u_2)
- Friction ratio (R_f)
- Pore-water pressure ratio (B_q)
- Normalised cone resistance (Q_t)
- Normalised friction ratio (F_r)
- Soil behaviour type index (I_c)
- Relative density (D_r)
- Undrained shear strength (s_u)

The geotechnical parameter bounds for the above soil units were determined by engineering judgement considering the recommendations in Section 7.3. It should be noted that geotechnical profiles are only presented for q_c , q_t , f_s , D_r and s_u . Table 7-4 summarises the geotechnical profiles with depth and parameter calculations. Section 7.9.1.1 presents derivation of relative density (D_r).

Table 7-4 - Measured and derived CPT parameters

Measured and derived CPT parameters		
Parameter	Calculation	Geotechnical profiles
Measured cone resistance (q_c)	As measured in situ	LE, BE, HE
Total cone resistance (q_t)	$q_t = q_c + u_2(1 - \alpha)$	LE, BE, HE
Net cone resistance (q_n)	$q_n = q_t - \sigma_z$	LE, BE, HE
Measured sleeve friction (f_s);	As measured in situ	LE, BE, HE
Measured pore-water pressure (u_2)	As measured in situ	—
Friction ratio (R_f)	$R_f = f_s/q_t$	—
Pore-water pressure ratio (B_q)	$B_q = \Delta_u/q_n$ $\Delta_u = u_2 - u_0$	—
Normalised cone resistance (Q_t)	$Q_t = q_n/\sigma'_z$	—
Normalised friction ratio (F_r)	$F_r = f_s/q_n$	—
Soil behaviour type index (I_c)*	$I_c = [(3.47 - \log Q_t)^2 + (\log F_r + 1.22)^2]^{0.5}$	—
Notes: * = Soil behaviour type index (I_c) determined according to (Robertson, 2016) α = Cone area ratio Δ_u = Net pore pressure u_0 = hydrostatic pore pressure σ_z = Total vertical stress — = Geotechnical profiles not derived		

7.9.1.1 RELATIVE DENSITY

Relative density (D_r) was determined using the relationship proposed by (Jamiolkowski, 2001). It should be noted that this methodology for determining relative density is developed for clean silica sand. Hence, the D_r determined using this method maybe unrepresentative due the varying fines contents observed in the soils and should be considered with caution (Fioravante et al., 2023). No adjustment for fines was performed.

7.9.2 STATIC UNDRAINED SHEAR STRENGTH

Field estimates of S_u were provided using Torvane (TV) and pocket penetrometer (PP) tests. The TV and PP were performed in the offshore laboratory immediately after sample recovery. These two methods provide quick, in-situ assessments of the soil's strength without requiring extensive laboratory testing. However, it's important to note that these are index test methods and may not provide accurate results. Therefore, these index strength tests were not considered in the geotechnical bounding.

Undrained shear strength (s_u) was determined from laboratory tests performed both offshore and onshore. s_u was determined from unconsolidated undrained triaxial (UU) tests performed both offshore and onshore. While, miniature lab vanes (MLV) and advanced laboratory strength tests including direct simple shear (DSS) tests, and consolidated triaxial (CIUc, CIDc, CAUc) tests were performed in the onshore laboratory.

s_u was also determined from CPT data using Equation 7-1.

$$s_u = q_n / N_{kt}$$

Equation 7-1

Where:

N_{kt} = Empirical factor relating net cone resistance to undrained shear strength

An assessment was performed to determine the appropriate N_{kt} empirical factor to be applied for each cohesive geotechnical unit. This was performed using the UU, CIUc, CAUc and DSS data within each geotechnical soil unit. The s_u determined from DSS, UU, CIUc were corrected to equivalent s_u from CAUc and then used in performing the N_{kt} assessments. Table 7-5 summarises the N_{kt} factors determined for the site.

Table 7-5 - N_{kt} empirical factors

Nkt empirical factors			
Geotechnical Unit	Nkt factor		
	LE	BE	HE
Ib	15	20	25
IIIa1	15	20	25
IIIb1	15	24	40
IIIb4	10	24	40
IIIb5/b6	15	21	40

7.9.3 REMOULDED UNDRAINED SHEAR STRENGTH

At the southern site, remoulded undrained shear strength ($s_{u(R)}$) testing was performed and determined from miniature lab vanes (MLV). $s_{u(R)}$ can be approximated directly from CPT data based on the recommendation below from Quiros and Young (1988).

$$s_{u(R)} = f_s$$

Equation 7-2

7.9.4 SENSITIVITY

Soil sensitivity (S_t) is defined as the ratio of peak to the remoulded undrained shear strength. This parameter provides an indication as to how much strength loss should be expected upon sample disturbance, remoulding or when subjected to monotonic or cyclic loading that cause large deformations.

S_t was determined from CPT data and MLV laboratory tests. S_t from CPT data was determined using the method proposed by (Schmertmann, 1978) as described by Equation 7-3.

$$S_t = N_s / R_f$$

Equation 7-3

Where:

N_s = Empirical constant

The value of N_s is determined by various factors such as OCR and mineralogy. Therefore, for this assessment an N_s value of 7.5 was adopted.

7.9.5 STRESS HISTORY AND CONSOLIDATION

The state of consolidation is an important indicator of stress state and stiffness of soils, which are important design considerations. To compute the state of consolidation, Venterra used the incremental loading (IL) consolidation tests on selected, relatively undisturbed specimens. Those test results together with the CPT data provided important insight into the behaviour of the cohesive units.

7.9.5.1 OVERCONSOLIDATION RATIO

Overconsolidation ratio is determined as the ratio of maximum preconsolidation stress to the effective vertical stress as defined by Equation 7-4.

$$OCR = \sigma'_p / \sigma'_{vo}$$

Equation 7-4

Where:

σ'_p = preconsolidation pressure

In addition to OCR being determined from laboratory test data, OCR was also estimated from CPT tip resistance data using the empirical correlation by (Kulhawy, 1990) (Equation 7-5).

$$\sigma'_p = k(q_t - \sigma_{vo})$$

Equation 7-5

Where:

q_t = cone tip resistance corrected for boundary effects

σ_{vo} = estimated in-situ total vertical stress

k = empirical factor equal to 0.33

OCR was also estimated indirectly estimated from s_u data determined from triaxial test data where available. The relationship proposed by Ladd (1970) as presented in Equation 7-6 was used.

$$OCR = \left(\frac{(s_u/\sigma'_{vo})_{OC}}{(s_u/\sigma'_{vo})_{NC}} \right)^{1/\lambda_0}$$

Equation 7-6

Where:

$(s_u/\sigma'_{vo})_{OC}$ = Ratio for overconsolidated soil

$(s_u/\sigma'_{vo})_{NC}$ = Ratio for normally consolidated soil of 0.25

$\lambda_0 = 0.85$

The preconsolidation pressure estimated from CPT data was used to develop OCR profiles and compared to laboratory test results. Geotechnical LE, BE and HE profiles were determined by engineering judgement. Appendix C presents the OCR profiles.

7.9.6 COEFFICIENT OF LATERAL EARTH PRESSURE AT REST

The lateral earth pressure coefficient at rest (K_0) is defined as the ratio of horizontal effective stress to vertical effective stress (Equation 7-7).

$$k_0 = \sigma'_{ho} / \sigma'_{vo}$$

Equation 7-7

Where:

σ'_{ho} = horizontal effective stress

σ'_{vo} = vertical effective stress

This ratio is commonly used to quantify the lateral pressure a soil exerts on a structure when loaded vertically. This ratio is also important in evaluating the depositional history and consolidation state of the soil. A higher k_0 indicates an increase in consolidation state. k_0 can

be determined for uncemented sands and clays of low to medium sensitivity as described in Equation 7-8.

$$k_0 = (1 - \sin\phi')OCR^{\sin\phi'}$$

Equation 7-8

Where:

OCR = over consolidation ratio

ϕ' = effective friction angle

Since k_0 is a function of ϕ' , the (Kulhawy, 1990) expression was used. OCR was set to 1.0 for cohesionless soils. With increasing OCR, k_0 is limited by the passive earth pressure coefficient (k_p) where passive failure supersedes.

7.9.7 EFFECTIVE STRESS PARAMETERS

7.9.7.1 GENERAL

The following effective stress parameters were determined for both cohesive and cohesionless soils:

- Peak friction angle
- Interface friction angle
- Critical state friction angle

Effective stress parameters for cohesive soils were determined from CAUc and CIUc test data. For cohesionless soils were determined from CIDc test data. Engineering correlations were also considered in the derivation of effective stress parameters.

7.9.7.2 PEAK FRICTION ANGLE

The peak friction angle (ϕ') represents the resistance to sliding and shear deformation along a potential failure plane within a soil mass. It is a measure of the internal frictional resistance between soil particles and is one of the key factors governing the shear strength of soils. ϕ' was determined from CID test data.

ϕ' was also determined from CPT data using the strength and dilatancy framework proposed by (Bolton, 1986) A critical state friction (ϕ'_{cv}) angle of 32° was used in the assessment of ϕ' . It should be noted that the Bolton correlation has been developed for clean sand and should be considered with caution in sands with fines contents.

A relatively good match was observed between the CID test data and CPT derived ϕ' based on Bolton (1986). Appendix C presents the peak friction angles and the geotechnical profile bounds. The bounds were determined by engineering judgement.

7.9.7.3 INTERFACE FRICTION ANGLE

Interface friction angle (δ) were determined based on API recommendation no test data was available. Equation 7-9 was used to determine δ .

$$\delta = \phi' - 5^\circ$$

Equation 7-9

7.9.7.4 CRITICAL STATE FRICTION ANGLE

Critical state friction angle (ϕ'_{cv}) was determined from available triaxial test data. Global review of the ϕ'_{cv} was performed due to the limited triaxial test data available.

7.9.8 STIFFNESS PARAMETERS

Unit specific stiffness parameters consisting of small strain shear modulus (G_0) were determined and are presented in this section. G_0 was determined from:

- PS logging data
- Seismic CPT data
- CPT data

7.9.8.1 P-S LOGGING

P-S logging was performed at two BH locations from 70 m below seafloor (BSF) to between 6.0 m and 18.0 m BSF. Both P and S waves were picked and processed.

7.9.8.2 SEISMIC CPT

Seismic CPT was performed at two locations across the entire site. The seismic shear wave values (V_s) as presented in the factual report were adopted.

7.9.8.3 CPT DATA

Shear wave velocities (V_s) were inferred from CPT data. The relationship proposed by (Mayne, 2006) was adopted to determine V_s . The V_s values determined from CPT data were calibrated against the P-S logging data. A calibration factor of 1.6 was applied for the sediments and 3.0 was applied for the unlithified Chalk.

7.9.8.4 SMALL STRAIN SHEAR MODULUS

Small Strain Shear Modulus (G_0) was determined using the V_s values determined from P-S logging, SCPT and as inferred from CPT data. Equation 7-10 was hence used to determine G_0 .

$$G_0 = \rho V_s^2$$

Equation 7-10

Where:

ρ = Bulk density of the soil [Mg/m^3]

V_s = Shear wave velocity [m/s^2]

Appendix C presents the G_0 values for each geotechnical unit. Geotechnical bounding was determined based on engineering judgement.

7.9.8.5 STRAIN AT 50% PEAK DEVIATOR STRESS

The strain at 50% of the maximum deviatoric stress (ε_{50}), is used in the formulation of traditional lateral load-deflection (p-y) curves in cohesive layers and is derived from triaxial test stress-strain plots. ε_{50} was determined from the CIUc, CAUc and UU test data. Appendix C presents the ε_{50} profile with depth.

7.10 ROCK PARAMETERS

7.10.1 GENERAL

Rock was encountered at varying depths across the site. The rock identified at the southern site was Chalk with top to bedrock varying between 1.4 m and 48 m BSF. The Chalk consisted of:

- Unlithified Chalk – Class Dm/Dc
- Lithified Chalk – Class A1 to B4

Design in Chalk should be considered with caution as it may lead to excessively long piles or premature refusal during installation. This will be dependent on the Chalk structure and properties.

CPTs were able to penetrate into the unlithified chalk but not into the lithified chalk. This is because the unlithified chalk is encountered as a structureless chalk slightly sandy silty gravelly to very gravelly. The thickness of the unlithified Chalk varied in thickness from less than 5m to greater than 10m. The unlithified Chalk was underlain by the structured lithified Chalk where CPTs terminated at top and were recovered by coring.

This section of the report discusses the characterisation of rock parameters in view of the laboratory test results, which included point load tests, unconfined compressive strength (UCS), and UCS with young's modulus.

7.10.2 RQD

Rock quality designation (RQD) is a measure of quality of rock cores recovered in a borehole. RQD is described as the ratio of solid core pieces longer than 100 mm length per core run. An RQD of 75% or greater indicates good quality rocks and 50% or less indicates poor quality rock cores. RQD was determined mainly for the lithified (structured) Chalk (GU Vb). Appendix C presents that RQD with depth. It can be observed that most of the rock cores had an RQD greater than 80% indicating a good quality structured Chalk.

In the unlithified structureless Chalk where coring was performed. RQD of between 0% and 100% was acquired in the few core runs performed in the unlithified Chalk. This shows the unlithified Chalk (GU Va) to be very variable consisting of both structureless and structured Chalk. This variability in GU Va should be considered with caution in the foundation design.

7.10.3 POINT LOAD TESTS

A total of 23 Point Load Tests have been performed to determine Point Load Index (PLI) for rock samples. PLI assesses the rock strength by applying a concentrated load at a specific point and measuring the applied load at failure. The shape of the rock selected for the PLI

will determine if the test will be performed diametral (D), Axial (A), Irregular lump (I) or random (U). PLT observed to have failed early or incorrectly were not included.

7.10.4 UNCONFINED COMPRESSIVE STRENGTH

A total of 33 UCS tests were performed to determine the uniaxial compressive strength of rock samples. Out of the 33 tests, 15 included strain measurements to calculate Poisson's ratio and Young's modulus. All the tests with strain measurements have been interpreted by using a secant method.

Several samples did not have an acceptable L/D ratio. For samples with L/D outside of the 2.0 to 2.5 range per ASTM or 2.5 to 3.0 range per ISRM, the results may therefore be biased. Venterra used the method recommended by (Tuncay, E, 2019) to correct the UCS for samples with low L/D.

PLT tests were converted to an equivalent UCS value as described by Equation 7-11. It should be noted that only the axial PLT were considered which is representative of a similar failure condition to UCS.

$$UCS = I_{S50}k$$

Equation 7-11

Where:

I_{S50} = Adjusted point load value

k = conversion factor

Appendix C presents a comparison of PLT and UCS test results with bulk density. A review of this plots shows a k factor of 13 was determined to be applicable for converting PLT to equivalent UCS results. Geotechnical bounding has been presented based on engineering judgement biased towards the UCS results

7.10.5 INTACT YOUNGS MODULUS

Intact young's modulus (E_i), tangential at 50% of the UCS failure mode, of the Chalk was determined from UCS strength tests with Youngs modulus. Appendix C presents the E_i plots where measured.

8 HAZARDS AND GEOHAZARDS

8.1 SEAFLOOR HAZARDS

A summary is provided below of the individual seafloor hazards identified by (GEOxyz, 2024). The associated risks to development are considered minimal as they have been previously investigated and are summarised here for a complete overview of the site. The level of risk for the described hazards is expected to be reduced further with the future site investigations required for the development of the site.

8.1.1 BOULDERS AND DEBRIS

A total of 243 targets were interpreted on the SSS (173) and MBES (70) data to be related to the presence of boulders. These vary in diameter between approximately 0.5 and 2.8 m, and in height between 0.05 and 1.15 m. A significant amount of scarring affects the seafloor. It is possible that some of the contacts interpreted as boulders represent just mounds of sediments developed during anchor-drag or trawl-related scarring. Additional targets were interpreted as sediment accumulation, wrecks, metallic anomalies and unknown. This is a relatively low amount of seafloor targets identified for a site and the risks related to this are considered minimal.

The site contains two levels of boulder field classification based on their density value for a 100 x 100 m area, that were provided and referenced by GeoXYZ in their report (GEOxyz, 2024). However, the delivered shapefiles for these areas contain a variation in classification to that reported. The report describes of classifications 1 and 2 representing a density of 40-80 boulders and >80 boulders, respectively. However, the delivered shapefiles contain classifications 1a, 1b and 2a. Because this cannot be clarified, Venterra have simplified them to class 1 and 2 as per the formally reported classifications.

8.1.2 DEPRESSIONS

Linear depressions were identified on the SSS and MBES data throughout the site and interpreted as trenching associated with the installation of the underwater cables. Several linear magnetic anomalies were identified in the immediate vicinity of known underwater cables and pipelines across the site (Figure 6-12). Some magnetic anomalies indicate the presence of additional subsea infrastructure, which was not previously identified.

Small, isolated depressions, (Figure 6-10), have been interpreted across the site. They occur most frequently in the northern and northeastern section as clusters of closely spaced depressions. These depressions are mostly 5-10 m in diameter, reaching up to 15 m maximum. They are rather shallow and gently sloped, the depth ranges between 0.4 -0.6 m.

Given the nature of the underlying sediments these depressions may be interpreted as pockmarks. Possible gas blanking was observed on seismic data, which in combination with pockmarks might suggest shallow gas presence. Potentially, these pockmarks were created by gas escaping from beneath the seafloor. Given the density and spread of the features identified across the site, the risks related to this are considered minimal.

8.1.3 SEAFLOOR SCARRING

Extensive seabed scarring was found in the eastern section of the site as well as a larger area in the centre (Figure 6-9). These scars were interpreted to be associated with fishing activity and offshore operations in the area. In the east, these scars appear deeper and more erratic in their shape and positioning to other scars, compared to further west where the scars are more equally spaced and shallower with defined paths across a wider area. Some of the identified depressions were deemed anthropogenic in origin due to their small horizontal extents relative to their depths, which generated high seafloor gradients, probably as a result of anchor operations, as presented in Figure 6-3 and Figure 6-9. As these areas are defined and the associated seabed slope values are low, the risks related to this are considered minimal.

8.1.4 SLOPE

Slopes across the site are generally not significant (under 1°), with an average of 0.3° and therefore the risks related to this are considered minimal. The widespread bottom trawling scars are associated with steeper slopes, predominantly between 2 and 5°, though very isolated occurrences of more than 5° were occasionally documented. Additionally, localised areas with slopes greater than 5°, rarely up to 32°, can be seen either within depressions or in areas affected by scouring.

8.1.5 WRECKS

A single area of elevated bathymetry and high gradients in the southeastern part of the site area was interpreted as potentially related to a shipwreck (GEOxyz, 2024). Based on their findings reported that it is the wreck of the Birgit Ehlers vessel. The feature consists of a cluster of targets potentially representing the shipwreck and its associated debris, as shown in Figure 6-6. This isolated feature and possibly related debris present a low risk to development as the features have been mapped and can be incorporated into development planning.

8.1.6 OTHER

Out of the 63 mapped magnetic targets, eight were interpreted as anthropogenic in origin, these targets correlated with the C-Lion cable crossing the site in southwest-northeast direction. The source of the remainder of the mapped targets remains unknown.

8.2 SUB-SEAFLOOR HAZARDS

8.2.1 BOULDERS AND COARSE SEDIMENTS

Unit IIIb which consists of lower glaciolacustrine deposits, in places displays a relatively higher density potentially associated with a small pocket of cobbles/gravel/coarse sediments, as suggested by its interpreted sedimentary environment. Numerous hyperbolic reflections with varying amplitudes can also be seen within unit Va and were not picked individually. Based on the geology in the region, these are considered to be flint nodules in the chalk bedrock, although it is also possible that they are artificial features created during seismic processing.

8.2.2 SHALLOW GAS

The Arkona Basin, which is located east of the site, is characterised by shallow gas rich sediments with different levels of saturation. Geoacoustic investigations show gas accumulations in pockmark areas, and in regions with homogeneous deposited organic rich sediments (Mathys, et al., 2005). The gas present in Arkona Basin sediments is of biogenic origin and originates from the generation of methane by methanogenic bacteria. However, only little is known about heterogenous distribution of methane in the Arkona Basin (Mathys, et al., 2005).

Gaseous sediments can be characterized by high acoustic impedance contrast and elastic contrast in relation to the surrounding medium such as non-gaseous sediments, as seen in Figure 8-1, determining high acoustic energy scattering properties (Jaśniewicz D., 2018).

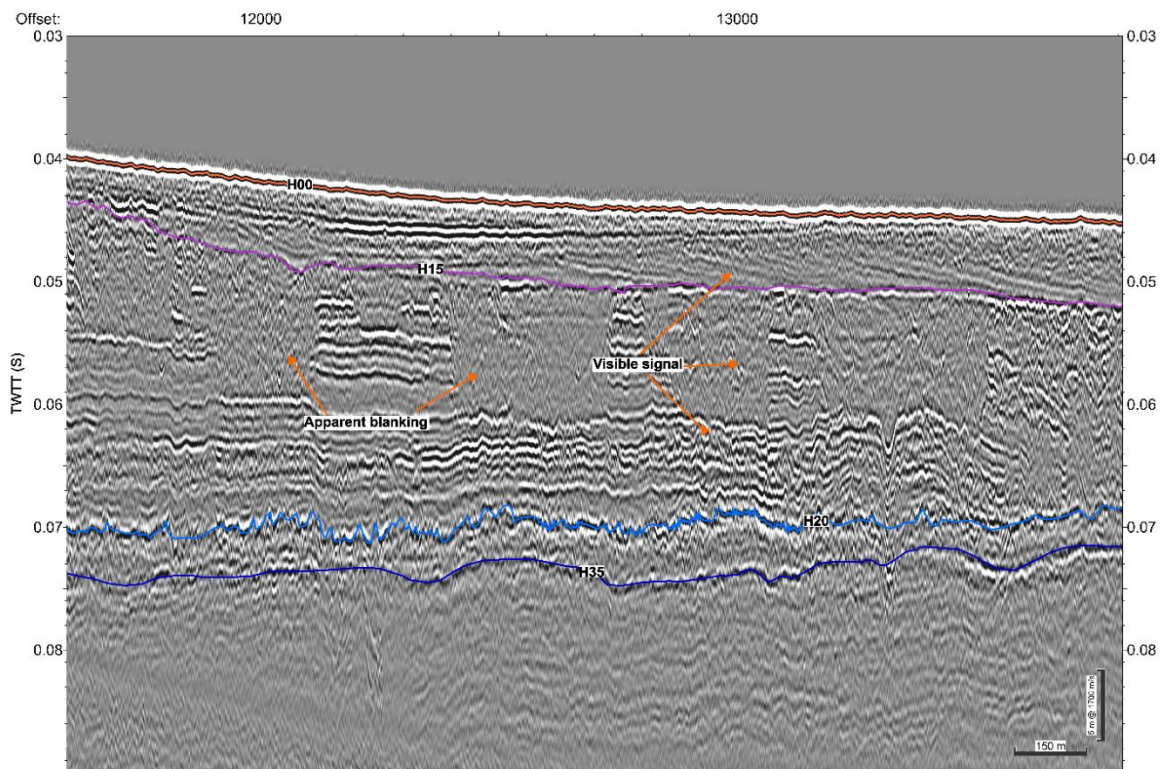


Figure 8-1 - Apparent acoustic blanking on seismic line KS_L024_UHR_T_MIG_STK

Evidence of possible shallow gas has been observed across the site on the SBP and UHRs datasets (Figure 8-1). As discussed in section 6.2.3.1, although areas of apparent signal blanking are present, because the seismic signal is still visible (although at a much lower amplitude) above, below and within the area of blanking, this does not represent signal blanking typically found where gas is present. It is possible that this may be attributed to the seismic survey set up. Observations from the seismic data reveal the presence of features that show resemblance to gas chimneys. They appear as columnar disturbances that range to 30-40m in width through relatively continuous and parallel reflectors. These possible

chimneys do not reach the seafloor and do not produce local depression or pockmarks on the seafloor.

Intrusive works were carried out without incidents. Insufficient record lengths, and/or the use of water column muting, in available seismic records, prevented possible observation of gas release into the water column during survey.

It is important to note that if abundant and under pressure, shallow gas could represent a blow-out risk for intrusive surveys and its' release in the water column can also destabilise vessels. Shallow gas may impact the development in different ways. Where present within permeable layers, potential influx of gas into a borehole and drill string providing pathways to the drill deck during site investigations should be considered as a hazard. This can represent a risk to the safety of operations and to human life. Free gas within impermeable soils may result in localised decreases in shear strength and stability. Characterisation of shallow gas is challenging and results in additional uncertainty in design parameters. However, further investigations are needed to assess the impact of shallow gas on the sediment load-bearing capacity in the site area.

8.2.3 CHANNELS AND CHANNEL INFILL

Evidence of possible channel incisions and infills were observed across the site. In the southwestern corner there are higher amplitude, dipping reflectors indicating a possible channel incision in the top of the bedrock, as presented on Figure 6-29. From the available seismic lines, this feature was seen to extend both south and west of the site boundary. The feature ranges from 1.7 km wide and approximately 80 m deep. Without targeted geotechnical data, it is not possible to determine the potential infill material or confirm that this is in fact a form of channel.

There is evidence of possible incisions features within Unit IIIb, typically in the central and eastern areas where the unit has transitions from the sand wedge to more laminated clay deposits. Examples are presented in Figure 8-2. Given that the depositional environment of Unit IIIb is interpreted as late glacial to glacio-lacustrine, the presence of small, infilled subglacial channels is expected

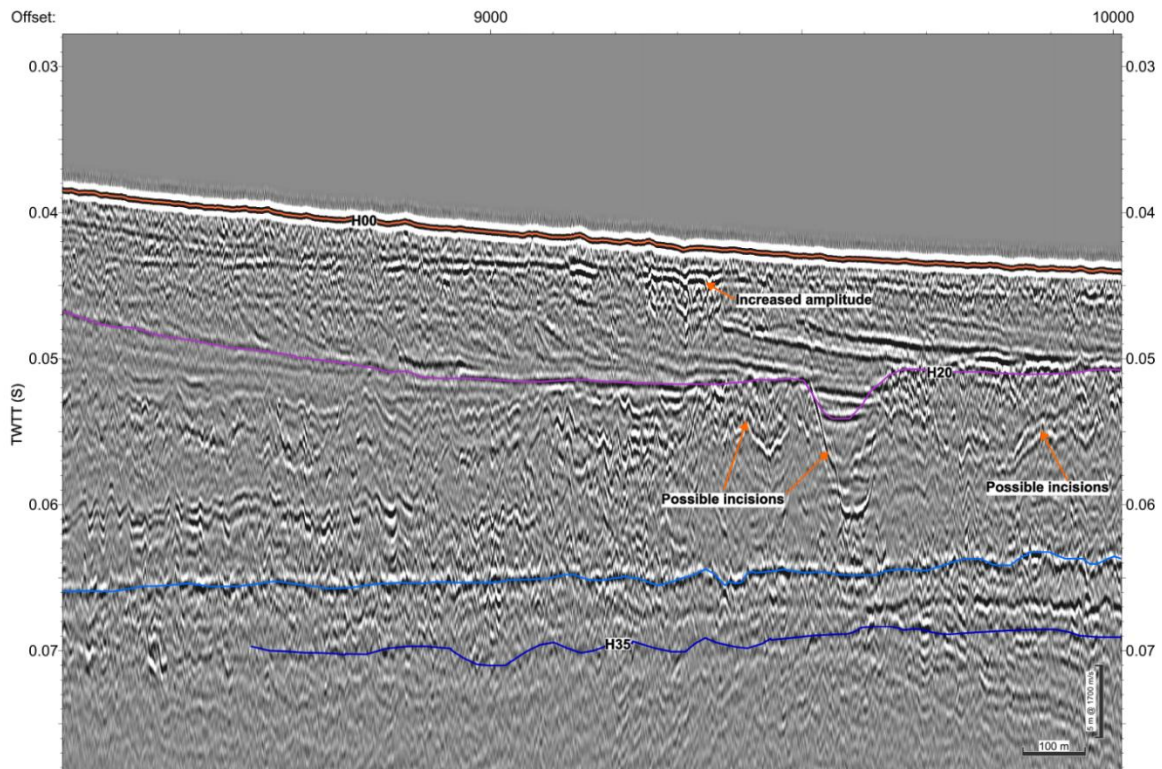


Figure 8-2 - Example of small incisions on seismic line KS_L018_UHR_T_MIG_STK

These features display a contrasting seismic signature to the incised units, with occasional high negative or positive acoustic impedance contrasts, which suggest an abrupt change in lithology, potentially accompanied by a change in physical properties.

In the literature, there are known examples of the aforementioned features formed in a similar environment. Few field sections have been documented with insight into the geological characteristics of subglacial channels. Small channels often occur at the bases of subglacial deposits and they are incised into outwash deposits below. Figure 8-3 presents documented in-filled incisions associated with Scandinavian Ice Sheet: A) Saalian glaciation, Lower Lusatia, eastern Germany; B) Weichselian glaciation, Island of Funen, Denmark; C) Weichselian glaciation, Limfjorden, western Denmark; D) Weichselian glaciation, Island of Rügen, north-eastern Germany; E) Weichselian glaciation, Brügge, north-western Germany (Kehew, et al., 2012).

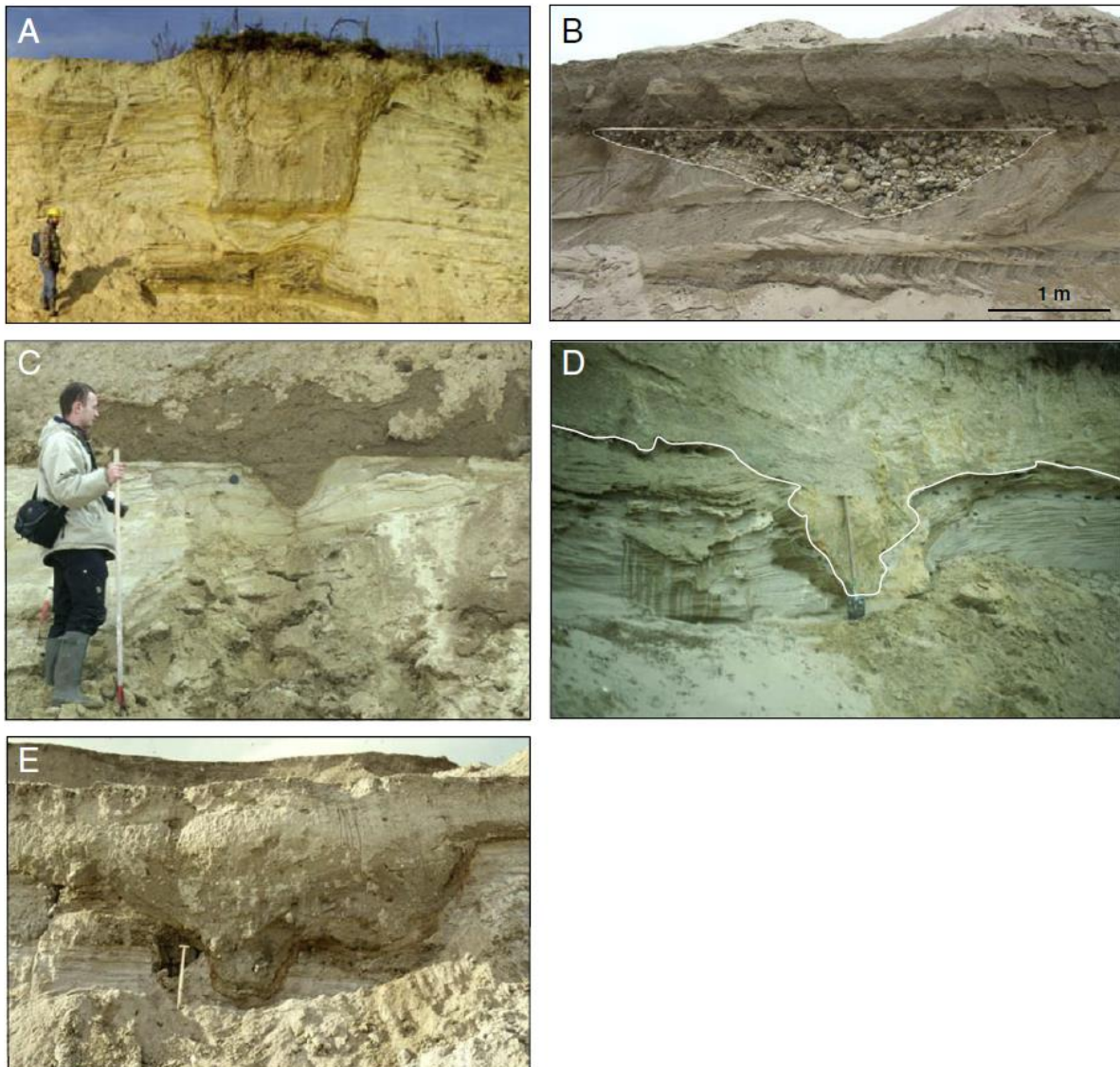


Figure 8-3 - Small subglacial channels at the southern fringe of the Scandinavian Ice Sheet (Kehew, et al., 2012).

8.2.4 FAULTS AND FAULTING

Two pre-Quaternary faults are marginally intersecting the site, in the northern and western corner, based on the EMODnet database (EMODnet, 2023). However, no clear evidence of faulting corresponding to these two expected features was observed at the bedrock level. No displacement associated with these inferred faults nor additional faults were observable within the Quaternary section. As such, sediment movement associated with fault activity is not an expected occurrence in the site.

Bedrock faults are not well imaged, though faults are almost certainly present, some UHRS lines do show weak evidence for the position of fault planes. These ancient faults were reactivated during the Late Cretaceous/Early Palaeocene and, in this area, likely generated inversion. The high potential for erosion of the top of the bedrock (especially over the last 1.1 million years of ice advances) makes it difficult to attribute features at the top bedrock surface to tectonic activity. The tectonic relief may well have been planned off by ice (GEOxyz, 2024).

8.2.5 GLACIAL FEATURES

The Quaternary geological evolution of the study area is defined by an alternation of glacial and interglacial periods. Scandinavian inland glaciers advanced several times through the Baltic area in the direction of Middle and Western-Europe (Mathys, et al., 2005). The nearby Arkona Basin has a complex geologic setting, with Cretaceous bedrock made of chalk successions, which were subsequently glacially overprinted and covered by glacial till, sands, and clays, fine-grained brackish to marine organic-rich deposits.

From literature, in the Arkona Basin there are no traces of ice marginal forms. The only glacial feature encountered across the site is a channel mentioned in section 7.2.2, potentially it can be glacial-related and constitute a tunnel valley. The infills can display similar physical and geotechnical properties to the adjacent units.

8.2.6 LOW STRENGTH SEDIMENT

Low strength fine grained sediments have been sampled by the geotechnical data within seismic units I to III. Unit 1 is comprised of marine sediments and exhibits a change in lithology from sands to silty sands, which are interpreted to be a low strength. The distribution of glacial sediment facies in unit III is in general chaotic with alternating sections of clays and parallel-bedded, well sorted sands with laminated silt and clay interbeds. The sampled sediments from Unit III include very closely to closely spaced thin laminations of organic matter. In the west of the site, the clay is confined to the base of Unit IIIb and increases in thickness to the east, whereby it is the main sediment type of the unit (section 6.2.3 and Figure 6-23 and Figure 6-24).

The low strength sediments are observed close to seafloor and at depth below high strength sediments. The low strength sediments will cause the following challenges to foundation design and installation:

- High risk of punch through where the low strength sediments underlie high strength sediments such as very dense sand.
- Excessive settlement of foundations.
- Jack-up placement challenges due to punch through, spudcan sliding, rapid or deep leg penetration, leg extraction challenges
- Excessive long and thick-walled piles maybe designed.

8.2.7 SHALLOW BEDROCK

The site is located at the margin of the Arkona Basin. Thus, the bedrock geology is represented by Upper Cretaceous chalk. The depth to bedrock varies from 3.8 to 51.0 mBSF, from the gridded surfaces. Most of the site is characterised by depths to bedrock less than 30.0 mBSF, exceptions occurring in the southwestern trough and additional smaller scale incisions. In the northeastern part of the site, the bedrock is shallowing to less than 15.0 mBSF. Bedrock is not interpreted to crop out based on the available seismic data. Section 11 presents the challenges of design and installing piles in the shallow rock.

9 RISK REGISTER

A Risk Register is provided in Appendix D. Risks are graded by likelihood of occurrence and severity (pre-mitigation) based on the criteria and scoring system defined in the respective parts of the document. An overall risk level is determined from the risk matrix in Figure 9-1 - Risk Matrix (Vamanu, et al., 2016). The associated risks for the hazards identified on the site(s) are assessed and scored based on the available literature for risks within the marine environment and offshore renewable energy activities. These include:

- Documentation from the International Organization for Standardization (ISO) (International Organization for Standardization, 2017).
- Standards from the British Standards Institution (BSI) (British Standards Institute, 2003; British Standards Institute, 2013; British Standards Institute, 2021).
- Carbon trust risk assessment guidance (Carbon Trust, 2015).
- Documentation on Marine Geohazards from the European Marine Board (European Marine Board IVZW, 2021).
- Offshore wind farm risk management codes of practice from VdS (VdS, 2014).
- International Association of Oil & Gas Producers (IOGP) Risk management guidance for geophysical operations (International Association of Oil & Gas Producers, 2017).
- Offshore risk assessment guidance from the European Commission and the Joint Research Centre (Vamanu, et al., 2016).

The final risk classifications are graded with reference to the European Commission and Joint Research Centre report for offshore risk assessment (Vamanu, et al., 2016). The resultant Low, Medium, and High levels can be described as:

Low

"The risk of the occurrence of the event is acceptable, and no risk reduction/mitigation actions are required; the risk must however be part of the continuous risk management process, for further reduction."

Medium

"The risk should be monitored, yet at the current moment it is controlled as low as reasonably practicable (ALARP)."

High

"The risk is intolerable and risk reduction/mitigation actions must be put into place."

The identified foundation risks focus on selection and installation concerns relate specifically to the southern site. It should be noted that in most cases the identified levels of risk can be mitigated by acquisition of additional information or development of avoidance strategies: these measures are not necessarily required to inform conceptual foundation design. Timing of any mitigation measures should be determined based on the project development strategy.

			Severity				
			Low	Minor	Moderate	Major	Severe
			1	2	3	4	5
Likelihood	Very Likely	5	Medium	Medium	High	High	High
	Likely	4	Medium	Medium	Medium	High	High
	Possible	3	Low	Medium	Medium	Medium	High
	Unlikely	2	Low	Low	Medium	Medium	Medium
	Very unlikely	1	Low	Low	Low	Medium	Medium

Figure 9-1 - Risk Matrix

10 RECOMMENDATIONS

10.1.1 DESK STUDIES

A shallow gas hazard assessment would provide added benefit to the understanding of the site conditions. As discussed in section 6.2.3.1 and section 8.2.2, the observed transparent facies (with reduced amplitude) does not exhibit typical behaviour of acoustic blanking attributed to the presence of gas. Mainly due to the fact that signal is still visible, above, below and often within these affected parts of the record.

10.1.2 DATA RE-PROCESSING

Reprocessing of the UHRS dataset to provide improved visibility of reflectors for the sections of the data affected by the seabed de-multiple process. The current dataset provides a preliminary coverage of the site, though it is limited in that the remnant processing artefacts affect the continuity and interpretation of the H20 and H35 reflectors of Unit Va and Vb, respectively (Figure 6-23). Re-processing the existing data would reduce costs for immediate data acquisition and may provide improved results to constrain the associated uncertainty around the till and unlithified chalk interface, as well as inform on the behaviour of the deeper H35, top of lithified chalk reflector.

10.1.3 FURTHER SURVEYS AND INVESTIGATIONS

A significant source of uncertainty in the IGM is due to the current UHRS data line spacing of approximately 250 m (Section 5.5). At this distance, significant extrapolation was required to create grids for the mapped seismic units. Where seismic units change significantly in depth between or along lines, the gridded surfaces can produce unrealistic trends that can give a false impression of changes in the depth of a unit. To alleviate this, additional seismic data should be acquired and added to the IGM to fill in gaps, reduce extrapolation distances, and subsequently improve reliability of unit depths. These additional surveys are advised to be undertaken with an adequate (narrower) line spacing for both 2D UHRS and SBP (e.g. Innomar) data, or even consider 3D UHRS. . A revision to the IGM ought to follow each data acquisition milestone to address remaining knowledge gaps.

The acquisition of additional seismic and geotechnical data would allow for further improvements and refinement of the velocity model. If the unitisation of the subsurface changes based on new data, then the associated velocity model would need to account for this to allow for accurate conversion of the interpreted model.

The geotechnical and geophysical data has shown that the ground conditions vary both laterally and axially across the site. Hence, for detailed design, it is recommended to perform location specific geotechnical testing at each foundation location to determine the ground conditions.

Bedrock consisting of unlithified (unstructured) and Lithified (structured) chalk was observed across the site. The testing at the site mainly targeted the lithified chalk with few classification testing performed within the unlithified chalk. However, considering the deep penetration of some of the CPTs into the unlithified chalk; this unit will be most critical for foundation design. The behaviour of chalk is very variable as noted by various authors such as (Jardine, R.J.,

Chow, F.C., Overy, R. & Standing, J. R. , 2005) . Hence, additional targeted testing is recommended to determine the geotechnical properties of the unlithified (unstructured) chalk as well as the lithified (structured) chalk.

A limited geotechnical testing scope was performed at the southern site. Additional geotechnical testing is recommended to properly capture the geotechnical properties such as shear box testing, electrical resistivity, triaxial extension tests and permeability tests etc

11 CONCLUSION

An IGM has been developed based on the integration of the recently acquired geophysical and geotechnical datasets, building on the results of the PGM (GEOxyz, 2024) and constraining the site as much as possible. Interpreted seismic units have been revised and correlated with independently interpreted geotechnical unit top markers. Based on this integration, a velocity model (appropriate to this stage of investigation) was developed and used for the depth conversion of the seismic dataset and interpretation. Though uncertainties remain, this model forms the basis of future detailed and targeted investigations that are required to further constrain the model and further understand the behaviour of the subsurface across the site.

Within the seismic data, three seismic units were differentiated based on their internal seismic facies and correlated with 12 geotechnical units. Seismic Unit I (marine sediments) consist of up to 2.8 m of surficial sands and clay, overlying the older glaciolacustrine deposits. Seismic Unit II (not interpreted as part of this study) corresponds to the post-glacial transition deposits. Minimal evidence of the unit was observed on SBP data below the truncating Unit I base reflector, and as such there was insufficient coverage to produce a usable interpretation (Chart 24004-PRO-006-22-00).

Seismic Unit III has been interpreted to consist of two subunits based on the characteristics of the seismic facies across the proposed site. Unit IIIa is present beneath Unit I and at the seabed (in isolated areas) as a layer of very low to low strength clay and silty sand, up to 8.4 m thick. This unit represents the upper glaciolacustrine unit as discussed by (GEUS, 2023; Jensen, et al., 1997) and was separated from the lower glaciolacustrine subunit (Unit IIIb) by the typical prograding to subparallel internal reflectors. The base of the unit, along with the base of Unit I and the seabed, represent the top of the lower glaciolacustrine unit - Unit IIIb. This unit is characterised by a variable lithology from west to east across the site (as summarised in Table 6-2, corresponding to the sand-wedge deposits of the western extent of the Arkona basin, transitioning to a predominantly clay-based deposit in the east (Figure 6-23). Internally this unit's seismic facies show clear change from eastwards prograding sigmoid clinoforms (western extent of the sand wedge) to continuous to discontinuous parallel reflectors in the east of the site. The area of transition is illustrated at a high-level in Figure 6-22 and as shown in a cross section in Figure 6-23. The current data do not allow for a clear reflector to be interpreted to bound this transition and potentially subdivide the unit further. The unit is at its thickest (51 m) in the west of the site where it is present up to the seabed (Figure 6-22).

The base of Unit IIIb represents the top of Unit Va, which is interpreted as unlithified chalk (Dm/Dc, H1). In the PGM provided by (GeoXYZ, 2024) this surface was initially interpreted to represent the top of till. The recovered geotechnical data (boreholes) do confirm a presence of till, though from the integration across the site, this surface has been interpreted as the top of unlithified chalk. The till, though present, has not been interpreted within the seismic data as no clear acoustic reflection or change in facies was observed. As discussed in sections 6.2.3 and 6.2.4, the thickness of the till overlying the unlithified chalk (Figure 6-25) may be insufficient to allow for a large enough difference in acoustic impedance (coupled with seismic

resolution) that would allow the interface to be distinguishable in the seismic data. Unit IV, glacial till, has not been interpreted within this model, though as the geotechnical results show, it is present within the subsurface and presents an uncertainty in the model that requires targeted future investigations.

Unit V (bedrock A1-B4, H2) is split into two subunits based on the recovered geotechnical data. These are Unit Va unlithified chalk and Unit Vb lithified chalk. Unit Va is bounded by the high amplitude, continuous reflector of Unit IIIb and is present across the site. A thickness for the unit is not available due to the reliability of the deeper lithified chalk surface reflector. In the southwest of the site, uncertainty remains for the bedrock unit due to the presence of a possible incision/channel feature (Figure 6-27). Unfortunately, there is no available geotechnical data for this area to confirm the lithology and so it is unknown if the current base of Unit IIIb (H20 reflector) represents any till or infill surfaces in this area. A preliminary interpretation was produced, though it was decided by the client that they did not want to pursue this. This area requires future investigations to determine the till to bedrock interface and to determine the suitability of this part of the site for foundations.

The current IGM presents limitations and uncertainties due to the coverage of the UHRS data and remnant processing artefacts, and the limited number of geotechnical locations and retrieved samples. As a result, there is reduced accuracy between gridded UHRS lines, which is increased when there is more variability in interpretation along the survey line. The remnant processing artefacts in the seismic data prevented the tracking of otherwise continuous reflectors to inform on key surfaces and interfaces.

Hazards and geohazards were identified within the proposed site. They include boulders and debris, seafloor depressions and scarring, a single wreck and a confirmed cable crossing the site. The subsurface hazards include possible incisions and channels within the glacial units (Unit III), potential faults (Quaternary), low strength sediment, shallow bedrock and possible gas deposits (Section 8).

Four geotechnical provinces and 12 geotechnical units were identified across the site. The geotechnical zones represent broadly similar ground conditions laterally and vertical across the site. Geotechnical units represent similar geotechnical properties e.g. clay or sand.

The provinces were delineated based on the depth to top of bedrock and considering the quaternary deposits above the bedrock. Generally, bedrock identified as both structureless (Grade Dc/Dm) and Structured (Grade A1/ B4) Chalk was encountered across the site at varying depths. Province 1, Chalk bedrock was encountered less than 10 m BSF. This province was observed in limited areas in the Northeast and Northwest edges of the site. Low strength sediments overlying the chalk are observed at this site. Province 2, Chalk was encountered between 10m and 20 m BSF. This province is spread across the North of the site. Very loose to dense sediments overlie low strength to extremely high strength clays. Province 3, Chalk was encountered between 20 m and 30 m BSF. The province is spread across the centre of the site. The sediments consist of medium dense to very dense sands becoming medium dense to dense overlying very low to extremely high strength Clays. Province 4, Chalk is at a depth greater than 30 m and dependent on the foundation depth,

Chalk may not be encountered. Sediments consist of predominantly medium dense to very dense Sand overlying transitional soil consisting of Silt, Clay Till or Sand Till.

The following should be considered when installing foundations within each of the provinces:

- Design of foundations in Chalk may result in excessively long heavy piles. Installation in Chalk presents an increased risk of premature refusal during installation due to competent Chalk layers or flint beds, requirement of specialised installation techniques such as drive-drill-drive or drilled and grouted piles which maybe expensive.
- Jack-up placement where low strength sediments are observed close to the seafloor or at great depths should be considered with caution as they may result in excessive leg penetration, spudcan sliding, uneven leg penetration, punch through, etc.
- Very dense sands are observed overlying very low to low strength clays. Design of foundations in these soil layers should be considered with caution due to high risk of punch through, excessive length of piles being designed, pile run risks etc
- Very dense sands are observed close to seafloor and at shallow depths. Installation of foundations in these sands may be challenging due to limited penetration, early refusal etc.
- Transitional soils are observed across the site which may behave as drained or undrained dependent on the design conditions. Geotechnical units IIIb4, IIIb5, IIIb6 may behave as a transitional soil and should be considered with caution by a geotechnical engineer.
- Clay Till was observed overlying the Chalk bedrock. Installation of foundations in this unit may results in pile tip buckling, premature refusal or punch through into the lower strength unlithified Chalk considering the gravelly sandy very high to extremely high strength properties of the unit.

Unitised geotechnical parameters were determined to describe the geotechnical properties across the site. LE, BE and HE geotechnical profile bounds were assigned to some of the unitised geotechnical parameters. The geotechnical profile bounds were determined either statistically and/or by engineering judgement.

Unit IIIa and IIIb, consist of predominantly dense to very dense sands. This may pose a challenge to the installation of piles.

Bedrock was encountered within the engineering foundation depth across the site. Bedrock consisting of unlithified (structureless) and lithified (structured) chalk was observed across the site. The unlithified chalk varied laterally across the site with varying thicknesses. Limited testing was performed within the unlithified chalk, and it is recommended that additional testing is performed to fully characterise this unit.

This IGM presents the assessment of ground conditions at the Krieger's Flak II Southern Site OWF. Geophysical and geotechnical data acquired for the site were reviewed, integrated and analysed to develop an IGM with unitised geotechnical parameters. The main ground risk identified were the thick Seismic Unit (SU) IIIb deposits encountered predominantly at the southwest of the site and bedrock consisting of Chalk at shallower depths towards the north

of the site. The bedrock varied from 10 m BSF to greater than 30 m BSF from north to south of the site; however, it should be noted that at localised areas at the north of the site, bedrock was encountered at less than 10 m BSF. SU IIIb is very variable consisting of a mix of sand, silt and clay. The silt and sandy clay or clayey sand may behave as drained or undrained dependent on the design conditions and should be considered with caution during design. SU IIIb was split into six geotechnical units to enable characterisation of similar geotechnical properties. The depth of bedrock may influence the foundation typology, foundation design and installation methodology dependent of the foundation depth. The site was split into four zones based on the depth to top of bedrock, depth of the thick seismic unit IIIb, geotechnical and geophysical data. The zones will aid in the initial planning of the turbine layout, foundation concept and design based on the engineering characteristics. Geotechnical parameters for each unit were also presented representing the range of engineering properties. It is recommended that the end user of this report performs an independent review of the IGM and parameters in respect to the proposed foundation typology and construction methodology.

12 REFERENCES

- Jardine, R.J., Chow, F.C., Overy, R. & Standing, J. R. , 2005. *ICP design methods for driven piles in sands and clays*, London: Thomas Telford Ltd.
- Binzer, K., Lykke-Andersen, H. & Stockmarr, J., 1994. *Geological map of Denmark, 1:500 000. Elevation of the Pre-Quaternary surface. The Danish land area and the Kattegat, inland waters and the waters around Bornholm*. s.l.:GEUS Dataverse.
- Bolton, M., 1986. The strength and dilatancy of sands. *Géotechnique*, 36(1), pp. 65-78.
- British Standards Institute, 2003. *BS EN ISO 19901 4:2003 - Petroleum and natural gas industries — Specific requirements for offshore structures — Part 4: Geotechnical and foundation design considerations*, London: British Standards Institute Limited.
- British Standards Institute, 2013. *BS 6349-1-1:2013-Maritime works –Part 1-1: General – Code of practice for planning and design for*, s.l.: BSI Standards Limited.
- British Standards Institute, 2021. *BS ISO 19901-10:2021-Petroleum and natural gas industries — Specific requirements for offshore structures-Part 10: Marine geophysical investigations.*, s.l.: BSI Standards Limited.
- Carbon Trust, 2015. *Cable Burial Risk Assessment Methodology-Guidance for the Preparation of Cable Burial Depth of Lowering Specification.*, London: Carbon Trust.
- DGU, 1992. *Geological map of the Danish underground*. s.l.:Varv.
- Emeis, K.-C., Endler, R. & Struck, U., 2002. The post-glacial evolution of the Baltic Sea . In: G. Wefer & W. Berger, eds. *Climate Evolution in NW Europe in the Holocene*. Berlin: Springer-Verlag.
- EMODnet, 2024. *EMODnet Central Portal*. [Online]
Available at: : <https://www.emodnet.eu/>
[Accessed 01 2024].
- Erlström, M. & Sivhed, U., 2001. *Intra-cratonic dextral transtension and inversion of the southern Kattegat on the south-west margin of Baltica – Seismostratigraphy and structural development*. Östervåla: Geological Survey of Sweded.
- European Marine Board IVZW, 2021. *Marine Geohazards - Safeguarding society and the Blue Economy from a hidden threat.*, Ostend: European Marine Board IVZW.
- Expedition 347 Scientists, 2014. *Baltic Sea Basin Paleoenvironment: paleoenvironmental evolution of the Baltic Sea Basin through the last glacial cycle. IODP Prel. Rept., 347*, s.l.: Integrated Ocean Drilling Program.
- Flanders Marine Institute, 2023. *Maritime Boundaries Geodatabase: Maritime Boundaries and Exclusive Economic Zones (200NM), version 12*. Available online at <https://www.marineregions.org/>. <https://doi.org/10.14284/632>, s.l.: Marine Regions.
- Galsgaard, J., 2014. *Flint in the Danian København Limestone Formation*. [Online]
Available at: https://www.geo.dk/media/1951/flint-in-the-danian-koebenhavn-limestone-formation_jgalsgaard_2014.pdf
[Accessed 18 1 2014].
- Gardline, 2024. *Volume II: Measured and Derived Geotechnical Parameters (Report Ref: 53101)*, s.l.: Gardline.
- GEOxyz, 2024. *Geophysical and Geological Survey Report For Kriegers Flak II North and South (BE5376H-711-03-RR)*, s.l.: GEOxyz.
- GEUS, 2022. *Geological Screening of Kriegers Flak North and South*, s.l.: s.n.
- GEUS, 2023. *Screening of seabed geological conditions for the offshore wind farm areas Kriegers Flak II North and Kriegers Flak II South*, s.l.: s.n.
- GEUS, 2024. *Denmark's Geology Portal*. [Online]
Available at:
<https://data.geus.dk/geusmap/?lang=da&mapname=denmark#baslay=&optlay=&extent=5296.6026>

[83329023,5932375.391217925,1107654.6090847922,6468052.484953636&layers=dkskaermkort](#)
 [Accessed 18 01 2024].

Graversen, O., 2004. Upper Triassic - Cretaceous stratigraphy and structural inversion offshore SW Bornholm, Tornquist Zone, Denmark. *Bulletin of the Geological Society of Denmark*, Volume 51, pp. 111-136.

Graversen, O., 2009. Structural analysis of superposed fault systems of the Bornholm horst block, Tornquist Zone, Denmark. *Bulletin of Geological Society of Denmark*, Volume 57, pp. 25-49.

International Association of Oil & Gas Producers, 2017. *Risk management in geophysical operations - 432-02*, London: International Association of Oil & Gas Producers.

International Organization for Standardization, 2017. *ISO 19901-2:2017-Petroleum and natural gas industries — Specific requirements for offshore structures — Part 2: Seismic design procedures and criteria*, Geneva: International Organization for Standardization.

Jakobsen, P. R., Rohde, M. M. & Sheldon, E., 2017. Structures and stratigraphy of Danian limestone, eastern Sjælland, Denmark. *GEUS Bulletin*, Volume 38, pp. 21-24.

Jamiolkowski, M. L. D. a. M. M., 2001. Evaluation of Relative Density from Cone Penetration Test and Flat Dilatometer Test. *Soil Behavior and Soft Ground Construction (GSP 119)*, pp. 201-238.

Jaśniewicz D., K. Z. B.-G. A. B. J., 2018. Acoustic investigations of shallow gas in the southern Baltic Sea (Polish Exclusive Economic Zone): a review. *Geo-Marine Letters*, Volume 39, pp. 1-17.

Jensen, J. B. et al., 1997. The Baltic Ice Lake in the southwestern Baltic: sequence-, chrono- and biostratigraphy. *Boreas*, Volume 26, pp. 217-236.

Jensen, J. B., Kuipers, A., Bennike, O. & Lemke, W., 2002. The Baltic Sea without frontiers. *Geologi*, Volume 4.

Jensen, J. B., Moros, M., Endler, R. & Members, I. E. 3., 2017. The Bornholm Basin, southern Scandinavia: a complex history from Late Cretaceous structural developments to recent sedimentation. *Boreas*, Volume 46, pp. 3-17.

Jensen, J. B. & Nielsen, P. E., 1998. *Treasures hiding in the Sea Marine raw material and Nature Interests*, s.l.: s.n.

Karlsrud, K. C. C. A. P., 2005. *Bearing Capacity of Driven Piles in Clay, the NGI Approach, Norwegian Geotechnical Institute*. Oslo: s.n.

Kehew, A. E., Piotrowski, J. A. & Jørgensen, F., 2012. Tunnel valleys: Concepts and controversies — A review. *Earth-Science Reviews*, Volume 113, pp. 33-58.

Kulhawy, F. a. M. P., 1990. *Manual on Estimating Soil Properties for Foundation Design*. s.l.:Electric Research Institute, EPR.

Lemke, W., 1998. *Sedimentation und paläogeographische Entwicklung im westlichen Ostseeraum (Mecklenburger Bucht bis Arkonabecken) vom Ende der Weichselvereisung bis zur Litorinatransgression*. s.l.:IOW, Bibliothek.

Mathys, M., Thießen, O., Theilen, F. & Schmidt, M., 2005. Seismic characterisation of gas-rich near surface sediments in the Arkona Basin, Baltic Sea. *Marine Geophysical Researches*, Volume 26, pp. 207-224.

Mayne, P., 2006. *The 2nd James K. Mitchell Lecture: Undisturbed sand strength from seismic cone tests. Presented at GeoShanghai, 6-8 June 2006. Intl. J. Geomechanics & Geoengineering*. London, Taylor & Francis Group.

Michel, G. e. a., n.d. Stratigraphic and palaeo-geomorphological evidence for the glacial-deglacial history of the last British-Irish Ice Sheet in the north-western Irish Sea.. *Quaternary Science Reviews*, Volume 300.

Mogensen, T. E. & Korstgård, J. A., 2003. Triassic and Jurassic transtension along part of the Sorgenfrei–Tornquist Zone in the Danish Kattegat. *GEUS Bulletin*, Volume 1, pp. 437-458.

Moreau, J. et al., 2016. Early diagenetic evolution of Chalk in eastern Denmark. *The Depositional Record*, 2(2), pp. 154-172.

- Moros, M. et al., 2002. Regressions and transgressions of the Baltic basin reflected by a new high-resolution deglacial and postglacial lithostratigraphy for Arkona Basin sediments (western Baltic Sea). *Boreas*, Volume 31, pp. 151-162.
- Pedersen, S. A. S., 1998. "Isrande.zip", *Kort over israndslinjer og lokaliteter i Skandinavien*. [Online] Available at: <https://dataverse.geus.dk/file.xhtml?persistentId=doi:10.22008/FK2/XOOWSR/HQ8T4F> [Accessed 22 01 2024].
- Robertson, P., 2009. Interpretation of cone penetration tests – a unified approach.. *Canadian Geotechnical Journal*, Volume 43, pp. 1337-1355.
- Robertson, P., 2016. Cone penetration test (CPT)-based soil behaviour type (SBT) classification system – an update. *Canadian Geotechnical Journal*, 53(12), p. 1910–1927.
- Robertson, P. C. K. 2., 2010. *Estimating soil unit weight from CPT, 2nd International Symposium on Cone Penetration Testing*. Huntington Beach, CA, s.n.
- Rosentau, A., Bennike, O., Uscinowicz, S. & Miotk-Szpiganowicz, G., 2017. The Baltic Sea Basin. In: N. C. Flemming, et al. eds. *Submerged Landscapes of the European Continental Shelf: Quaternary Paleoenvironment*. s.l.:John Wiley & Sons Ltd..
- Schmertmann, J., 1978. *Guidelines for cone penetration test: Performance and design (Report no. FHWA-TS-78-209)*. s.l.:Federal Highway Administration, US Department of Transportation .
- Schneider, J. R. M. M. P. a. R. N. 2., 2008. Analysis of Factors Influencing Soil Classification Using Normalized Peizocone Tip Resistance and Pore Pressure Parameters. *Journal of Geotechnical and Geoenvironmental Engineering*, 134(11), pp. 1569-1586.
- Tuncay, E, O. N. T. K. A., 2019. An Approach to Predict the Length-to-Diameter Ratio of Rock Core Specimen for Uniaxial Compression Tests. *Bulletin of Engineering Geology and the Environment*, Volume 78, pp. 5467-5482.
- Vamanu, B., Necci, A., Tarantola, S. & Krausmann, E., 2016. *Offshore Risk Assessment - An overview of methods and tools*, ISPRA: European Commission.
- VdS, 2014. *VdS 3549 2014-01 (01) International guideline on the risk management of offshore wind farms - Offshore code of practice*, s.l.: Gesamtverband der Deutschen Versicherungswirtschaft.
- Vejbæk, O. V. & Britze, P., 1984. *Top præ-Zechstein. Danmarks Geologiske Undersøgelse Map series 45*. s.l.:s.n.

13 APPENDICES

APPENDIX A – CHARTS AND DIGITAL DELIVERABLES

Table A- 1 - Charts and digital deliverables overview

Charts and digital deliverables overview					
Type	File Type	File Name	Deliverable	Unit (if applicable)	Comment
Chart	PDF	24004-OVR-001-02-01	Site overview	N/A	
Chart	PDF	24004-BSF-002-05-01	Top of unit depth below sea floor	I	
Chart	PDF	24004-BSF-002-06-01	Top of unit depth below sea floor	IIIa	
Chart	PDF	24004-BSF-002-07-01	Top of unit depth below sea floor	IIIb	
Chart	PDF	24004-BSF-002-08-01	Top of unit depth below sea floor	Va	
Chart	PDF	24004-MSL-003-05-01	Top of unit elevation to MSL	I	
Chart	PDF	24004-MSL-003-06-01	Top of unit elevation to MSL	IIIa	
Chart	PDF	24004-MSL-003-07-01	Top of unit elevation to MSL	IIIb	
Chart	PDF	24004-MSL-003-08-01	Top of unit elevation to MSL	Va	
Chart	PDF	24004-ISO-004-04-01	Unit Isochore (thickness)	I	
Chart	PDF	24004-ISO-004-05-01	Unit Isochore (thickness)	IIIa	
Chart	PDF	24004-ISO-004-06-01	Unit Isochore (thickness)	IIIb	
Chart	PDF	24004-HAZ-005-02-01	Site geohazards	N/A	
Chart	PDF	24004-Zon-007-02-01	Geotechnical zonation	N/A	
Chart	PDF	24004-BTH-008-02-00	Bathymetry	N/A	
Grid	ASCII	GeoTIFF	Top_Unit_I_mBSF	Top of unit depth below sea floor	I
Grid	ASCII	GeoTIFF	Top_Unit_IIIa_mBSF	Top of unit depth below sea floor	IIIa
Grid	ASCII	GeoTIFF	Top_Unit_IIIb_mBSF	Top of unit depth below sea floor	IIIb
Grid	ASCII	GeoTIFF	Top_Unit_Va_mBSF	Top of unit depth below sea floor	Va
Grid	ASCII	GeoTIFF	Top_Unit_I_mMSL	Top of unit elevation to MSL	I
Grid	ASCII	GeoTIFF	Top_Unit_IIIa_mMSL	Top of unit elevation to MSL	IIIa
Grid	ASCII	GeoTIFF	Top_Unit_IIIb_mMSL	Top of unit elevation to MSL	IIIb
Grid	ASCII	GeoTIFF	Top_Unit_Va_mMSL	Top of unit elevation to MSL	Va
Grid	ASCII	GeoTIFF	Unit_I_Isochore	Unit Isochore (thickness)	I
Grid	ASCII	GeoTIFF	Unit_IIIa_Isochore	Unit Isochore (thickness)	IIIa

Charts and digital deliverables overview						
Type	File Type	File Name	Deliverable	Unit (if applicable)	Comment	
Grid	ASCII	GeoTIFF	Unit_IIIb_Isochore	Unit Isochore (thickness)	IIIb	
Grid	ASCII	GeoTIFF	Base_Unit_I_mBFSF	Base of unit depth below sea floor	I	Venterra additional deliverable
Grid	ASCII	GeoTIFF	Base_Unit_IIIa_mBFSF	Base of unit depth below sea floor	IIIa	Venterra additional deliverable
Grid	ASCII	GeoTIFF	Base_Unit_IIIb_mBFSF	Base of unit depth below sea floor	IIIb	Venterra additional deliverable
Grid	ASCII	GeoTIFF	Base_Unit_I_mMSL	Base of unit elevation to MSL	I	Venterra additional deliverable
Grid	ASCII	GeoTIFF	Base_Unit_IIIa_mMSL	Base of unit elevation to MSL	IIIa	Venterra additional deliverable
Grid	ASCII	GeoTIFF	Base_Unit_IIIb_mMSL	Base of unit elevation to MSL	IIIb	Venterra additional deliverable
Geodatabase	GDB		N/A		N/A	

APPENDIX B - SEISMIC CROSS SECTIONS

APPENDIX C - UNITISED GEOTECHNICAL PARAMETERS

APPENDIX D - RISK REGISTER

APPENDIX E - GEOTECHNICAL CROSS-SECTIONS



We **develop** and **engineer** major global wind farm projects across the **entire** wind farm life cycle.



FIND OUT MORE

Environmental | **Advisory** | **Survey** | **Geoscience** | **Design**



Venterra Group,
3rd Floor, Standbrook House,
2-5 Old Bond Street,
London, W1S 4PD



venterra-group.com



Follow us